DEVELOPMENT OF IMPROVED AND LOW-COST DRILLING FLUIDS AND CEMENT SLURRIES IN OIL WELLS

PhD Thesis

By:

Emine Yalman

Petroleum and Natural Gas Engineer

University of Miskolc, Faculty of Earth Science and Engineering, Petroleum and Natural Gas Institute

Mikoviny Sámuel Doctoral School of Earth Sciences
Head of the Doctoral School: **Prof. Dr. Péter Szűcs**

Supervisor: **Assoc. Prof. Gabriella Petra Federer Kovácsné**

Miskolc, 2022

HUNGARY

Declaration

We as the members of the Doctoral Defense Committee declare that we accept Emine Yalman's thesis work, 'Development Of Improved And Low-Cost Drilling Fluids And Cement Slurries In Oil Wells', as original and independent work containing new scientific results and achievements and as a PhD theses.

Miskolc, 2022.08.23.

Dr Szabó Norbert .....

Chair of the committee

Dr Turzó Zoltán .....

Member of the committee

Dr Vadászi Mariann .....

Member of the committee

Dr Koncz Ádám .....

Member of the committee

Dr Zsuga János .....online participant.....

Member of the committee

Miskolci Egyetem
Kőolaj és Földgáz Intézet

ACKNOWLEDGMENTS

I would like to express my gratitude to my esteemed supervisor Dr. Gabriella Petra Federer Kovácsné, who guided me with a great devotion at every stage of my thesis and shared her all valuable knowledge and experience from the beginning to the end of my thesis work.

I sincerely thank to Prof. Dr. Tolga Depci for sharing his knowledge and experience, guiding me and collaborating in the publication of the thesis results throughout the thesis work.

I would like to thank to the Phd student Hani Al Khalaf for his helping in the performing of laboratory experiments and for his cooperation in publishing our results.

I greatly acknowledge to the Institute of Raw Materials Preparation and Environmental Processing. Especially Prof. Dr. Gábor Mucsi, who supplied me fly ash for my thesis, guided me about geopolymer and supported my work. I also would like to thank to Dr. Ádám Rácz, Dr. Roland Szabó for helping me in the grinding processes and PhD students Mária Ambrus and Tamás Kurusta for helping me laboratory experiments conducted in Institute of Raw Materials Preparation and Environmental Processing.

I would also like to thank to PhD student Nagham Amer Sami who is my office mate, with whom we started the doctoral journey at the same time, for her friendship and support throughout the thesis period.

Finally, I would like to thank to my dear husband Yusuf Yalman for his love, support and encouragement throughout the thesis process, and my family, who always supported me under all circumstances.

ABSTRACT

Drilling fluid and well cementing are indispensable components of drilling operations. In general, it is desirable that the drilling fluid used be simple and contain few additives additives at maintaining its high performance. Thus, the maintenance of the drilling mud and the monitoring of the parameters that need to be followed becomes easier. However, the flow characteristics of the drilling mud, which is in constantly circulation in the well, differ at the entrance and exit of the well. Therefore, a wide variety of drilling fluid additives are mixed into the drilling mud to maintain the flow properties such as viscosity, weight, gel strength and filtration of the drilling mud at the required levels. These additives are often quite expensive, which results in an increase in the overall cost of drilling operations. On the other hand, cementing operation is also crucial for the successful completion of well drilling. Cement is used to fill the gap called annulus between the casing lowered into the well and the formation. The cementing process is applied to the placement of the drill string, to prevent mud leaks, to prevent uncontrolled fluid flow from the formations to the surface through the well, to abandon the wells and to close the formations that are no longer produced. Generally, ordinary portland cement is employed as a binder in the world. Although a very significant amount of cement is produced every year, it is predicted that it will increase even more in the future. A significant amount of CO_2 is released during cement production, which causes a serious environmental concern. In addition, cement production is a costly process as it requires a significant amount of energy.

The aim of the thesis is to develop improved, cost effective and environmentally friendly water-based drilling fluid and cement slurry systems, which have superior rheological and filtration properties and are able to meet the requirements of the drilling operation, using fly ash (FA) and rice husk ash (RHA). An extensive experimental work was conducted to achieve the relevant goal. To this end, several different types of drilling fluid systems were designed using FA and RHA, and their rheological and filtration properties were measured and analyzed at ambient and elevated temperature and potential of differential sticking tendency of the drilling fluid was studied considering the effect of different particle size of FA by grinding in a stirred media mill. Subsequently, the cement used in the cementing operation was initially partially replaced by FA and RHA, then completely replaced by FA by forming geopolymer material to reduce or eliminate the amount of cement required. The performance of the relevant cement slurries has also been analyzed both under ambient conditions and increased temperature as well as when exposed to drilling mud contamination. On the other hand, effect of particle size of FA in both driling fluid, cement and geopolymer slurries was examined by conducting the with the different times of grinding process in a thumbling ball mill. In addition, hydraulic performance of the driling fluids formulated with FA depending on increasing temperature were calculated by considering parameters cutting carrying index, flow behaviour index and minimum annular velocity required to clean bottom of the well efficiently and rheological model analysis of the fluid was performed.

In conclusion, in the thesis, different types of drilling muds with improved hydraulic performance were developed with FA, which is a large amount of industrial waste, and RHA, which also constitutes a large amount of agricultural waste at ambient and elevated temperature. Also, cement and geopolymer with improved rheological and filtration properties were designed by partially changing the amount of cement with FA and RHA and completely replacing cement by FA, respectively. In addition, it was reveal that particle size of fly plays a great role on the rheological and filtration properties of driling fluid, cement and geopolymer slurries and Herschel-Bulkley model provides the estimation of the

rheological parameters of drilling fluid with high accuracy. Consequently, an alternative method was developed for the recycling of FA and RHA, as well as contributing to the reduction of drilling costs and environmental problems with the drilling mud and cement slurries developed in this thesis. Also, with the determined Herschel Bulkley model, more accurate assessment of well hydraulic could be achieved. Finally, it worths to be noted that the new comprehensive findings obtained in this thesis can be used as a guide for future studies.

2022, 129 pages.

Key words: Drilling fluid, cement, geopolymer, fly ash, rice husk ash, rheology, temperature

CONTENTS

LIST OF TABLES

Table **Page**

LIST OF FIGURES

Figure **Page**

1. INTRODUCTION

In the today's world technology is developing and the population is increasing day by day. It is known that the energy consumption increases proportionally with increasing population. The increase in energy consumption is also directly proportional to the development level of the countries. Many energy sources are used to meet the increasing energy need. Today, although the share of alternative energy resources has increased, most of this energy need is met from fossil resources, particularly oil and natural gas. In order to benefit from these resources, high-cost drilling operations have been carried out.

Drilling mud is one of the most important components of the drilling operation and undertakes many critical tasks in the well. Some of the important tasks undertaken by drilling mud are as follows: to clean the well by moving the drilled cuttings to the surface, to prevent the collapse that may occur in the well by keeping the formation pressure in balance, to prevent the drilled cuttings from accumulating at the bottom of the well by keeping the cuttings suspended in case of stoppage, to cool and lubricate the drill string, to prevent corrosion. The flow properties of drilling mud must be adjusted according to the well conditions to fulfill these duties (Bourgoyne, 1991; Caenn, 2011; Rabia, 2001).

It is known that approximately 15 to 18% of the oil drilling cost is directly caused by drilling fluids (Khodja et al., 2010). Therefore, selection of appropriate drilling fluid plays a key role in the success and total cost of drilling operations. Improper rheological properties of drilling fluid may causes serious drilling problems such as inadequate hole cleaning, formation damage, excessive torque and drag, lost circulation, pipe sticking and wellbore instability, which can even lead to well abandonment and cost hundreds of millions dollars.

Cementing is one of the most important operation of drilling and well completion operations an indispensable component in the oil industry to successfully complete wells and put them into production. The main purpose of cement is to provide zonal isolation by filling the space called the annulus between the casing and the formation, as well as preventing mud leaks and uncontrolled flow of fluid from the formations to the surface through the well. The cementing operation is also vital to ensure the stability of the well, avoid contamination of the production zones and continue the production efficiently (Bourgoyne et. al., 1991). Improper cementing operation causes serious operational difficulties, significant environmental problems and high

remedy cost. Therefore, cement is required to have certain properties suitable for well conditions to perform these functions.

It is vital importance that the cement completely fills the space between the casing and the formation, in terms of the well-being to fulfill its functions throughout its life (Azar and Samuel, 2007). The effective and safe filling of the cement prepared on the surface into the well depends on the rheology of the cement. It is desirable that the cement maintain its rheology until it reaches the desired areas. The more it maintains its rheology, the lower will be the pump pressure required to pump the cement from the surface. The rheology of cement slurry determines its pumpability.

Fly ash (FA) is an industrial waste generated by the combustion of coal. Approximately 10% to 15% of hard coal (anthracite) used in thermal power plants and 20% to 50% of lignite coal is produced as ash. 75% to 85% of this ash comes out of the boiler with flue gases and these are called FA. Generally, high efficiency electrofilters are used to retain FA in flue gases (Morrison, 1970). FA has been used in several applications. Construction sector is the leading sector in which FAs are evaluated. In addition, FA is used in various fields such as ceramics, glass, glass-ceramic, zeolite synthesis, agricultural amendment, environmental protection, catalysis and valuable metal recovery (Yao et al., 2015; Blissett and Rowson 2012; Ahmaruzzaman, 2010). The use of FA as a binder is not only economical but also environmentally friendly, so its use is important.

Rice husk is one of the most important by-products of rice production that occurs during the processing of rice and is one of the lignocellulosic substances that can be widely used with its high ash content. In many countries, rice husks are burned industrially. In addition to providing energy, the combustion process enables the production of rice husk ash (RHA), which is a by-product rich in silica and can be used industrially. The RHA is employed several applications such as concrete, steel, ceramic production, brick, activated carbon, insulator, bio-char, detergents and soap, catalysts and energy storage (Prasara and Gheewala, 2017; Pode, 2016; Kumar et al., 2013).

These informations clearly show how effective the drilling fluid and cement properties are on both the success and cost of the drilling operation, as well as FA and RHA are some kind of wastes and have been used in various industries.

2. PROBLEM STATEMENT

Generally, it is desirable that drilling fluid employed is simple and contains a few additives and to be considered that high/optimum performance of drilling fluid is the key/primary issue in applied drilling fluid technology. Thus, the maintenance of the drilling mud and the monitoring of the parameters that need to be followed becomes easier. However, the flow characteristics of the drilling mud, which is in constantly circulation in the well, differ at the entrance and exit of the well. Therefore, a wide variety of drilling fluid additives are mixed into the drilling mud to maintain the flow properties such as viscosity, weight, gel strength and filtration of the drilling mud at the required levels.. For this purpose, weighting agents, viscosifiers, filtration control materials, lubricants, thinners and pH controllers are used (Rabia, 2001; Caenn, et al., 2011).

Table 2.1 shows additives commonly used in water-based drilling fluids. These high cost drilling mud additives increase the drilling costs significantly. Therefore, researchers have currently studied on developing an alternative drilling mud system that is less expensive, environmentally friendly, easy to apply, stable and capable of performing the necessary functions, and how the properties of the drilling mud can be improved.

Generally, ordinary portland cement is employed as a binder in the world and approximately 4 billion tons of cement was produced in 2013 (Statista, 2014). It is estimated that the annual production amount of cement will increase by 25% in the next 10 years. Today, global warming is an important issue and 7% of the CO_2 released worldwide is caused by cement production.. (Malhotra, 1999). Approximately 820 kg of CO_2 is emitted from 1 ton cement production. This released CO_2 is a problem for the environment, cement producers and people. Cement production also requires a significant amount of energy. Therefore, there is a urgent need to use new materials that can be used as a substitute or to reduce the amount of portland cement.

Table 2.1. Additives commonly used in water-based drilling fluids (Yalman et al., 2021a; Modified by Rabia, 2001).

Fluid loss controller	Bentonite, polymers, starches and thinners or deflocculants (PAC, CMC etc.)
Weighting	Barite, haematite, galena, magnetite, siderite
Thinners	Plant tannins, lignitic materials, lignosulfonates, low molecular weight, synthetic, water soluble polymers.
Viscosifiers	Bentonite, xanthan gum, guar gum, synthetic polymers, resins, silicates
Alkalinity and pH control materials	NaOH, KOH, $Ca(OH)_2$, $NaHCO_3$ and $Mg(OH)_2$
Lubricating material	Oil, surfactants, fatty alcohol, graphite, asphalt, gilsonite, and polymer or glass beads
Shale stabilizing materials	Polyacrylics, asphaltic hydrocarbons, potassium and calcium salts, glycols, and certain surfactants and lubricants.
Lost circulation material	Granules, fiber, flake
Emulsifier	Lignosulfonate, lignite, detergent
Special Additivies	Flocculants, defoamers

In the past, FA produced from coal combustion was simply trapped in flue gases and released into the atmosphere. However, due to the increase in industrialization, the production of FA has increased and this situation has started to cause environmental and health problems. Today, more than 65% of the FA produced from coal plants worldwide is dumped in landfills and ash ponds. Moreover, as a result of rice production, an excessive amount of rice husk is produced and 20% of this amount of husk consists of ash. In this context, with the production of 500 million tons of rice, 100 million tons of rice husk comes out and 20 million tons of ash is produced by burning this husk (Malhotra, 1993). Therefore, FA and RHA cause pollution by forming a significant amount of waste.

Although FA and RHA are utilized in many industrial areas, a significant component of them is still untreated due to their excessive production and appears as a serious waste. At this point, there is an urgent need to investigate new and innovative areas where these ashes can be used for their recycling.

3. GAP STATEMENT

Literature study shows that FA and RHA are used in a wide variety of applications, particularly in the construction industry. In addition, a great number of additives are studied by researchers to improve the rheological and filtration properties of drilling fluid systems. However, there

have been limited published data with respect to the use of FA and rice husk in drilling fluid and also these ashes have never been studied in some drilling fluid systems. In addition, although researchers have studied extensively in the construction sector with FA and RHA regarding of cement, especially the investigation of rheological and filtration properties in wellbore cementing has not been studied extensively. To the best of the author knowledge, this thesis is the first attempt to investigate FA and RHA in both drilling fluid systems and borehole cementing operations simultaneously.

4. OBJECTIVES

The objective of the thesis is to develop improved, cost effective and environmentally friendly water-based drilling fluid and cement slurry systems, which have superior rheological and filtration properties and are able to meet the requirements of the drilling operation, using FA and RHA. Thereby, a new application area of FA and RHA will be investigated, as well as the reduction of the design cost of drilling mud and cement slurry, and it will contribute to the reduction of the environmental problem arising from both FA and RHA and cement production. An extensive experimental work was conducted to achieve the relevant goal. To this end, several different types of drilling fluid systems were designed using FA and RHA, and their rheological and filtration properties were measured and analyzed. Subsequently, the cement used in the cementing operation was initially partially replaced by FA and RHA, then completely replaced by FA by forming geopolymer material to reduce or eliminate the amount of cement required. The performance of the relevant cement slurries has also been analyzed both under increased temperature and when exposed to drilling mud contamination.

5. BACKGROUND

5.1. Flow characteristics of drilling fluid

Drilling fluid is defined by American Petroleum Institute (API) as a water, oil or gas based circulation fluid supplemented with different additives used to perform some functions needed in the drilling process. It is desirable that the designed drilling mud be effective in meeting potential drilling problems. Today, thanks to the advenced technological developments in the drilling industry, high performance drilling fluids can be developed in well conditions. It should be noted that the success of the drilling process and majority of drilling costs depend on the performance of the developed fluid and its ability to perform certain functions properly.

The branch of science that studies the flow properties of materials and the deformation of fluids is called rheology (Schramm, 1994). Rheological properties, flow profile, viscosity, well cleaning ability, pressure loss and equivalent circulation density of the drilling fluid can be considered a key in the success of drilling operations as it enables the analysis of well hydraulics in general (Amoco, 1994). In cases where the flow properties of the drilling mud are insufficient, it may cause problems such as well enlargement, low drilling speeds, circulation losses and stuck pipe. It is very important to regularly control and monitor the rheological properties of the drilling mud, both the completion time of the well drilling operation and the drilling cost. At the same time, it provides to take early precautions for some serious drilling problems that may occur and to make direct effective decisions and foresight in the process such as abandoning the well when necessary.

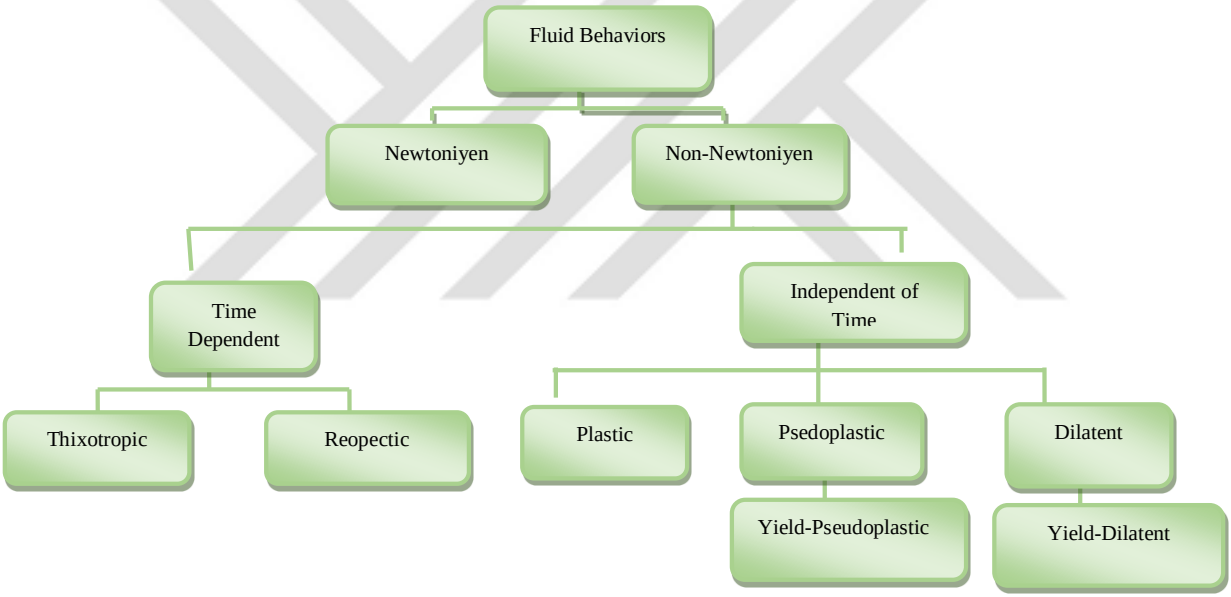

Figure 5.1. Classification of fluids based on rheological behaviour (Derived from Barnes et al., 1989; Avci, 2018).

The shear velocity-shear stress plot is known as the Flow Model, depending on the fluid being tested. Fluids are divided into newtonian and non-newtonian fluids according to the their rheogram profile. The rheological behavior classification and rheogram of fluids were given in Fig.5.1 and Fig.5.2 respectively. Curve representing shear stress versus shear rate relationship is known a flow curve (rheogram), can be see in Fig.5.2, and this relationship is based on the rheological classification of viscous fluids.

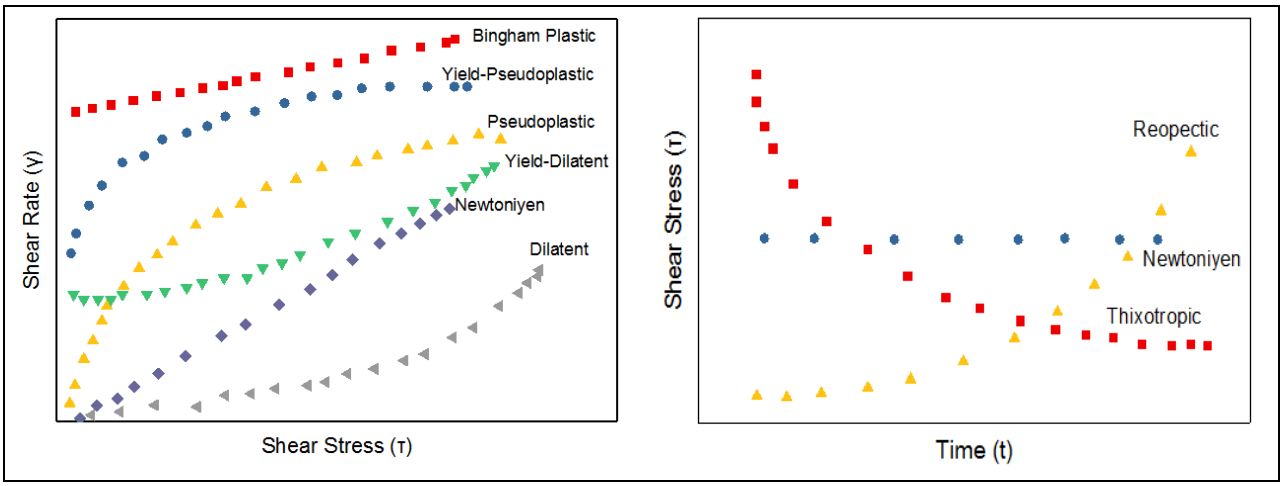

Figure 5.2. Rheogram of fluids (Derived from Barman et al., 2016)

Newtonian Fluids: The fluids in which the relationship between shear stress and shear rate are linear are called newtonian fluids and viscosity is constant for newtonian fluids (Barnes, 1989). Non-Newtonian Fluids: It is the type of fluid in which there is no direct ratio between shear stress and shear rate, or the shear stress-shear rate graph does not start from the origin. The behavior of drilling fluids whose viscosity is not constant at different shear rates are called non-newtonian fluids (Barnes, 1989). As seen in Fig.5.2, bingham plastic, pseudoplastic, yield pseudoplastic, dilatant, yield dilatant are non-newtonian fluid types.

Drilling mud, within the rheological classification given in Figure 5.2, is classified as non-newtonian fluids due to its structure and generally exhibits a non-linear flow curve, although it has a yield stress. With this feature, drilling mud is included in the yield pseudoplastics group of non-newtonian fluids with and shows shear thinning behaviour. In addition, drilling mud exhibits thixotropic behavior as its rheological behavior changes with time as an unstable fluid.
Apparent viscosity: It is the viscosity of the fluid when it is flowing under a certain force or at a certain speed (Rabia, 2001; Caenn, 2011).
Plastic viscosity: It is the component of resistance to flow that occurs due to mechanical friction. This friction occurs between the solids in the mud, between the solids and the surrounding liquid and due to the sliding of the liquid itself (Amoco, 1994; Caenn, 2011).
Yield point: It is the component of resistance to flow that occurs due to the attractive force between particles. This tensile force is due to electric charges on the surfaces of suspended solids in the fluid (Amoco, 1994; Caenn, 2011).
Gel strength: Gel strength is the measurement of the thixotropic properties of a drilling fluid under static conditions. While the force created by the attractive forces is the yield point when

the mud is in motion, the gel strength is explained as the force created by the same forces when the mud is at rest (Amoco, 1994; Caenn, 2011).

Filtration: The filtration and cake properties of drilling mud are inevitable for drilling and well completion operations. In case the hydrostatic pressure of the mud is greater than the formation pressure, while the drilling mud gives the liquid part to the permeable formations, the solid part accumulates on the surface of the permeable formation and forms a mud cake, and this phenomenon is known as filtration. Preferably, it is desired that a thin and impermeable cake forms on the surface of the formation and that the loss of liquid is as low as possible. The filter cake need to be in the interval between 1 to $2/_{32}$" and should never exceed 3" (Rabia, 2001). Thus, it is beneficial in terms of preventing important drilling problems such as pipe sticking and hole instability, as well as preventing the productive formations from being polluted and allowing the well log to be evaluated correctly (Amoco, 1994; Caenn, 2011).

Density: Mud density is one of the most important parameters controlled during drilling operation. The density of the mud highly affects the rate of penetration. Necessary hydrostatic pressure can be controlled by the mud density to ensure the stability of the well by balancing of the formation pressure. Thus, the invasion of undesired formation fluids into the well is prevented. In addition, unnecessarily high mud density should be avoided and the hydrostatic pressure of the drilling mud should be at a level that will not crack the drilled formation (Amoco, 1994; Caenn, 2011).

5.2. Cement and geopolymer

Cement: Cement is defined as a hydraulic binder material obtained by grinding a mixture of natural limestone stones and clay after heating at high temperature (Van Oss and Padovani, 2003). Today, cement is used in a wide range of areas such as mineral exploration and extraction, road, tunnel, ground surveys, oil and natural gas drilling and well completion operations.

Cement raw materials are clay, limestone, marl and gypsum. Limestone is a sedimentary rock. Limestone can be found in nature as a rock composed of calcite and aragonite crystals, or it can be found in the form of double carbonate, that is, dolomite. It has up to 90% calcium carbonate ($CaCO_3$) in its chemical composition (Hewlett and Liska, 2019).

The secondary raw material of cement is clay. The main source of alkalis in cement is also clay components. The main feature of clay minerals is that they contain aluminum oxide (Al_2CO_3) in their chemical composition and are composed of hydrated aluminum silicate.

In the cement production, initially limestone and clay are crushed into size less than 10 centimeters. Then, they are milled to produce fine powder. Crushed and thinned clay and limestone are mixed and loaded into a cylindrical shaped rotary kiln and fired at a temperature of approximately 1400-1500 °C. The product obtained as solid particles is called clinker. Production of clinker process can be seen in Fig.5.3. Then, portland cement is obtained by adding some gypsum (2-3% by volume) to the clinker and grinding it into a very fine powder (Hewlett and Liska, 2019).

While the cement sector constitutes the third largest sector in energy consumption with 7% energy consume, it also constitutes the second largest sector in CO_2 emissions with 27% ((2.2 gigatonnes per year) in 2014. While 60-70% of the CO_2 emission originates from the calcination process of the limestone, which is the process of turning the limestone into lime, the remaining part (30-40%) comes from the combustion of the fuel required for the cement production process (IEA, 2018). In the calcination process, the large amount of CO_2 is formed as a result of the reaction given below. Calcium oxide formed is also known as quicklime and a key ingradient in formation of clinker.

$$CaCO_3 + \text{heat} \rightarrow CaO + CO_2$$

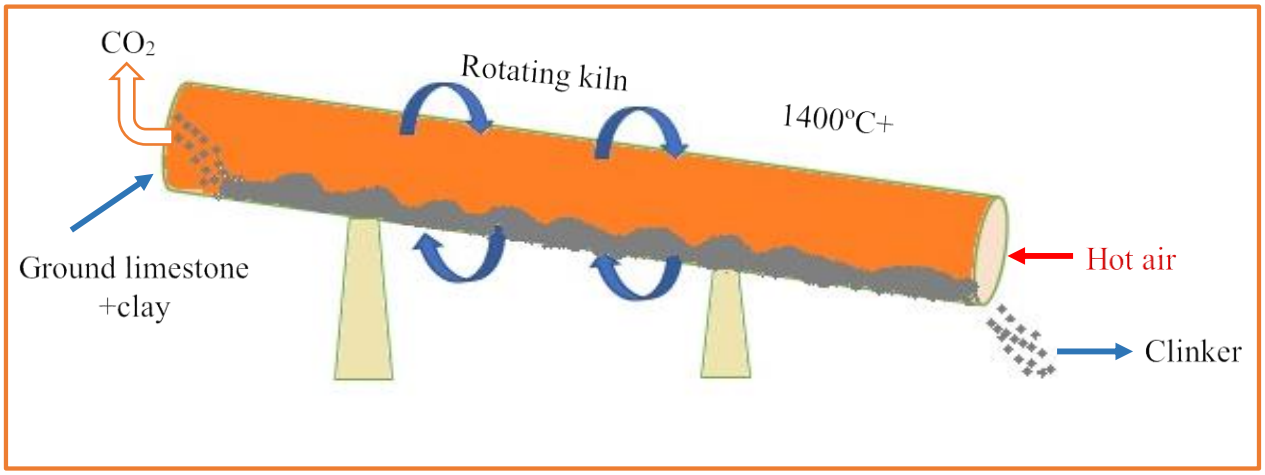

Figure 5.3. Production of clinker process (Modified from Carbon brief- Chatham house, 2018).

Cementing operations are crucial to the successful completion and production of wells in the oil industry. Cement is used in different ways during the drilling and completion of oil, natural gas and geothermal wells. It is used to fill the gap called annulus between the casing lowered into the well and the formation. The cementing process is applied to the placement of the drill string, to prevent mud leaks, to prevent uncontrolled fluid flow from the formations to the surface through the well, to abandon the wells and to close the formations that are no longer produced (Bourgoyne et al., 1991).

It is vital for the cement to completely fill the gap between the casing and the formation, in order to fulfill its functions throughout the life of the well. When cement mixture is mentioned in drilling technique, "powder cement+water" mixture is understood and this mixture is called as cement slurry. The effective and safe filling of the cement slurry prepared on the surface into the well annular space depends on the rheology of the cement slurry and the power of the cementing pump on the surface. It is desired that the cement slurry maintain its fluidity until it reaches the desired areas. The more it retains its fluidity, the lower the pump pressure will be required to pump the cement from the surface. The rheology of the cement determines the pumpability of the cement.

Table 5.1. Depth and temperature ranges where API cements are used with water content (Bourgoyne, 1991; Smith, 1990)

Well cement class	Water content, wt% of well cement	Depth range, m	Temperature range, °F (°C)
A	46	0-1830	80-170 (27-75)
B	46	0-1830	80-170 (27-75)
C	56	0-1830	80-170 (27-75)
D	38	1830-3660	170-260 (75-127)
E	38	1830-4270	170-290 (75-143)
F	38	3050-4880	230-320 (110-160)
G	44	0-2440	80-200 (27-93)
H	38	0-2440	80-200 (27-93)

Ensuring the stability of the cement sheath around casing is vital for zonal isolation and production zones not to be polluted and for the production to continue efficiently. Therefore, the cement should have the desired properties according to the well conditions. Cement types

that have been named by making different classifications can be found in different sources. Cement with different properties can be produced in today's industry, depending on the area of use and need. Portland cement, blast furnace slag cement, high-alumina cement, pozzolanic cement, low-heat cement and sulphate-resisting cement are some of the types of cement used in industry (Medeiros-Junior and Lima, 2016; Korsch and Walther, 2015). Portland cements are the most commonly used cements in drilling (Piklowska, 2017). There are different types of cements suitable for the depth to be drilled and the conditions to be encountered in the well. These types are symbolized by letters such as A, B, C, D, E, G, H. Cements specified by API as Class G and H are chiefly used in the petroleum industry (API, 1997). Therefore, in the thesis, G class of cement was preferred to work on it. The depth and temperature limits of these cement types are standardized by API, as can be seen Table 5.1.

Geopolymer: Recently, climate changes caused by global warming have become a major concern for the worldwide. The main factor causing global warming is the release of greenhouse gases such as carbon dioxide into the atmosphere. On the other hand, cement production require a significant amount of energy and limestone (calcium carbonate), which is the raw material of portland cement, is needed for the production of cement. Moreover, CO_2, which is produced during the production of this material, as outlined, has a share of approximately 6-7% among the elements that cause greenhouse gas effects worldwide. Also, it is predicted that the increase in portland cement demand will be 200% between 2010-2050 (Pacheco-Torgal et al., 2011). This situation has led scientists to research to produce more environmentally friendly and less costly products.

Geopolymerization is an innovative technology that can convert material containing alumina silicate into useful products called geopolymers or inorganic polymers (Yahya et al. 2015).

Geopolymers were formed with binding materials as a result of the activation of alumina silicate materials with alkaline or alkaline silicate solutions at the room conditions (Davidovits, 1989; 1991). Due to its excellent properties, it has become extremely important and many studies have been started in recent years (Cong and Cheng, 2021). Moreover, since the raw materials used are abundant, inexpensive and do not require high temperature in working conditions, its production have attracted great interest of researchers and is seen as an alternative to portland cement. In addition, another advantage is that high performance products can be obtained with

the use of large amounts of industrial waste and toxic gases are not released into the environment during their production. It should be noted that during the production of ordinary portland cement, the amount of CO_2 released to the atmosphere is about 80% higher than the production of geopolymer, which makes geopolymer an environmentally friendly material (Davidovits, 1994) In this way, environmental and economic contributions are provided to the country by using waste products as raw materials in production (Masi et al. 2014).

With the discovery of the concept of geopolymer, the use of geopolymer materials has increased and studies on a new type of binder material alternative to cement, called geopolymers or alkali-active cement, have achieved great interest from researchers and many geopolymer studies have been carried out based on the literature. It has been determined that geopolymers have been prepared using materials such as natural pozzolan, FA, blast furnace slag, calcined kaolin clay and talc.

Geopolymers are low temperature materials obtained from the mixture of sodium silicate, sodium hydroxide and potassium hydroxide solutions of inorganic materials such as FA, slag and metakaolin. FA is a cheap and abundant source of raw materials for geopolymer production. FA obtained as a result of the combustion of coal in thermal power plants contains high levels of silica and alumina. As a result of the reaction of silica and alumina with alkaline solutions, geopolymer production is carried out. Process of the production geopolymer can be seen in Fig.5.4.

Figure 5.4. Production of geopolymer (Modified from Zhuang et al., 2016).

5.3. Fly ash and rice husk ash

FA is fundamentally defined as the solid combustion by-product in thermal power plants coal fired as a result of the burning of coal in the boiler. Fig.5.5 shows the production process of FA. Accordingly, coal is pulverized in coal mills before being fed to be burned to boilers, then these pulverized coal particles are sent to the boiler with fresh air and burned. Coarse particles of ash, which are generated from combustion of coal and are called bottom ash, fall under the boiler and are removed from the system at this point. Ash, which are lighter and finer and called FA, are removed from the boiler with the help of fans together with the combustion gases and kept in the dust holding unit. Dust holding units can be in the form of electrostatic filters or bag filters depending on the plant design.

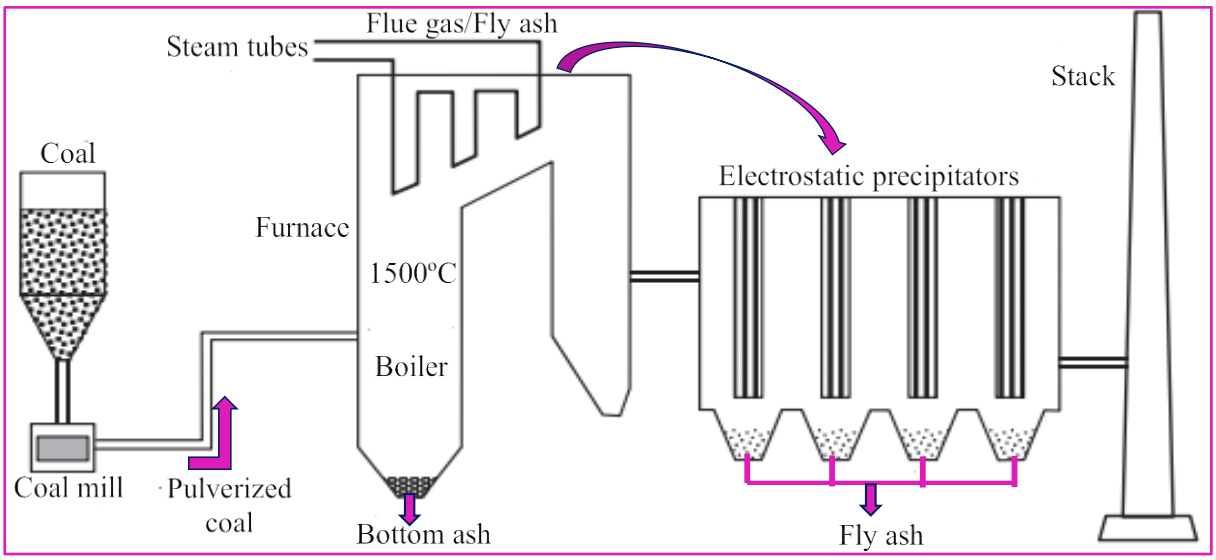

Figure 5.5. Production of FA (Modified from Forum, 2017).

The most obvious common feature of the produced FAs in terms of puzalonic, chemical, physical and mineralogical characteristics is that these properties differ from region to region and can be different even within the same region. This variability is mainly based on the following parameters (Ahmaruzzaman, 2010):

- The type and variability of the coal from which FA is produced,
- The degree of pulverization of the coal before it is burned,
- Boiler type,
- Combustion temperature and other operating parameters,
- Features and operation of ash collection and removal systems,
- Features arising from factors such as additives added to coal for environmental protection and that factors can change over time.

The physical and chemical properties of FA are briefly summarized below:

FA is a dark gray, very fine grained material. The darkness and lightness of its color depend on the coal it is obtained from and its burning properties. It is the unburned carbon in it that gives black color to the FA formed in case of incomplete combustion. FA formed as a result of good combustion is lighter in color than the other (Joshi and Lohita, 1997; Morrison, 1970).

The fineness of the FA primarily depends on the grinding degree of the coal supplied to the boiler, the second factor affecting the fineness is keeping the ashes as far as possible from escaping from the chimney.

When examined in terms of chemical composition, it is seen that FA consists of compounds including SiO_2, Al_2O_3, Fe_2O_3 and MgO. The amount of carbon that can be found in it varies according to the type of coal and the burning process. In addition, some may contain significant amounts of CaO, depending on the type of coal used (Joshi and Lohita, 1997; Morrison, 1970).

In terms of mineralogical and chemical properties, FA consists of hollow and voidless, glassy globules, spongy mineral particles and unburned particles. Si, Al, Ca and S have been available in their chemical structure as the basic element. The matrix of FA mainly consists of alumina silicates and Fe, Mg, Na, K, Ca, Ti with rare earth elements which can be found with them.. Elements such as As, Cd, Ga, Mo, Pb, Se and Zn, which are volatile or form volatile oxides, do not tend to enter the matrix (Yao et al., 2015; Nyale et al., 2014; Neupane and Donahoe, 2013) These elements are collected on the surfaces of the FA in such a way that their concentration is inversely proportional to the grain size.

Although they are not hydraulic binders themselves, they are natural or artificial materials that form binding compounds by reacting with calcium hydroxylde in a humid environment and at normal temperature when finely ground. Pozzolans are used in cement and concrete making, either by grinding together with clinker during cement production or by adding to cement at different rates depending on the structure of the construction site. The use of pozzolans gives cement and concrete many good properties apart from economy. In other words, cements with pozzolan can be called portland cements with corrected errors. FAs are also materials that can

be used as pozzolans due to their pozzolanic properties (Joshi and Lohita, 1997; Morrison, 1970).

Research on FA has gained great intensity in recent years. In the early days, studies on the general structure and properties of FA and its possibilities of use were developed over time with analyzes carried out in the laboratory and in the field. As a result, it has been revealed that the use of FA in the field of construction, especially in road construction, will provide a solution to the problem of removing this material, which is formed as a waste material at large amount in thermal power plants.. As a result of the studies carried out later, it has been revealed that the FA can be used in many applications given in Fig.5.6.

Referring to Fig.5.6, although FA is used in many applications, it is seen that a significant amount of FA have been left untreated and comes out as waste. This situation clearly shows that there is an urgent need to develop new methods of recycling of FA to convert the waste of the FA to value-added raw material.

Rice is an important food item for the world's population. As a result of rice production, excessive amount of rice husk emerges as a waste material and the rice husk cause to environmental pollution by covering around the regions where rice production is high (Prasara and Gheewala, 2017).

Rice husk is also an important by-product of rice milling and produced in excessive amount every year around the world. During the separation of shell, which are the wastes of rice production, from the grains, two husk are formed, as can be seen in Fig.5.7a. First shell; it is in the form of a thin membrane surrounding the rice grain and this is called bran. It is used as animal feed because it is rich in nutrients. The second shell is; it is the outermost husk of a rice grain. It is harder than the inner shell and this shell is called husk or hull. The husk contains silica and carbon. The silica in its structure forms the skeleton of the shells (Prasara and Gheewala, 2017).

RHA is obtained by burning of rice husk. Depending on the use of the ash, the burning method of the shell also changes. If the shell is used as fuel, it is not necessary to keep the combustion

conditions constant. However, when it is desired to be used as a building material (pozzolan), burning the shells and cooling the ash should be carried out under certain conditions.

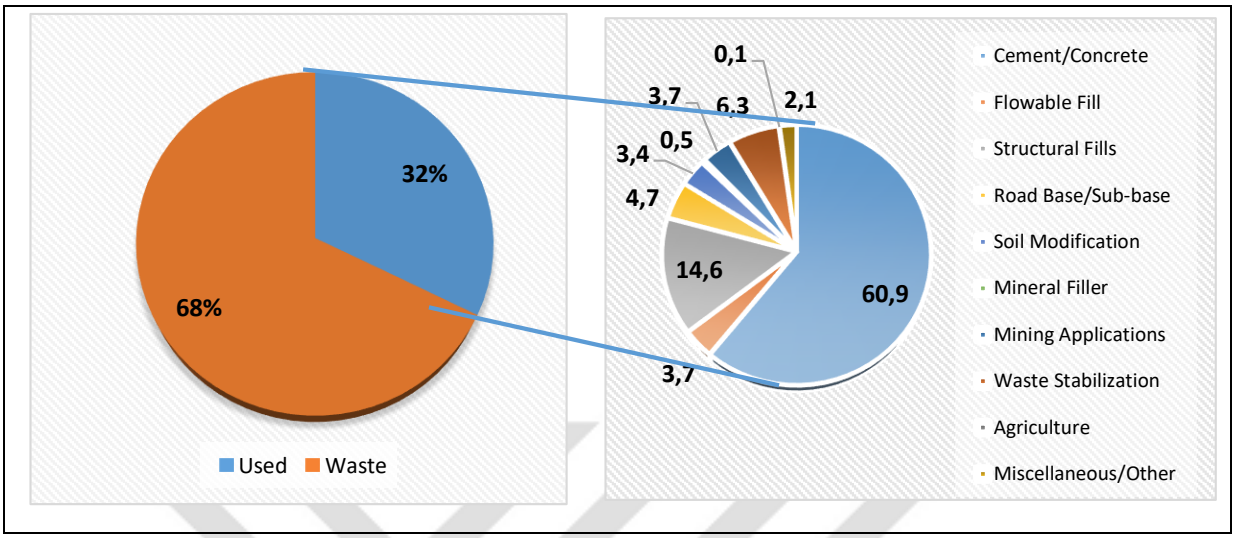

Figure 5.6. FA uses and waste (a) usage areas of FA (%) (b) Source:(Derived from USA Technical report, 2001).

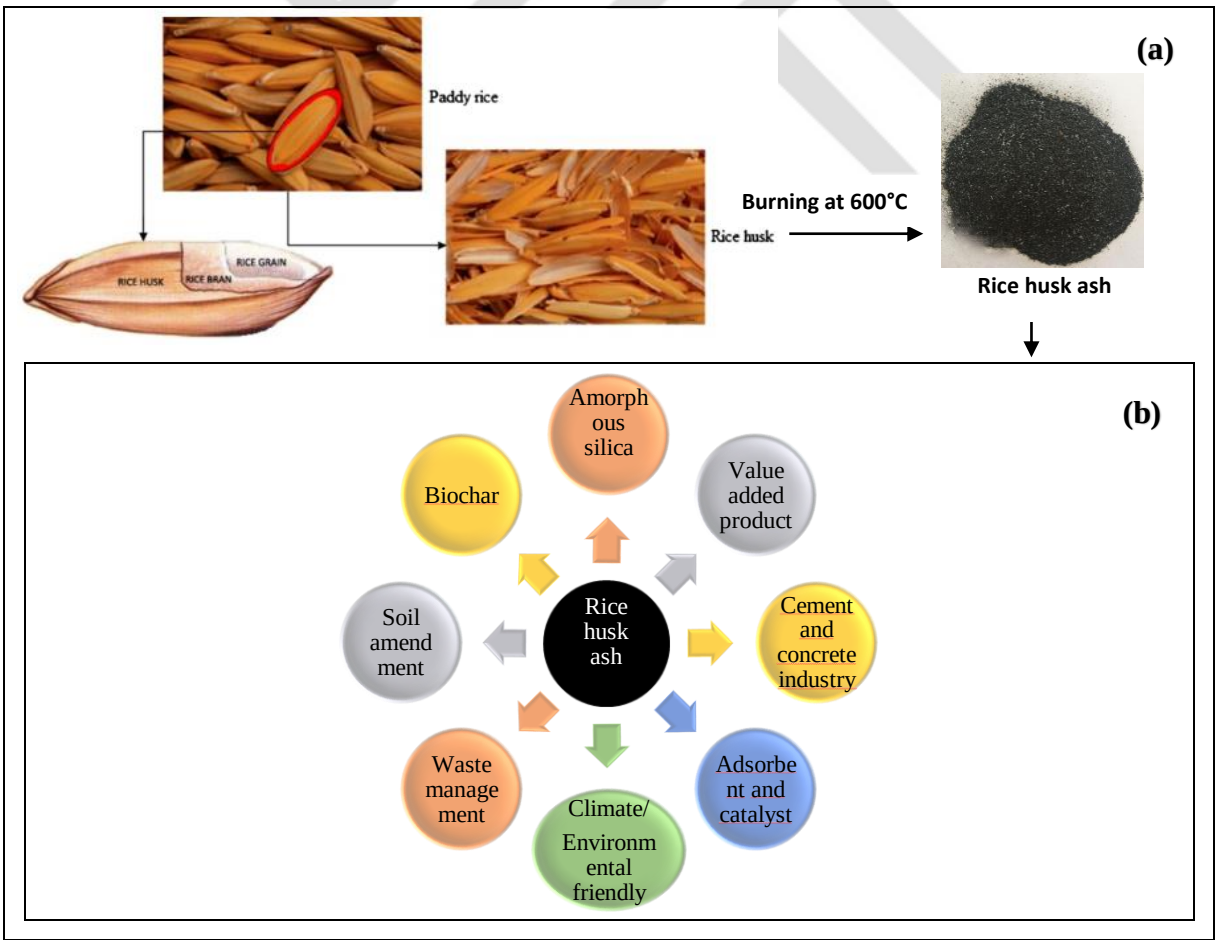

Figure 5.7. Production of RHA (a) and overview of its applications (b) (adapted from Pode, 2016; Moayedi et al., 2019 Fernandes et al., 2016; Buggenhout et al., 2013; Kieling et al., 2009).

Large amount of rice husk and RHA are used in industry around the world. As a result, there are many possible industrial applications of RHA (Soltani, et al., 2015). Rice husk is seen as a good alternative to traditional products as it is a renewable, biodegradable, low cost, easily available resource. Moreover, RHA is inexpensive, biodegradable, and available in abundance around the world. In developed countries, such products are seen as a new resource, not as waste. Therefore, such materials can be used for environmental protection and for the design of new materials. The main usage areas of RHA were given in the Fig.5.7b.

6. MATERIAL AND METHOD

In this section, the tools, equipment, materials used in the experiments, the computer program used in the theoretical study and the methods used in the experimental and theoretical studies are explained.

6.1. Material

In this thesis, Brown Coal Fly Ash (BFA) (Class F), Lignite Fly Ash (LFA) and Rice Husk Ash (RHA) were used as the main materials.

FA colour may from tan to dark gray according to the burning coal type and the way it is burned. The brownish color of LFA can be attributed the high iron content within whereas the grayish colour of BFA can be associated with high unburned carbon content. On the other hand, the color of RHA is dark gray, which can be seen in Fig.6.1.

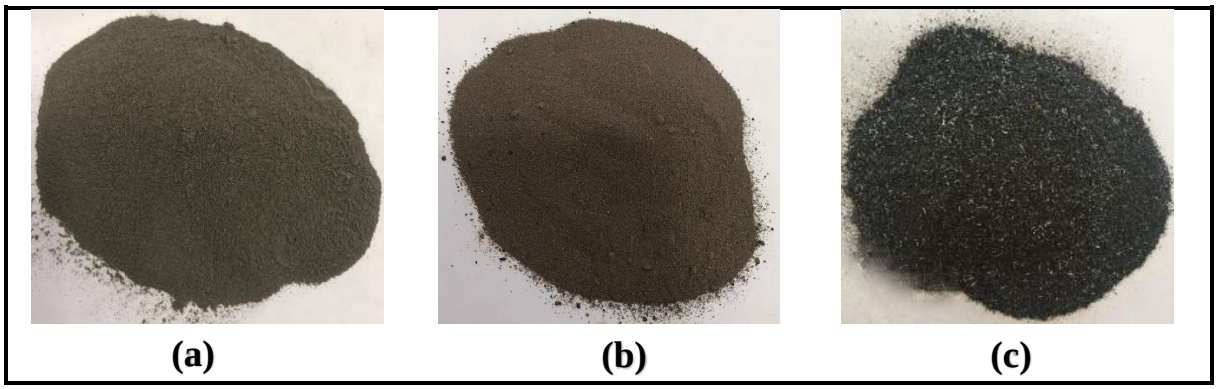

Figure 6.1. FAs (brown coal (a), lignite (b)) and RHA (c) samples used in the thesis

Chemical compositions of the materials were measured with a Rigaku Supermini 200 type XRF (X-ray fluorescence) spectrometer and were given in Table 6.1.

Table 6.1. The chemical composition (as oxides) of FAs and RHA

Oxides	BFA (wt.%)	LFA (wt.%)	RHA (wt.%)
SiO_2	58.8	39.8	97.3
Al_2O_3	24.0	14.0	0.2
MgO	1.17	3.41	0.51
CaO	1.92	12.1	0.65
Na_2O	0.91	0.54	0.13
K_2O	1.53	1.61	2.68
Fe_2O_3	5.51	11.2	0.14
MnO	0.032	0.176	0.195
TiO_2	0.605	0.495	0.011
P_2O_5	0.053	0.346	0.429

Samples	D_{10}, µm	D_{50}, µm	D_{90}, µm	SSA, cm^2/cm^3
RHA	44.53	102.39	218.45	831.47
BFA	21.28	84.11	187.89	1191.2
LFA	13.36	59.82	175.19	1799.3

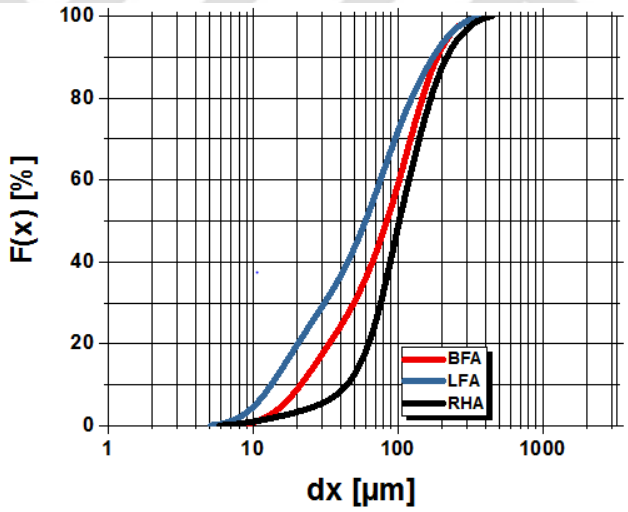

Figure 6.2. Particle size distribution curve of the studied FAs and RHA

Fly ash is mainly classified in two main categories according to American Society for Testing Materials (ASTM-C618, 2005). FA with a total composition of SiO_2, Al_2O_3 and Fe_2O_3 greater than 70% and the content of CaO is less than Fe_2O_3 is determined as type of Class F. Whereas, FA with a total composition of SiO_2, Al_2O_3, and Fe_2O_3 is between 50% and 70% and the content of CaO is greater than Fe_2O_3, is defined as Class C type. Results observed in Table 4.3 shows that the total composition of SiO_2, Al_2O_3 and Fe_2O_3 is 88.31% and also the percentage of CaO, which is 1.92%, is less than that of Fe_2O_3, which is 5.51% for BFA, while the total composition of SiO_2, Al_2O_3 and Fe_2O_3 is 65% and also the content of CaO, which is 12.1%, is higher than

that of Fe_2O_3, which is 11.2% for LFA. Therefore, the type of BFA and LFA used in this study was determined as Class F and Class C, respectively. More than 97% of the RHA consists of SiO_2.

Particle size distributions of the raw materials were measured with a a HORIBA LA-950V2 laser diffraction particle size analyser and results were presented in Fig.6.2. With a laser sizer software through the particle size distribution data, specific surface areas (SSA) of the materials were calculated. Moreover, morphologies of the materials were identified with LeO EVO 40 Scanning Electron Microscope (SEM) and EOL 8600 Superprobe type microscope and characterization results were presented in Fig.12.1-12.6 given in Appendix-A. Also, Fourier-transform infrared spectroscopy (FTIR) and X-Ray Diffraction (XRD) of the FAs and RHA were performed with Perkin Elmer Spectrum Two and X-ray powder diffraction using Rigaku Miniflex 600 with Cu Kα (40 kV, 15 mA, $\lambda = 1.54050$ Å) radiation, respectively.

6.2. Method

In this thesis, initially, BFA, and LFA was obtained from 900 MW power plant of Tiszaújváros-Hungary and 950 MW Mátra Power Station Visonta-Hungary, respectively. On the other hand, RHA was supplied from a food company of Turkey (Edirne). The RHA was obtained by burning rice husk under 600 °C.

6.2.1. Development of drilling fluids: For the development of water-based drilling muds in both different compositions and type as well as cement and geopolymer slurries were prepared based on API standards in order to investigate both a new application area for FA and rice husk and to improve the rheological characteristics and reduce differential pressure pipe sticking tendency of the drilling fluid. In this context, gypsum/polymer driling fluid, spud mud, KCl water based, shale inhibitor mud, bentonite mud with additive and barite weighted bentonite mud types, portland cement and FA based geopolymer were addressed.

Initially, field gypsum/polymer (inhibitive water based driling fluid) was obtained from an oil well driling and its composition can be seen in Table 6.2. Then, spud mud which consists only of bentonite and water was formulated whose composition was given in Table 6.3. The mud systems were designed both in absence and presence of two different type of FA, which are BFA and LFA 1.0, 3.0 and 5.0 (wt%) concentration of FAs were introduced into the

gypsum/polymer and spud mud and suspension formed was mixed using a five-spindle multi-mixer (model 9B) for 10 minutes to ensure a homogeneous mixture. Finally, a total of 14 mud samples were prepared, 7 of each from gypsum/polymer mud and spud mud.

Table 6.2. Formulation of Gypsum/Polymer drilling mud

Additives	Mass concentration (g/l)
Ca^{++} provider/Inhibitor	25
Viscosifier	30
Bactericide	1
Defoamer	1
Fluid-loss control-1	4
Fluid-loss control-2	2
Viscosifier	1
Corrosion inhibitor	1
Lubricant	5
Alkalinity control	0.5

Table 6.3. Formulation of spud mud

Bentonite (g)	Water (mL)
22.5	350

Rheological and filtration properties of the systems were measured and results were compared with the reference drilling fluid (without FA). At the end of this investigation, the effectiveness of FA in drilling mud was investigated and how different chemical structure of FA affects drilling mud was also revealed. The steps followed for gypsum/polymer and spud mud can be seen in Fig.6.3 and Fig.6.4, respectively.

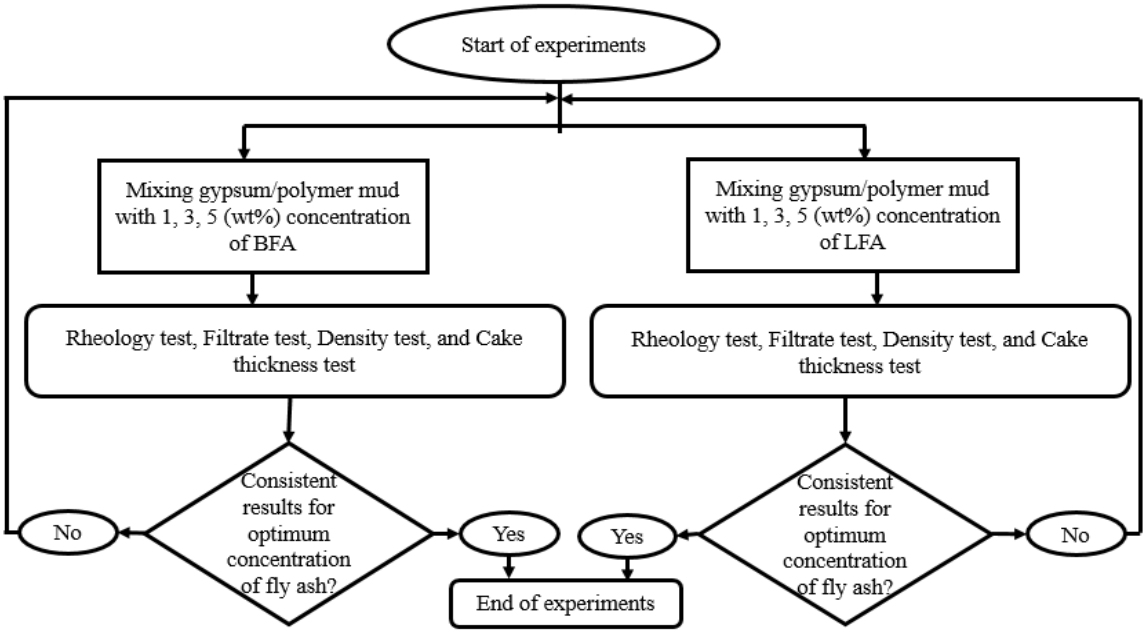

Figure 6.3. Flowchart for gypsum/polymer

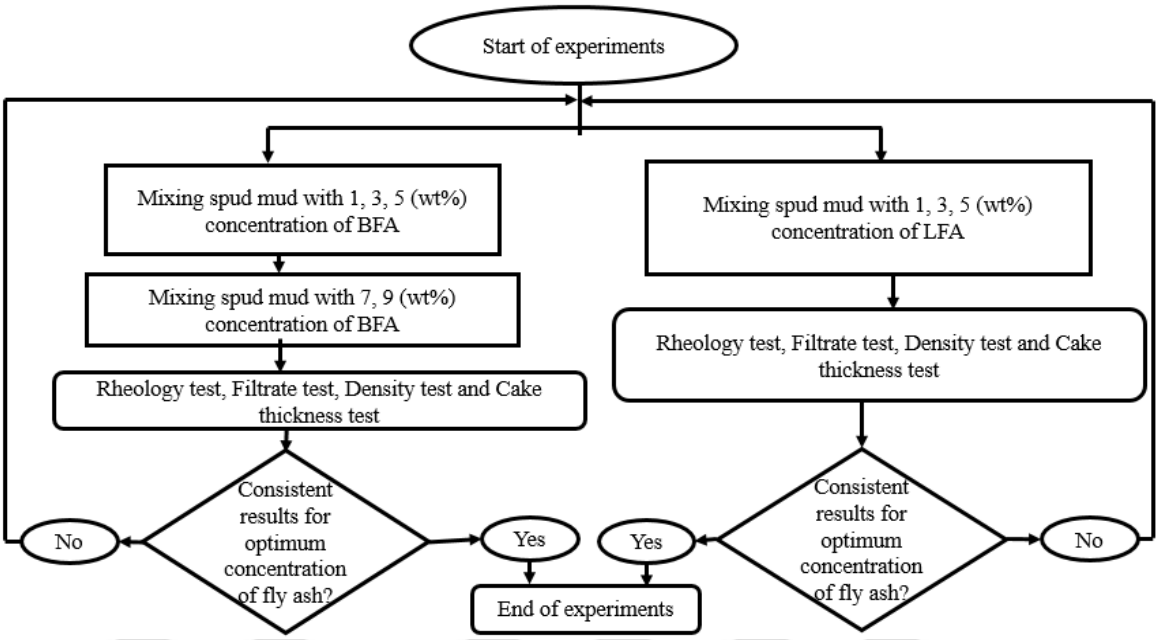

Figure 6.4. Flowchart for spud mud

After this investigation, an attemp was made to develop an improved inhibitive driling fluid system with FA and RHA. To this end, firstly, optimum concentration of FA was determined based on KCl water based drilling fluid whose composition given in Table 6.4.

Table 6.4. Formulation of KCl water based drilling mud

Additives	Concentration (g/l)
Alkalinity Controller	0.5
Viscosifier-1	30
Inhibitor	25
Bactericide	1
Defoamer	1
Secondary fluid loss controller	4
Viscosifier-2	1
Corrosion inhibitor	1
Viscosifier-3	2
Lubricant	5

The mud system was incorporated with BFA in the range of 1.0, 3.0, 5.0, 7.0 and 9.0 (wt%) content. Optimum concentration of FA was determined from this mud analysis based on their rheological and filration properties. Subsequently, determination of optimum particle size of FA was studied on shale inhibitor mud with 30 minutes, 60 minutes and 120 minutes ground FAs as well as sieved FA. The grinding process was perfomed in dry mode with a tumbling laboratory ball mill that was given in Fig.6.5. Composition of shale inhibitor mud was shown in Table 6.5 and further increasing concentration of FA (7 wt%, 9 wt%, 12.5 wt% and 15 wt%) was investigated in the mud.

Table 6.5. Formulation of shale inhibitor mud

Additives	Concentration (g/l)
Bactericide	0.5 – 1.0
Ionic Inhibition	35 – 40
Chloride-Free Ionic Inhibition	5 – 10
Rheology modifier	2.5 – 3.0
Fluid Loss Controller	10.0 – 12.0
Shale Inhibition	20.0 – 25.0
Density/Bridging	40.0 – 50.0
Density/Bridging	40.0 – 70.0
Density/Bridging	40.0 – 70.0
Corrosion Inhibition	2.0 – 3.0
Oxygen Scavenger	0.5 – 1.0

Figure 6.5. Tumbling laboratory ball mill

Moreover, optimum concentration of RHA was also studied in the shale inhibitor mud by employing RHA with 2 wt%, 4 wt%, 7 wt%, 9 wt% and 12.5 wt% dosages. Flow chart for this investigation and particle size distribution of raw and ground forms of FA and RHA was presented in Fig.6.6 and Fig.6.7, respectively.

Behaviour of the shale inhibitor mud with 7 wt%, 9 wt%, 12.5 wt% and 15 wt% concentration of FA was investigated under increasing temperature (30°C, 40°C and 50°C) to simulate bottom hole conditions. Drilling performance of the systems was analyzed based on cutting carrying index, flow behaviour index, minimum anular velocity required to clean bottom of the well efficiently.

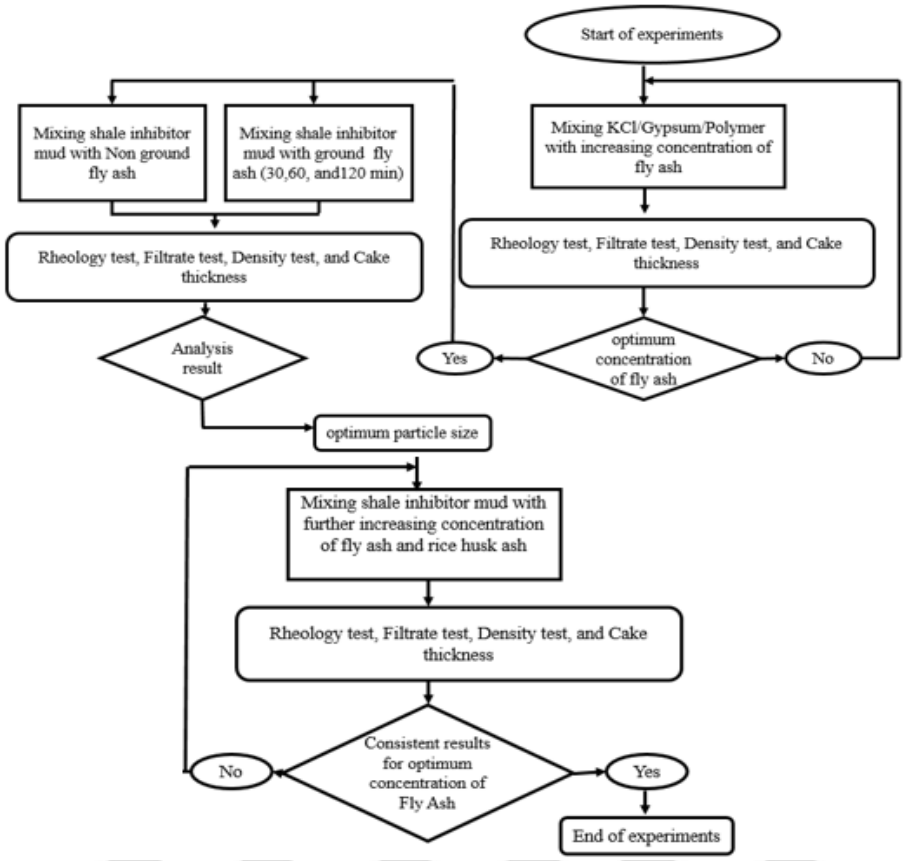

Figure 6.6. Flowchart of the experimental analysis conducted for KCl water based and shale inhibitor mud (Adapted from Yalman et al., 2022a)

Samples	D_{10}, µm	D_{50}, µm	D_{90}, µm	SSA, cm^2/cm^3
RHA	44.53	102.39	218.45	831.47
Sieved FA	21.25	67.89	117.90	1349
30 min. ground FA	7.26	18.25	48.74	4242.9
60 min. ground FA	5.61	13.75	28.90	5687.4
120 min. ground FA	3.46	9.38	17.61	9814.2

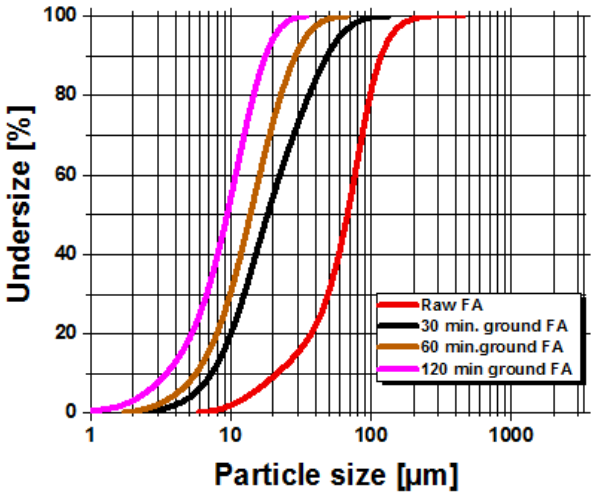

Figure 6.7. Effect of dry mode grinding on particle size distibution of FA (Yalman et al., 2022a).

Further different mud compositions were studied for a better understanding of effectiveness of FA and RHA in the muds. Five fresh water-based mud systems with bentonite, water, XG, CMC and FA based on specific concentrations whose formulation can be seen in Table 6.6 at drilling laboratory were prepared. For the first mud system (spud mud), after water weighted (350 cc) pouring into the Hamilton beach mixing cup, bentonite (6.4 wt%) was added and stirred for 20 minutes under stirring condition. Subsequently, XG (0.5 g) and CMC (1 g) were added into the mixing cup and stirring the mixture for 5 minutes sequentially and the mixture was rested for 24 hours before using it in the tests to ensure exact hydration of bentonite. Rheological and filtration properties of this mud system were measured and used as benchmark fluid for evaluation of performance of FA. Afterwards, desired concentrations of FA ranging from 1 wt% to 5 wt% were added to the mud system and continued to mixed by the mixer for 10 minutes until homogeneity to monitor change in flow behavior of the water-based mud and determine optimum concentration of FA by analyzing rheological reading (plastic viscosity, apparent viscosity), gel strength, density, fluid loss and cake thickness and comparing the benchmark fluid.

Table 6.6. Formulations of bentonite mud with additives

	Bentonite (g)	Water (mL)	XG (g)	CMC (g)
1	22.5	350	-	-
2	22.5 (6.4%)	350	0.5	1
3	28 (8%)	350	0.5	1
4	22.5	350	0.80	1
5	22.5	350	0.80	1.3

In the second step, same process was repeated by increasing bentonite concentration from 6.4 wt% to 8 wt%. In addition, first and second mud systems were rested for 48 and 72 hours at room temperature in absence and presence of optimum concentration of FA determined in first step for a better understanding of performance of FA based on different aging time by comparing first mud for 24 hours aging time and measuring rheological reading (plastic viscosity, apparent viscosity, yield point), gel strength, density, fluid loss and cake thickness. In third step, a mud system was developed in the same manner containing higher XG concentration (0.8 g) compared to the first and second mud systems resting for 24 hours. In the fourth step, a mud system was also developed in the same manner containing higher CMC concentration (1.3 g). Thereafter, optimum concentration of FA found in the first step was also introduced into the mud and stirring was continued again up to a homogeneous suspension was obtained. Plastic viscosity, apparent viscosity, yield point, gel strength, density, fluid loss and cake thickness of the muds were measured and compared with the benchmark fluid. It should

be noted that the second and third mud systems were formulated to further analyze of feasibility of FA at mud system with different composition. Formulation and code of the developed water-based muds were shown in Table 6.7 and flowchart of the part was given in Fig.6.8.

Table 6.7. Compositions and codes of the formulated muds at various conditions

	Composition					
Mud system	Water (cc)	Bentonite (g)	XG (g)	CMC (g)	FA (wt%)	Aging time (hour)
B1-24	350	22.5 (6.4 wt%)	0.5	1	-	24
B1-48	350	22.5 (6.4 wt%)	0.5	1	-	48
B1-72	350	22.5 (6.4 wt%)	0.5	1	-	72
B2-24	350	28 (8 wt%)	0.5	1	-	24
B2-48	350	28 (8 wt%)	0.5	1	-	48
B2-72	350	28 (8 wt%)	0.5	1	-	72
XGM	350	22.5 (6.4 wt%)	0.8	1	-	24
CMCM	350	22.5 (6.4 wt%)	0.5	1.3	-	24
B1-F4-24	350	22.5 (6.4 wt%)	0.5	1	4	24
B1-F4-48	350	22.5 (6.4 wt%)	0.5	1	4	48
B1-F4-72	350	22.5 (6.4 wt%)	0.5	1	4	72
B2-F4-24	350	28 (8 wt%)	0.5	1	4	24
B2-F4-48	350	28 (8 wt%)	0.5	1	4	48
B2-F4-72	350	28 (8 wt%)	0.5	1	4	72
XGM-F4	350	22.5 (6.4 wt%)	0.8	1	4	24
CMCM	350	22.5 (6.4 wt%)	0.5	1.3	4	24

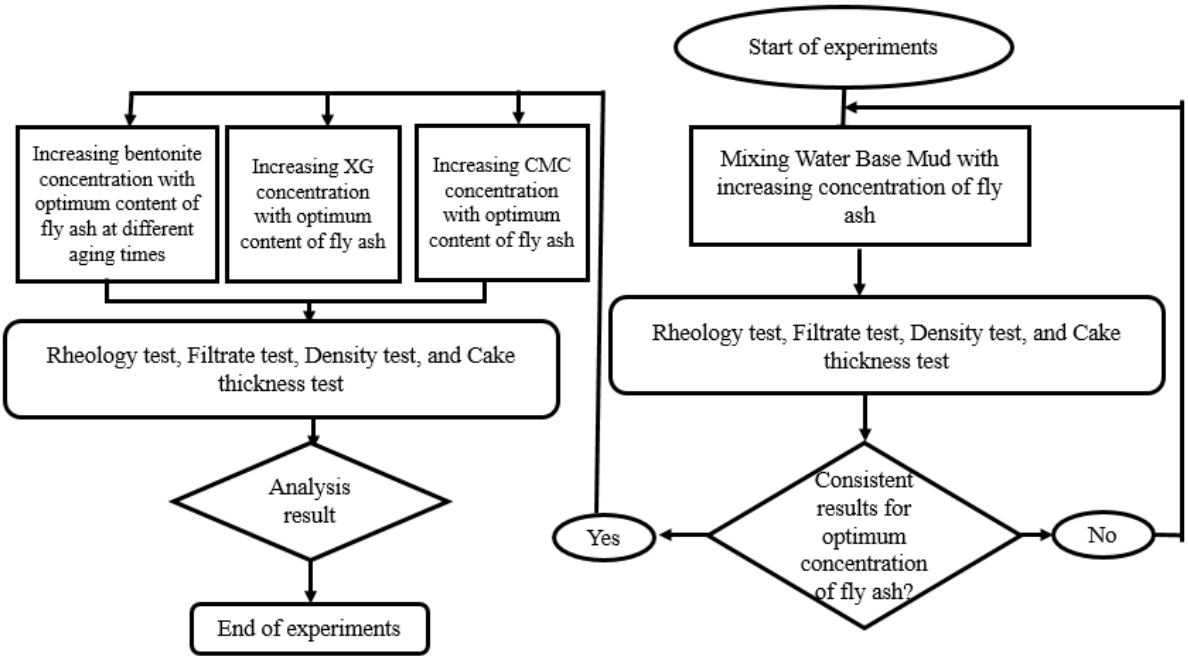

Figure 6.8. Flowchart of the experimental process for various conditions

The use of RHA in bentonite mud with additives was also investigated in the thesis. Different concentrations of RHA were introduced to the bentonite mud, the composition of which is given in Table 6.8, and its effect on the properties of the drilling mud was determined. To this end, firstly, reference mud without RHA was prepared by considering API standards. In this context, bentonite was mixed with fresh water with a drilling fluid mixer for 20 minutes until it had a homogeneous appearance, and then XG and CMC additives were added sequentially to prevent agglomeration, and mixed for 5 minutes each additive. Thereby, 7 drilling mud samples were prepared by adding various concentration of RHA (2, 4, 7, 9, 12.5 and 15 (wt%)) to the reference drilling fluid. In addition, the prepared drilling mud samples were kept at room temperature for 24 hours in order to fully hydrate the bentonite. Then, the rheological and filtration properties of the formulated drilling muds were measured at room temperature. In addition, the performance of RHA on wellbore hydraulics was evaluated by considering the cutting carrying index, minimum annular velocity needed for the well cleaning efficiently and flow behavior index parameters. Followed steps were given in Fig.6.9.

Table 6.8. Formulation of water based drilling mud for RHA

Additives	Compositions
Bentonite (g)	22.5 (6.4%)
Water (mL)	350
XG (g)	0.5
CMC (g)	1.0

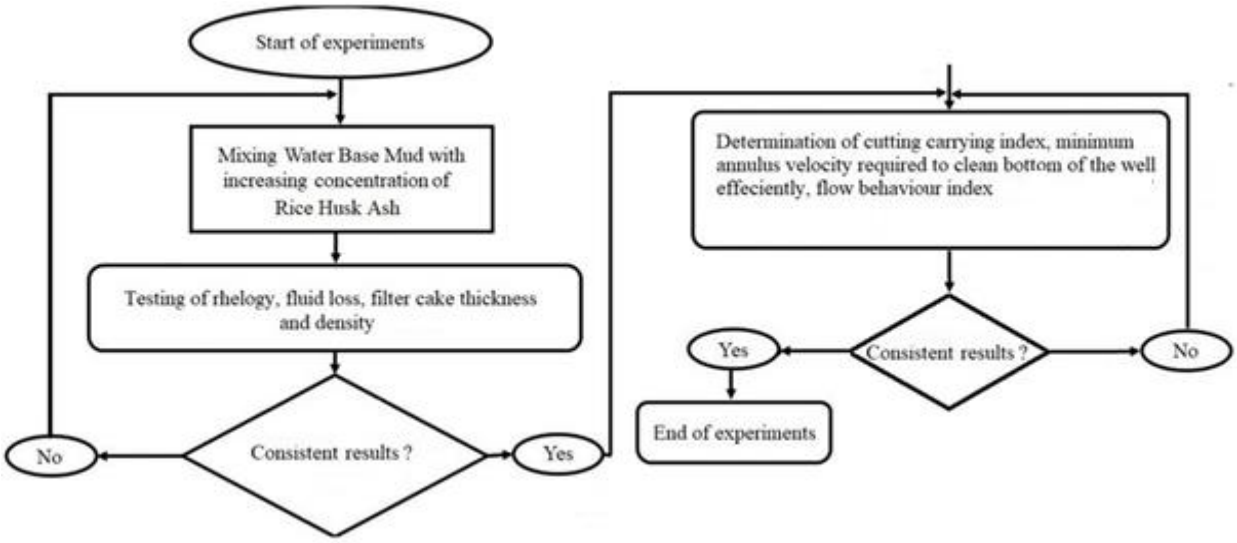

Figure 6.9. Flow diagram for performing study of RHA (Yalman et al., 2021b).

The method given in the literature was followed to evaluate the suitability of the rheological characteristics and the performance of the driling fluids with RHA. Cutting carrying capacity (CCI) of the drilling fluid was considered as a criterion for the assessment. CCI of the drilling fluid can vary depending on three controllable parameters which are average velocity of the fluid at the annulus, driling fluid viscosity (viscosity of the fluid defined by the power law rheology model, (K)) and driling fluid density and is defined as the ratio of the product of these three parameters to the value of 400.000 and is expressed in Eq. (6.1) below (Bourgoyne, 1991).

$$\mathrm{CCI} = \frac{Va\rho_{\mathrm{m}}\mathrm{K}}{400000} \tag{6.1}$$

CCI: Cutting carrying index, non-dimensional

Va: Annular velocity of the fluid, ft min

ρm: Density of driling fluid, ppg

K: Power law fluid viscosity index, cp

CCI value should be 1.0 or higher for adequate well cleaning. Based on the dial readings of the fluid at 600 and 300 rpm, parameters of power law fluid viscosity index (K) and flow behavior index (n) can be calculated by Eq. (6.3) and the by Eq. (6.2), respectively.

$$\mathrm{n} = 3.32\log\frac{\theta_{600}}{\theta_{300}} \tag{6.2}$$

$$\mathrm{K} = \frac{510\theta_{300}}{511^{\mathrm{n}}} \tag{6.3}$$

n : Power law fluid behavior index, dimensionless

θ_{600} : 600 rpm dial reading of fluid in viscometer, lb/100ft^2

θ_{300} : 300 rpm dial reading of fluid in viscometer, lb/100ft^2

K : Power law fluid viscosity index, cp

The mud formulation presented in Table 6.9 was used for the differential sticking tendency analysis. In this investigation, effect of particle size of FA was analyzed based on raw FA, sieved FA and 120 minutes ground FA. The ground FA was produced by stirred media mill that is given Fig.6.10 for 2 hours in wet mode. After the completion of grinding, the FA was left to dry for 72 hours. Differences between in particle size of FAs can be seen in Fig.6.11. Magnitude of mean partice size of FA (d_{50}) decreased from 84.110 μm to 0.270 μm at the end of grinding

process. After the grinding and sieving process, different concentrations of FA with the different forms of particle size were introduced to the drilling fluid system and sticking coefficent of the fluids was calculated with the following formula:

$$K_{SC} = \frac{0.001 * \text{average torque reading}}{\text{stuck cake Radius}^3} \quad (6.4)$$

Table 6.9. Formulation of barite weighted bentonite mud

Bentonite (g)	Water (mL)	CMC (g)	XG (g)	Barite (g)	Density (ppg)
25.71	400	0.6	0.5	131.42	10.2

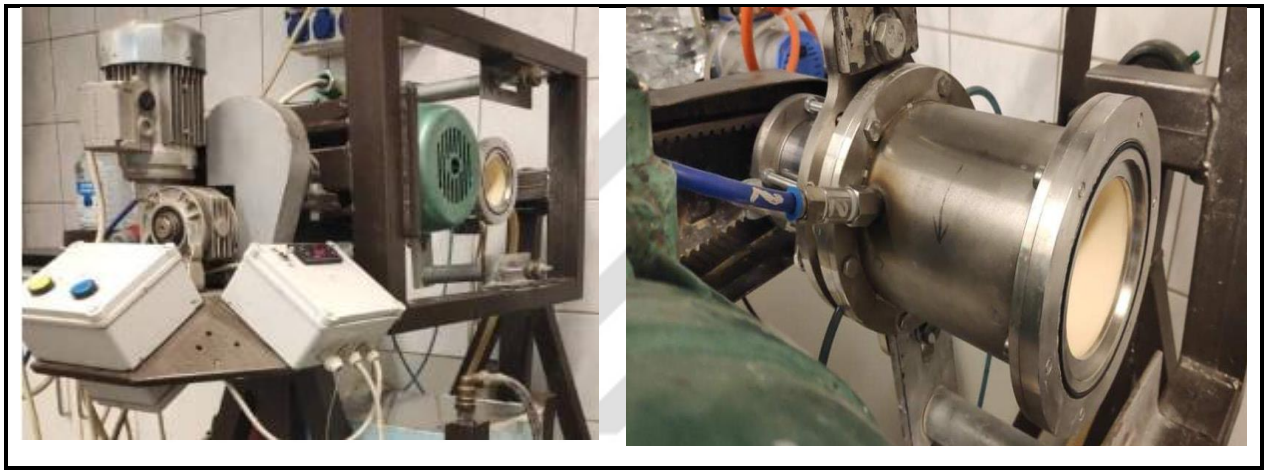

Figure 6.10. Stirred media mill

Sample	d10 [µm]	d50 [µm]	d90 [µm]	SSA [cm^2/cm^3]
Raw FA	21.280	84.110	187.890	1191
Sieved FA	21.257	67.893	117.907	1349
Ground FA	0.122	0.270	0.8783	257230

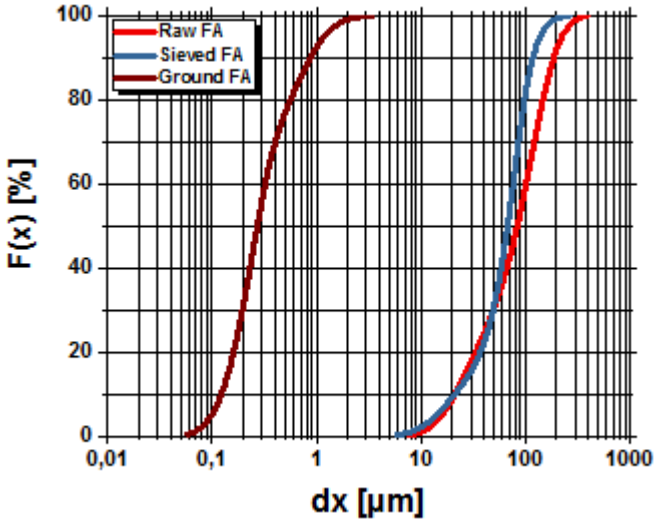

Figure 6.11. Effect of wet mode grinding on particle size distributions of FAs (Yalman et al., 2022b)

6.2.2. Development of cement slurry: In the thesis, portland cement slurry was prepared in ambient conditions according to API standards as a reference slurry in the development of cement slurry. In this context, distilled water was put into the cement blender and then cement powder was added and mixed at low speed for 15 seconds and then mixed at high speed for 35 seconds. Thus, portland cement slurry was prepared and its composition was given in Table 6.10.

Table 6.10. Formulation of portland cement slurry

Products	Mass (percent by weight of cement BWOC)
Class G Cement	100
Distilled Water	44

In the cement part, firstly optimum particle size of FA was determined by grinding FA that was produced with a thumbling laboratory ball mill given in Fig.6.5 for 30 minutes, 60 minutes and 120 minutes. Sieved FA obtained by using 106 μm sieve was also used in particle size determination. After grinding and sieving of FA, cement slurries were prepared. In the preparation of cement systems, cement amount (wt) was replaced by 30% with sieved and ground FAs by keeping the solid/water ratio constant. Optimum particle size of FA was determined of by analyzing density, rheology and filtration results of the prepared cement combination. Code of systems developed in the determination of optimum particle size of FA in cement was given in Table 6.11. After determination of the optimum particle size of FA, cement amount was replaced with 10%, 15%, 20%, 30% of FA by weight of cement with the condition of keeping solid/water ratio constant. Optimum percentage of FA could be substitue of cement was determined considering density, rheology and filtration results of the samples. After the determination of optimum percentage of FA cement was further replaced with 15% RHA by weight of cement.

Cement slurry and mud compatibility tests: Behaviour of the these combinations was investigated under 5% and 10% (by weight of cement) mud loading contamination, ambient temperature, elevated temperatures and constant temperatures. The mud introduced the cement is a gypsum/polymer water based drilling mud and obtained from a driling well. Composition of the mud was presented in the Table 6.12. Formulated all combinations were coded explanations of the codes were given in Table 6.13. Conducted experimantal steps were given in Fig.6.12.

Table 6.11. Code of systems developed in the determination of optimum particle size of FA in cement

P1F30-S	Replacement cement by 30% sieved FA
P1F30G-1	Replacement cement by 30 minutes ground FAwith 30%
P1F30G-2	Replacement cement by 60 minutes ground FA with 30%

Table 6.12. Composition of the driling fluid used in contamination

Additives	Mass concentration (g/l)
Biocide	1
Defoamer	1
Alkalinity	1
Filtrate reducer	7
Viscosifier	2
Lubricant	20
Ca++ source	25
Viscosifier	1
Filtrate reducer	3
Corrosion inhibitor	1
LCM/Bridging/Weighting	30

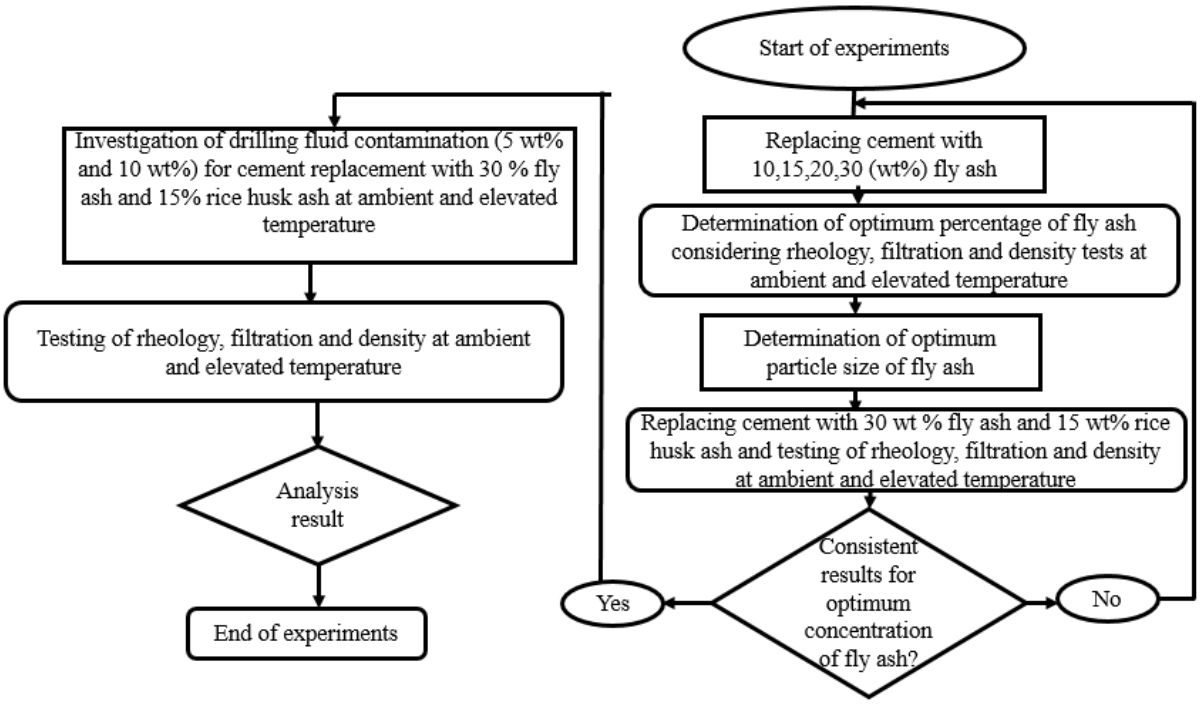

Figure 6.12. Flowchart of experimantal study for cement replacement

Table 6.13. Code of systems developed for cement

P1	Neat Cement
P1F-10	Replacement cement by 10% FA
P1F-15	Replacement cement by 15% FA
P1F-20	Replacement cement by 20% FA
P1F-30	Replacement cement by 30% FA
P1F30R15	Replacement cement by 30% FA and 15% RHA
P1M-5	Neat cement+5% mud
P1M-10	Neat cement+10% mud
P1F30M-5	Replacement cement by 30% FA+5% mud
P1F30M-10	Replacement cement by 30% FA+10% mud
P1F30R15M-5	Replacement cement by 30% FA and 15% RHA+5% mud
P1F30R15M-10	Replacement cement by 30% FA and 15% RHA+10% mud

In formulation of geopolymer, while sodium silicate (water glass) (Na_2SiO_3) and sodium hydroxide (NaOH) were used as alkaline activators, FA was used as raw material. Initially, an aqueous solution of sodium hydroxide at 12 molar concentrations was prepared. This prepared solution was left to cool in the laboratory for 24 hours. Subsequently, Na_2SiO_3 that is a compound consisting of NaOH and Na_2O was formulated with 27.5 (wt%) SiO_2, 8.3% (wt%) Na_2O, and 64.2 (wt%) H_20. Fig.6.13 shows the preparation process of the geopolymer.

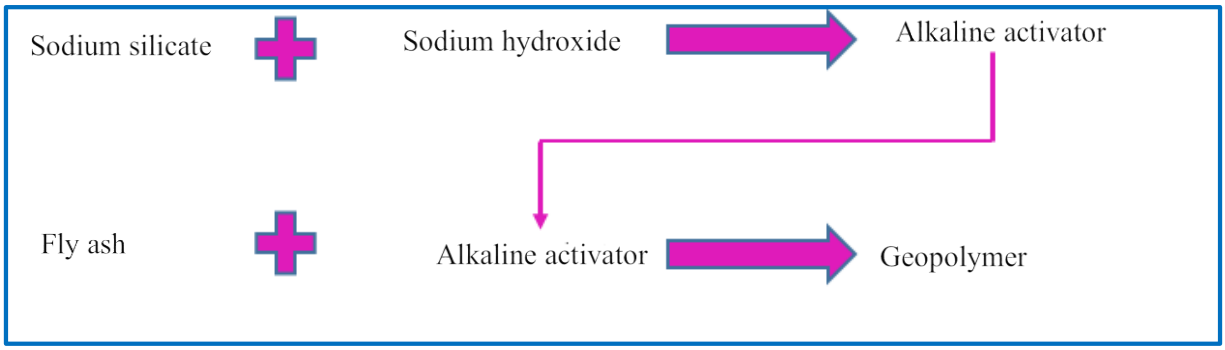

Figure 6.13. Geopolymer preparation process

Initially, optimum particle size of FA was determined in order to design geopolymer. To this end, FA was grinded in a a tumbling laboratory ball mill which was given in Fig.6.4 for the duration of 30 minutes, 60 minutes and 120 minutes. After grinding procedure of FA, geopolymer samples were prepared with the 45/55 liquid/solid ratio. Composition of the geopolymer in the determination of optimum particle size can be seen in the Table 6.14.

6.14. Composition of the geopolymers in the determination of optimum particle size

Liquid/Solid (wt.)	NaOH molarity	NaOH percentage	Water glass percentage
45/55	12 M	25	75

After the determination of optimum particle size of FA, an attempt was made to determine optimum liquid/solid ratio (L/S) based on 45/55, 42.5/57.5, 47.5/57.5 and 50/50 ratios. Composition of the designed geopolymers was given in Table 6.15. In this part, mud to cement conversion technology was applied on the geopolymers as well by comparing the portland cement systems. Geopolymer and cement slurries were replaced with the field water based drilling fluid (20%, 30%, and 40% by volume) whose composition given in the Table 6.12. Formulated systems were coded and presented in Table 6.16. Conducted experimantal steps were given in Fig.6.14.

6.15. Composition of the geopolymers in the determination of optimum L/S ratio

Liquid/Solid	NaOH molarity	NaOH percentage	Water glass percentage
45/55	12 M	25	75
42.5/57.5	12 M	25	75
47.5/52.5	12 M	25	75
50/50	12 M	25	75

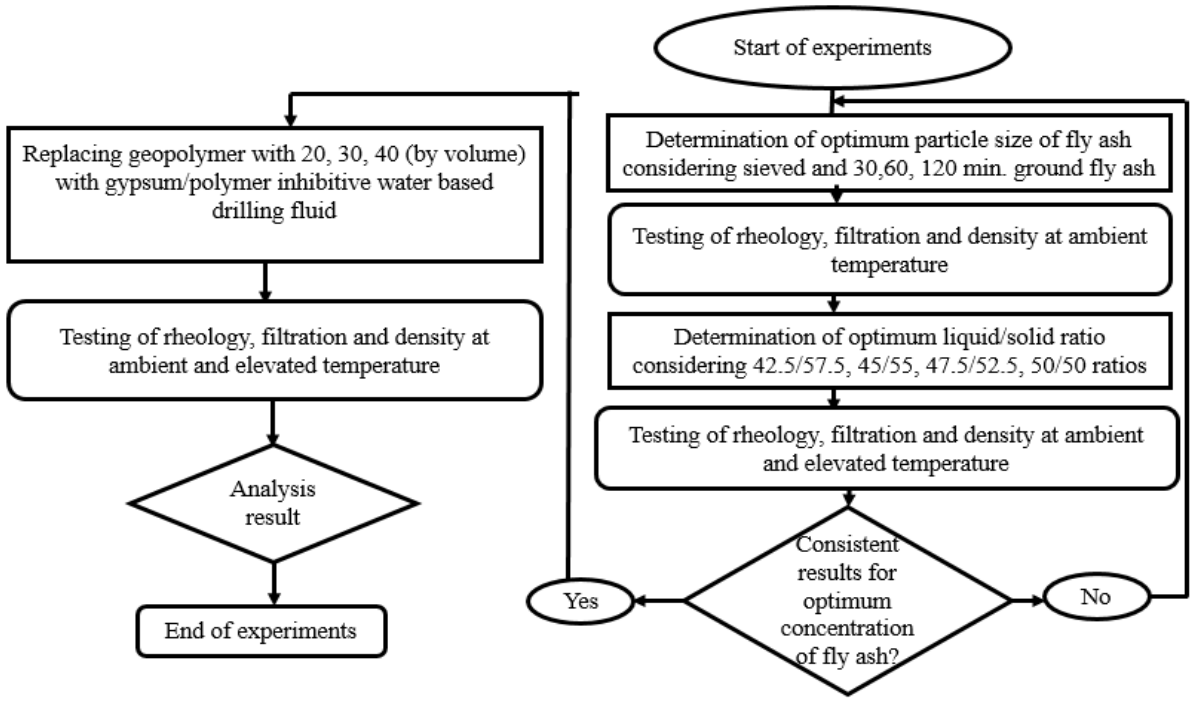

Figure 6.14. Flowchart of experimantal study for geopolymer

Table 6.16. Code of samples for mud to cement conversion

P1MC-20	Replacement cement with mud by %20
P1MC-30	Replacement cement with mud by %30
P1MC-40	Replacement cement with mud by %40
G1MC-20	Replacement geopolymer with mud by %20
G1MC-30	Replacement geopolymer with mud by %30
G1MC-40	Replacement geopolymer with mud by %40

6.3. Determination of properties of drilling fluid, cement and geopolymer

Properties of mud, cement and geopolymer are controlled by applying some tests and kept at appropriate values in order to avoid any problems during drilling and to fulfill their functions. All experimental measurements were carried out in accordance with the standards of the American Petroleum Institue (API) throughout the thesis (API, 2003). Details of the measured properties were presented below.

6.3.1. Measurement of viscosity

To measure the apparent viscosity (AV), plastic viscosity (PV), yield point (YP) and gel strength values of the prepared samples under ambient conditions, the Fann Model 35A rotates with 6 speeds viscometer (600, 300, 200, 100, 6 and 3 rpm) viscometer given in the Fig.6.14(a) was used. These parameters are the most basic parameters and constitute one of the features that must be measured continuously both in the laboratory and in the field.

In order to measure the relevant parameters, the mud, cement and geopolymer samples were filled up to the marked level in the viscometer cup after preparation and immersed in the test liquids up to the line on the rotor. The rotor was rotated at 600 rpm, and the reading of 600 rpm was recorded when the needle on the dial became stable. The same process was performed for the rotor speed of 300 rpm and when the pointer on the dial reached a fixed value, the reading was recorded as 300 rpm. Then, the relevant values were calculated with the help of the formulas given below.

Apparent viscosity (AV) in (cP)

$$= \theta_{600}/2 \tag{6.5}$$

Plastic viscosity (PV) in (cP)

$$= \theta_{600} - \theta_{300} \tag{6.6}$$

Yield point (YP) in (lb/100ft^2)
$= \theta_{300} - PV$ (6.7)

where θ_{600} is dial reading 600 rpm and θ_{300} is dial reading 300 rpm.

In order to measure rheology of cement and geopolymer systems under elevated temperature Fann model 35A viscometer with a heater cup given in Fig.6.15(a,b) was employed. In the measurement, heater cup was filled with the test fluid until there was a 1-in gap from the top and same procedure applied in the measurement at ambient conditions were performed.

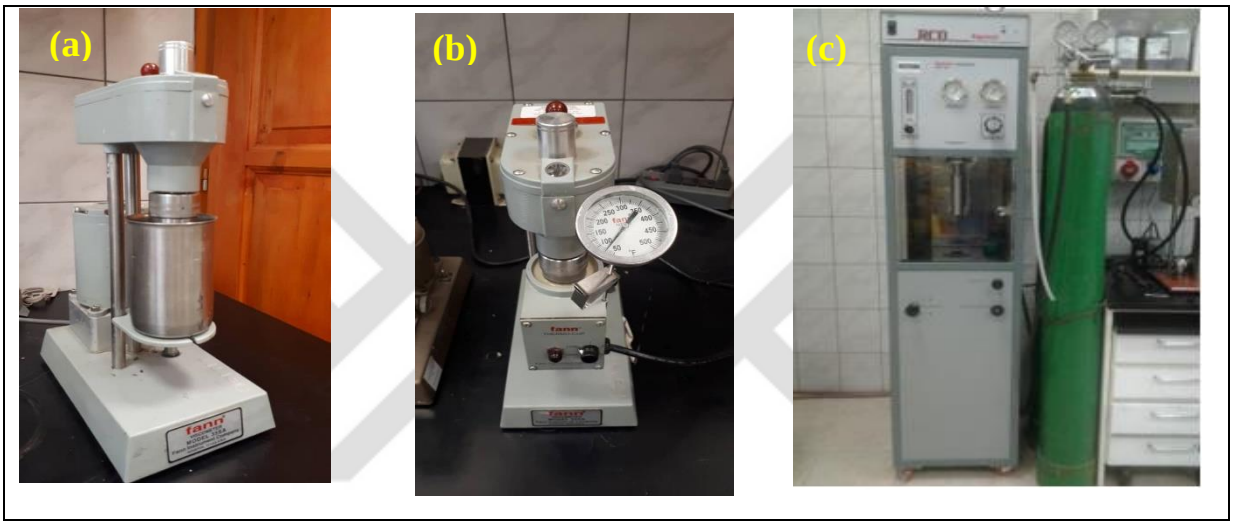

Figure 6.15. Viscometers, Fann 35A (a) for ambient condition, for elevated temperature (b) and Fann 50SL rheometer (c)

In the study, Fann Model 50 SL High Temperature-High Pressure (HTHP) Rheometer that is shown in Fig.6.15(c) was used to measure the rheological properties of muds at elevated temperatures. The rheometer is a high-precision, dual-cylinder rotary viscometer used to measure the viscosity of drilling fluids. This device has many advantages that measured data such as pressure, shear rate, shear stress, time and viscosity can be recorded under certain temperature.

The rheometer studied consists of a bob (B5) with a radius of 1.5987 cm and a length of 7.62 cm and a standard cup (R1) with an inside radius of 1.8415 cm. Due to the R1-B5 combination, the recommended value of 52 ml of test liquid was employed (Fann, 2015). When starting the experiment, firstly the raw torque value was checked and the bobbin was attached to the shaft. Then, temperatures of 30, 40, 50 (°C), speeds of 600, 300, 200, 100, 6, and 3 rpm, and the rotation time were set to take readings for 60 second per revolution. The excel file in which the

data were entered from the "Auto Test" section was loaded and saved with a desired name. Temperature of sample and bath, pressure, shear rate, shear stress, torque value and data showing how long each operation last were received at the end of the experiment. A measurement was perfomed every 5 seconds in each revolution and a total of 12 measurements results were obtained since readings were taken for 60 seconds. Calculations were conducted by taking the arithmetic mean of 12 measurements in each revolution. The data from the experiment were given in the excel file.

Gel strength was also measured with the Fann model 35A rotary viscometer. The test mud placed in the viscometer cup was stirred at 600 rpm for 10 seconds, then ceased for 10 seconds and then rotated at 3 rpm. The maximum value seen by the dial was recorded as 10 seconds gel strength. After the same process was repeated, waiting duration was kept for 10 minutes and the value read at 3 rpm was noted as 10 minutes gel strength.

6.3.2. Measurement of filtration

Measurement of filtration and filter cake properties is essential for the maintenance and control of drilling mud. The fluid loss was measured by API standard filter press, as shown in Fig.6.16. Both tests work on filling a test cell, which contains a backing screen below the filter paper. Once the test cell was filled and sealed, a graduated cylinder was placed underneath the assembly in order to collect the filtrate and the test cell was exposed to pressure of 100 psi for 30 minutes. When 30 minutes over, the pressure was interrupted and the filter fluid value accumulated in the graduated cylinder at the bottom of the test cell was recorded as the standard API fluid loss value. On the other hand, the cake thickness of the drilling fluid systems was measured by placing a ruler in the cake.

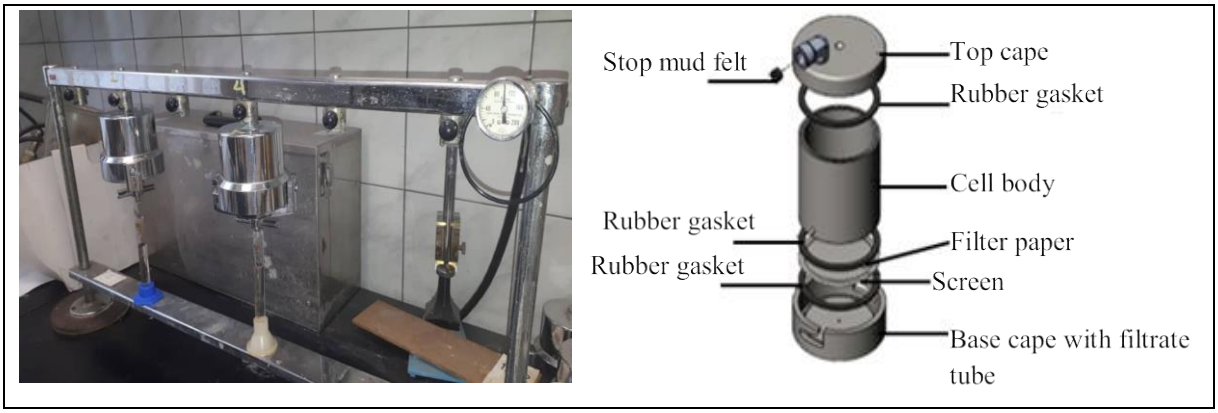

Figure 6.16. API standard filter press (left) and cell assembly (Ofite- manual, 2013) (right)

6.3.3. Measurement of density

The densities of the prepared systems were measured using the mud balance given in the Fig.6.17(b). After the mud to be measured was placed in the sample cup, lid of sample cup was placed on the cover of the cup. It was ensured that the sample cup is fully filled by ensuring that mud comes out from the hole on the lid. The overflowing mud was cleaned to prevent errors. The mud balance was placed at the fulcrum rest and balanced with the rider. After balancing, the value corresponding to the left of the rider was recorded as the mud density.

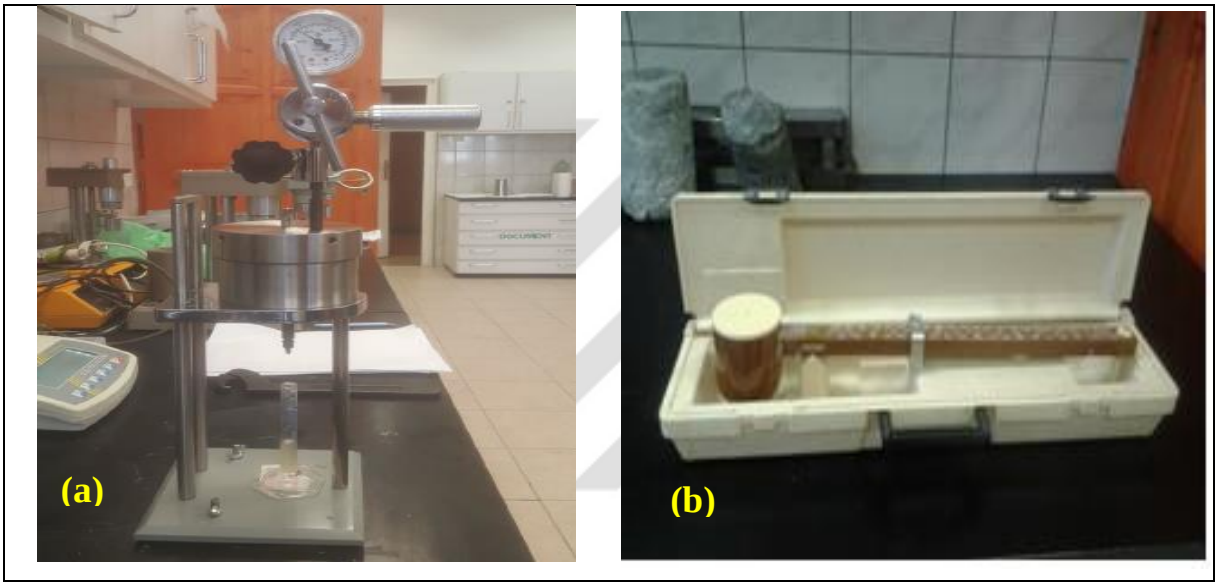

Figure 6.17. Differential sticking tester (a), mud balance (b).

6.3.4. Measurement of differential pressure pipe sticking

A number of devices have been developed so far to detect differential pressure pipe sticking of drilling muds. Even though the applicable temperature and pressure ranges of these devices are different, all of them basically simulate the pipe-wellbore geometry and mud cake formation process. In the thesis, the effectiveness of FA on the differential sticking tendency of drilling fluid was investigated by differential sticking tester (Fann Model 21150) in Figure 6.17(a), taking into account the different concentration and particle size as well as the grinding effect of FA. For measurement, the sample to be tested was first placed in the sample cup and exposed to nitrogen pressure of 500 psi for 10 minutes. The applied pressure caused the test sample to be filtered and the filtered liquid was collected with a graduated cylinder. After 10 minutes is completed, the torque plate was pressed with a lever for 2 minutes and the torque plate was adhered to the mud cake formed. Then, the torque plate was rotated using torque wrench and

the maximum torque value observed on the dial of torque wrench was recorded in lb-in. After waiting for 30 seconds, one more reading was recorded from the dial of torque wrench. This process was repeated every 30 seconds, recording a total of 6 readings. Finally, by taking the average of the recorded values, the sticking coefficients of the tested drilling muds were calculated using Eq.6.8.

$$K_{SC} = \frac{0.001 * \text{average torque reading}}{\text{stuck cake radius}^3} \quad (6.8)$$

7. RESULTS AND DISCUSSION

Before starting the experimental study, both types of FA and RHA samples were dried in a drying oven at 105˚C in order to remove moisture from the samples and reach the constant mass.

Based on the drilling mud, cement and geopolymer formulations whose compositions were given in Chapter 6, FA and RHA were used in different concentrations or conditions and the rheological and filtration properties of these fluids were measured under ambient conditions and elevated temperature. The stability of the cement and geopolymer slurry against drilling mud contamination was also measured under both ambient and elevated temperature. Finally, in the light of the data obtained drilling performance and rheological model analysis of the drilling mud was studied under increasing temperature. The detailed results obtained were presented below.

7.1. The role of fly ash type and concentration in assessment of flow behaviour of gypsum/polymer drilling mud

The steps given in the Fig.6.3 were followed by adding BFA and LFA at 1.0, 3.0 and 5.0 (wt%) concentrations into the gypsum/polymer whose composition were given in the Table 6.2. Results achieved were presented below.

The AV, PV, YP and gel strength noted from Fann viscometer were shown in Fig.7.1 and Fig.7.2. Results of effect of FA types and their concentration on the AV, PV, and YP of gypsum/polymer water-based mud was presented in Fig.7.1. As can be seen from the figure, as the FA concentration increases the AV and PV increase for both types of Fas and the highest AV and PV values are observed with BFA. Moreover, the yield point also increases with

increasing concentrations of BFA. However, the yield point decreased with LFA at 3.0 wt% concentration. Fig.7.2 revealed that the 10s gel strength, 1 min gel strength and 10 min gel strength increase at 1.0 wt% concentration for both types of FA, while neither the concentrations nor the type of FA has any effect on the gel strengths, above 1.0 wt% concentration.

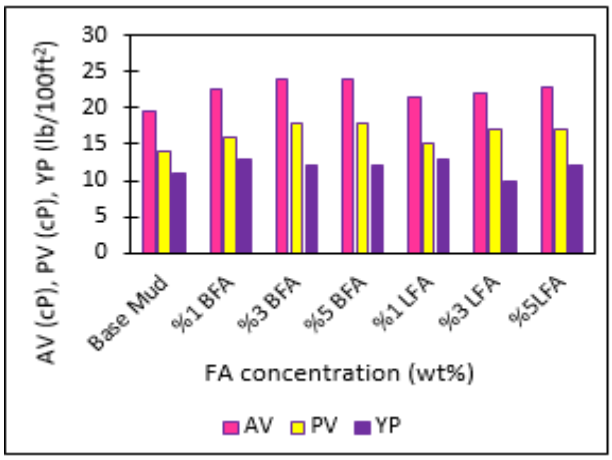

Figure 7.1. Variation of AV, PV and YP of gypsum/polymer mud with the increasing concentration of BFA and LFA

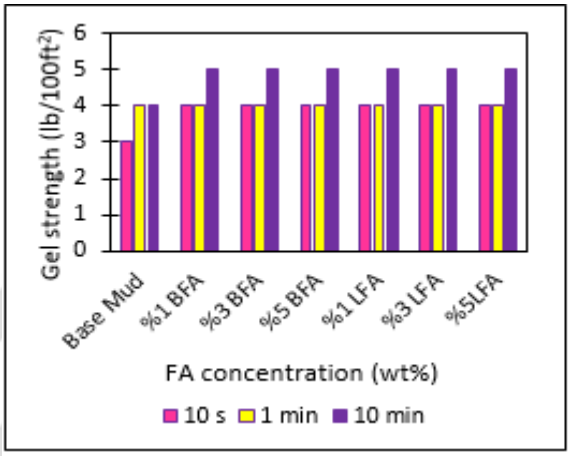

Figure 7.2. Variation of gel strength of gypsum/polymer mud with the increasing concentration of BFA and LFA

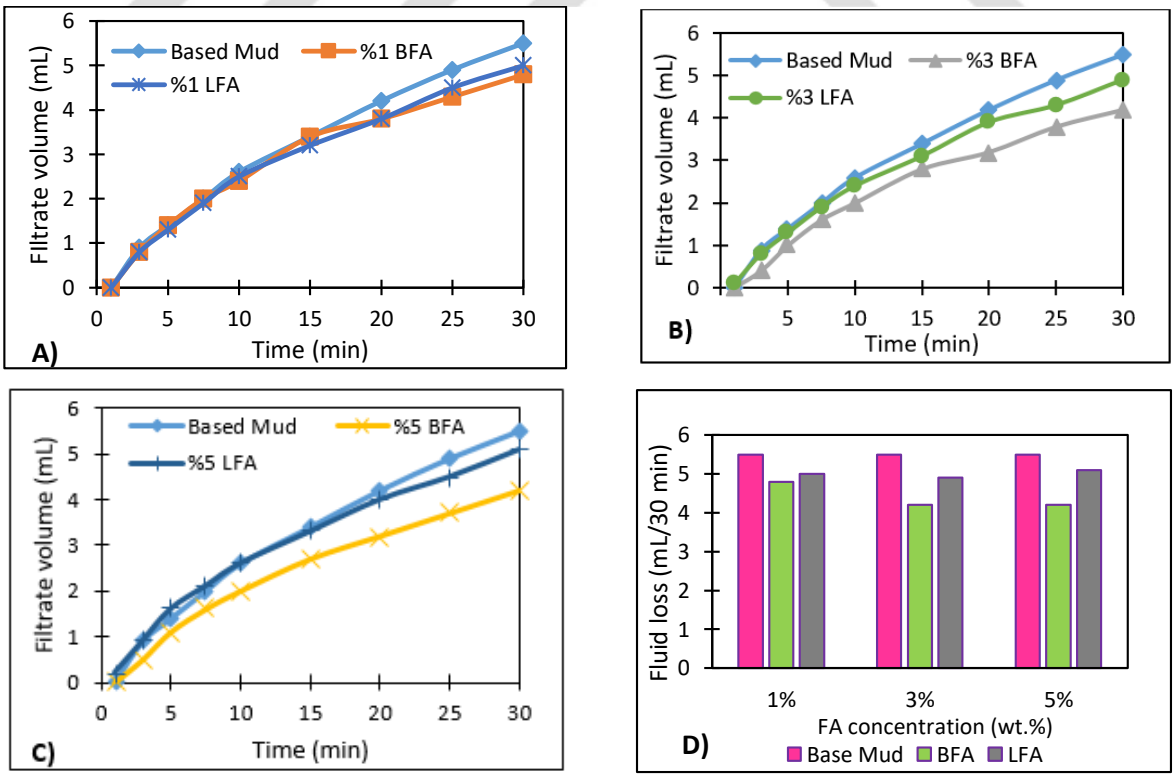

Figure 7.3. Variation of fluid loss of gypsum/polymer mud with the increasing concentration of BFA and LFA, A. Fluid loss versus time for 1.0 wt% concentration, B. Fluid loss versus time for 3.0 wt% concentration, C. Fluid loss versus time for 5.0 wt% concentration, D. Fluid loss for 30 min.

The effect of FA types and their concentration on fluid loss are presented in Fig.7.3 for gypsum/polymer drilling fluid. Fig.7.3(A-C) shows the filtrate volume against time for 1.0 wt.%, 3.0 wt.%, and 5.0 wt.% concentration, respectively for BFA, LFA and base mud. As can be seen from the figures, the samples with BFA show less fluid loss than the samples with LFA at all concentrations. Fig.7.3D shows filtrate volume collected for 30 min. From the figure, it can be seen that the 30 min of fluid loss of base mud decreases with increasing concentration of both types of FA samples. On the other hand, the percentage of decrease in filtrate volume collected increased up to 3.0 wt% for both types of FA. However, thereafter the percentage of reduction in fluid loss remains constant for BFA samples, whereas it increases slightly for LFA samples.

From Fig.7.4, it was observed from that while adding the BFA decreases the cake thickness of gypsum/polymer, the mud cake thickness increases with increasing concentration of LFA and the minimum cake thickness value was obtained with 3.0 wt% concentration of BFA in gysum/polymer mud. Being obtained more thick mud cake may cause various problems such as sticking of pipes, high swab and surge pressures, and excessive torque and drag (Avci et al., 2019).

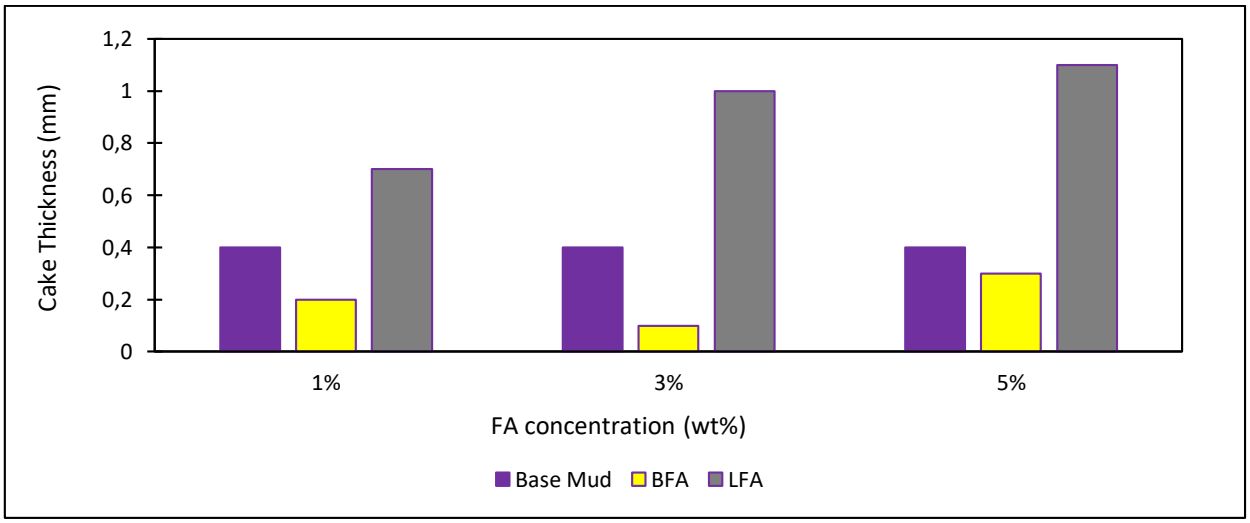

Figure 7.4. Variation of cake thickness of gypsum/polymer mud with the increasing concentration of BFA and LFA

7.2. The role of fly ash type and concentration in assessment of flow behaviour of spud mud

The steps given in the Fig.6.4 were followed by adding BFA and LFA at 1.0 wt%, 3.0 wt% and 5.0 wt% concentrations into the spud mud whose composition were given in the Table 6.3. Results achieved were presented below.

Fig.7.5 shows that while there is no effect BFA ash on the apparent viscosity, plastic viscosity and yield point of spud mud, all the rheological parameters increase as the LFA concentration increases. From Fig.7.6, it can be seen that while with adding BFA into the spud mud, the 10 s, 1 min. and 10 min. gel strength decreased slightly, all the gel strengths increased considerably with the increase concentration of LFA.

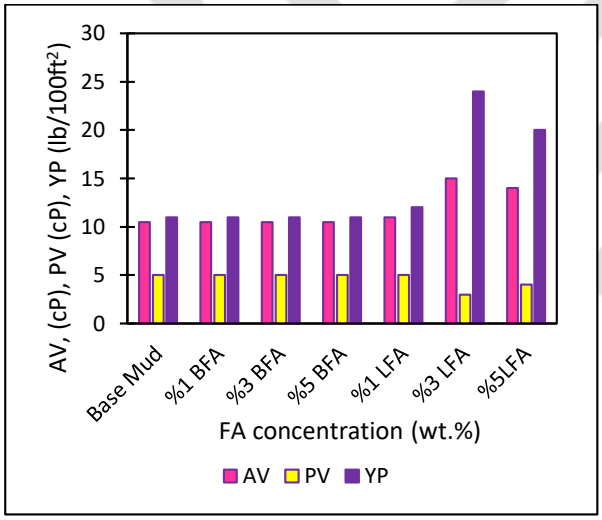

Figure 7.5. Variation of AV, PV and YP of spud mud with the increasing concentration of BFA and LFA

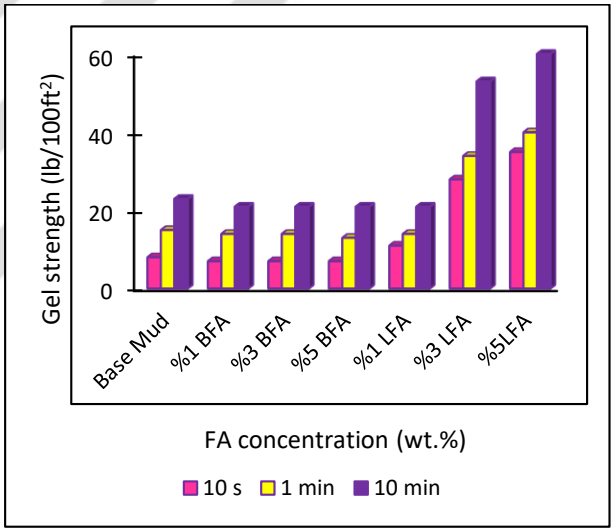

Figure 7.6. Variation of gel strength of spud mud with the increasing concentration of BFA and LFA

The effect of FA types and their concentration on fluid loss are presented in Fig.7.7 for spud mud. Fig.7.7(A-C) shows the filtrate volume against time for 1.0 wt%, 3.0 wt%, and 5.0 wt% concentration, respectively for BFA, LFA and base mud. As can be seen from the figures while the fluid loss decreases as BFA concentration increases, the fluid loss increased considerably with the increasing concentration of LFA. Fig.7.7D shows filtrate volume collected for 30 min. From the figure, it can be seen that the lowest filtrate rate is obtained with 5 wt% BFA.

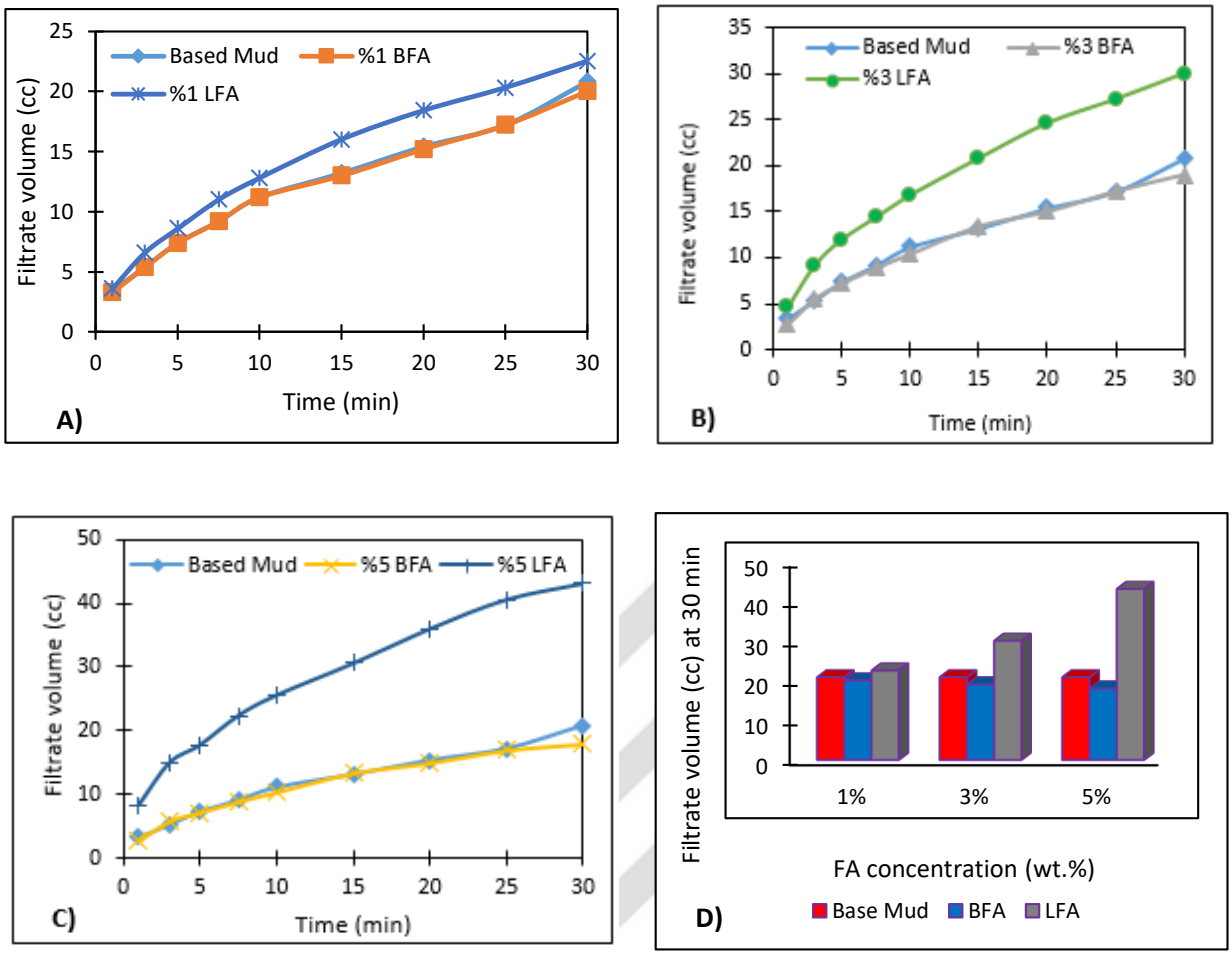

Figure 7.7. Variation of fluid loss of spud mud with the increasing concentration of BFA and LFA, A. Fluid loss versus time for 1.0 wt% concentration, B. Fluid loss versus time for 3.0 wt% concentration, C. Fluid loss versus time for 5.0 wt% concentration, D. Fluid loss for 30 min.

From Fig.7.8, similar to results of gypsum/polymer mud, it was observed from that while adding the BFA decreases the cake thickness of spud mud, the mud cake thickness increases with increasing concentration of LFA and minimum cake thickness value was obtained with 3.0 wt% concentration of BFA in the mud. Being obtained more thick mud cake may cause various problems such as sticking of pipes, high swab and surge pressures, and excessive torque and drag.

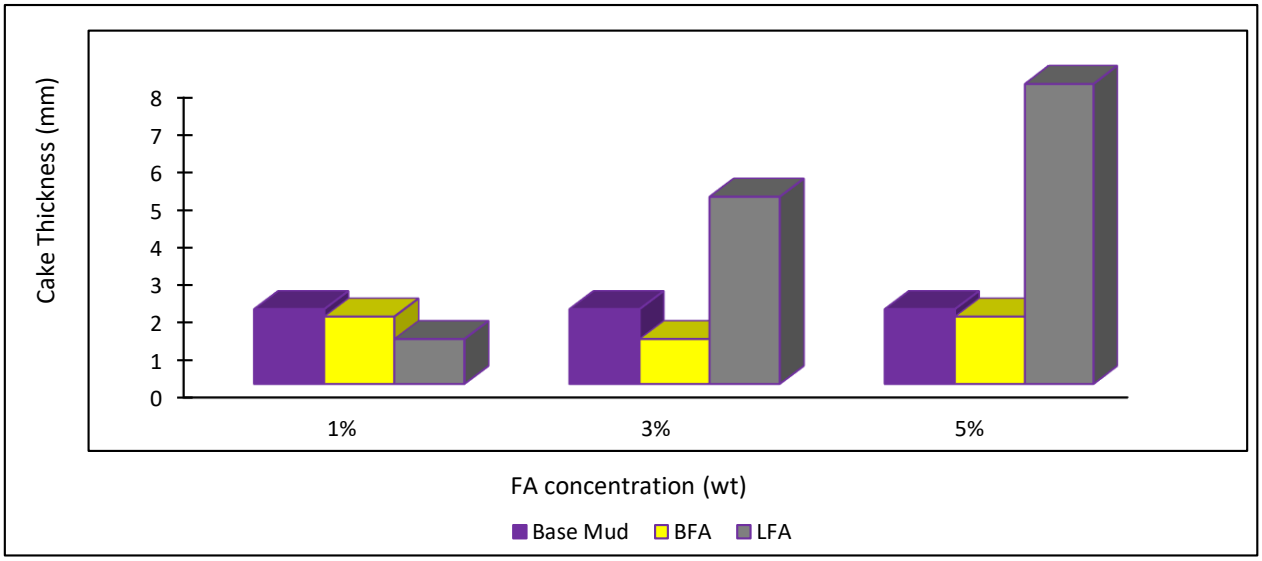

Figure 7.8. Variation of cake thickness of spud mud with the increasing concentration of BFA and LFA

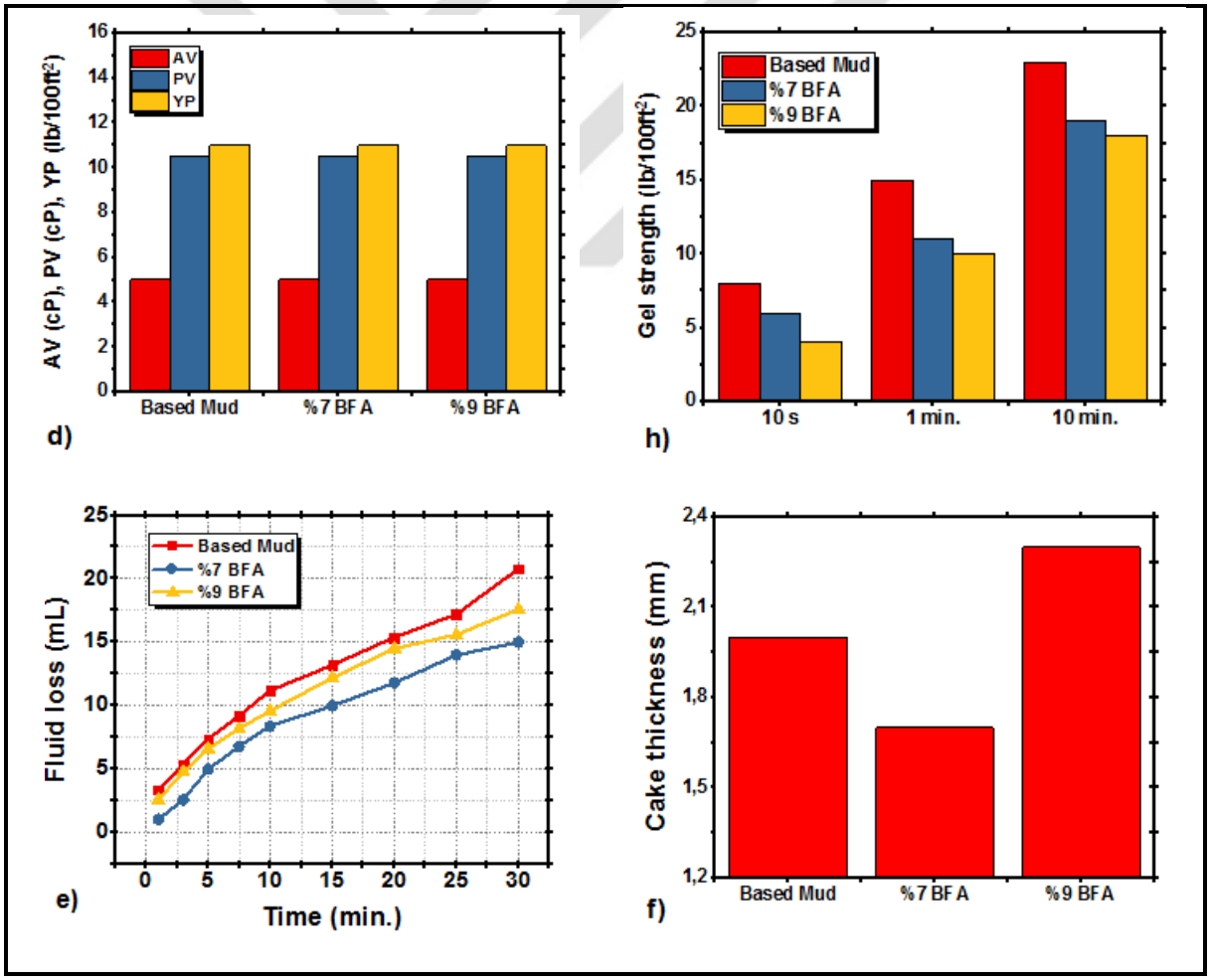

Figure 7.9. Variation of flow characteristic of spud mud with the further increasing concentration of BFA (Yalman et al., 2021c).

After studying the effect of low-concentration, BFA with further increasing concentration (7 wt% and 9 wt%) was introduced into the spud mud. Rheological and filtration properties of the fluid with 7 wt% and 9 wt concentration of FA were presented in Fig.7.9 by comparison with reference fluid. Result shows developed spud mud incorporated with 7 wt% concentration of BFA exhibited improved filtration properties as well as gel strength without significant variation on apparent viscosity, plastic viscosity and yield point compared to the reference fluid without FA. With the forming developed mud system API standard fluid loss and thixotopy of the reference fluid decreased by 22% and 9%, respectively (Yalman et al., 2021a).

After the determination that BFA showed better properties than LFA in both gypsum/polymer and spud mud, research continued with the BFA. Subsequent parts of the thesis were studied considering solely BFA.

7.3. The role of fly ash concentration in assessment of flow behaviour of KCl water based mud

In this part, an attempt was made to design an inhibitive drilling fluid with FA and RHA. To this end, 1.0 wt%, 3.0 wt%, 5.0 wt%, 7 wt%, 9 wt% concentrations of FA were introduced to KCl water based whose composition given in Table 6.4 and milestone given in Fig.6.6 were followed. Results obtained were provided below.

Apparent viscosity, plastic viscosity, yield point, and gel strength increased with the addition of BFA into the KCl water based mud, as shown in Fig.7.10 and Fig.7.11.

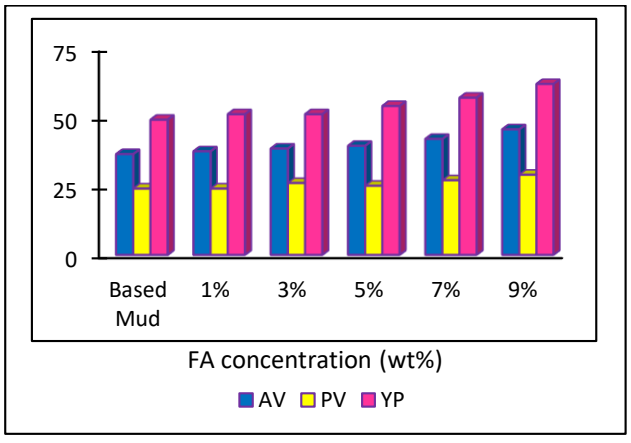

Figure 7.10. Variation of AV, PV and YP of KCl water based mud with the increasing concentration of FA

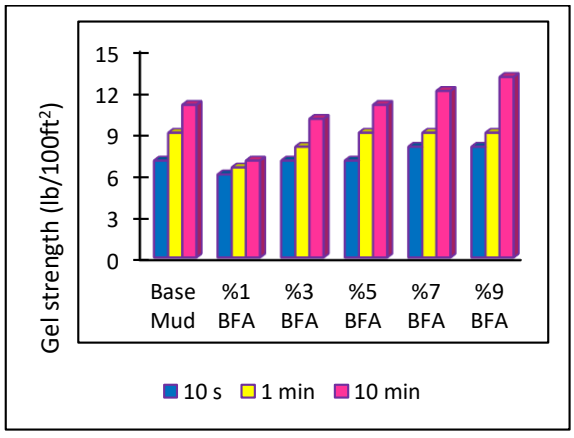

Figure 7.11. Variation of gel strength of KCl water based mud with the increasing concentration of FA

The effect of FA concentration on fluid loss was presented in Fig.7.12 for KCl water based drilling fluid. Fig.7.12 (A-C) shows the filtrate volume against time for 1.0 wt%, 3.0 wt%, and 5.0 wt% concentration, respectively for drilling fluid with FA and base mud. As can be seen from the figures as FA concentration increases, the fluid loss decreases. Fig.7.12D shows filtrate volume collected for 30 min. From the figure, it can be seen that the lowest filtrate rate is obtained with 9 wt% FA.

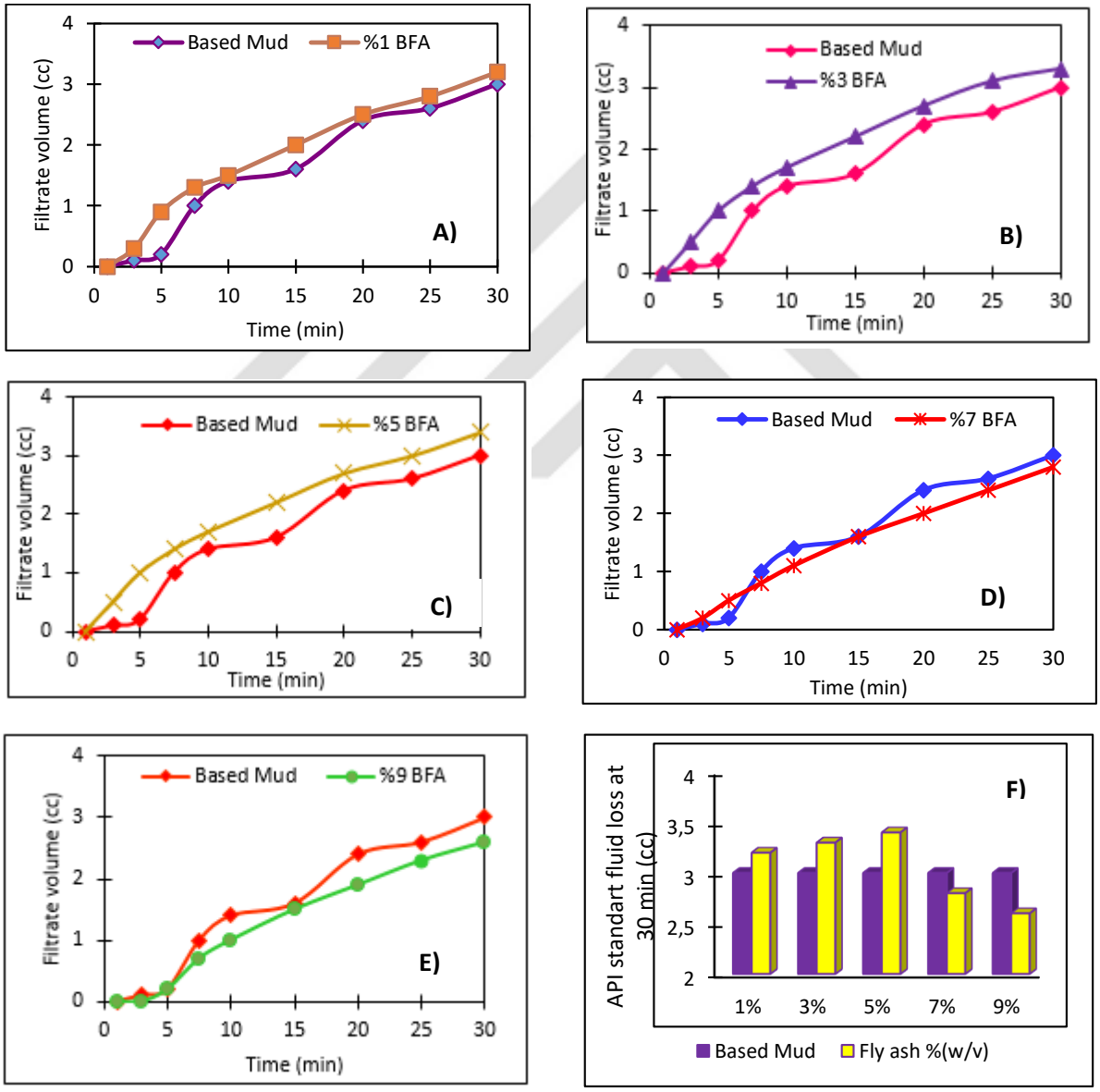

Figure 7.12. Variation of fluid loss of KCl water based mud with the increasing concentration of FA , Fluid loss versus time for 1.0 wt% concentration (A), 3.0 wt% concentration (B), 5.0 wt% concentration (C), 7.0 wt% concentration (D), 9.0 wt% concentration (E), Fluid loss at 30 min (F)

From Fig.7.13, it is clear that filter cake properties of the fluid improved with the increasing concentration of FA. Results shows as FA concentration increases filter cake thickness decreases. With the forming KCl water based mud with 9 wt% FA concentration of FA, mud cake thickness decreased by 65%.

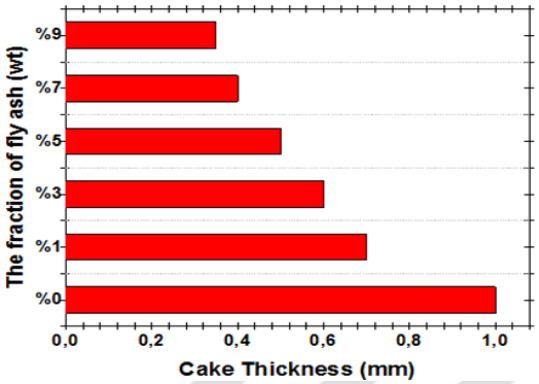

Figure 7.13. Variation of cake thickness of KCl water based mud with the increasing concentration of FA

7.4. Effect of finess of fly ash in shale inhibitor mud

Finess of FA generally have an important role in material which it is employed. The optimum concentration of FA that is 9 wt% in KCl water based mud was introduced to shale inhibitor mud in order to analyse role of finess of FA on rheological and filtration features of the mud. Fig.7.14 shows rheological properties of shale inhibitor mud with different grinding time of FA and unground FA. From Fig.7.14A, it is clear that grinding time had no affect on AV, PV and YP of shale inhibitor mud. In addition, drilling mud designed with unground FA showed a greater rheological parameters than drilling mud formulated with FAs subjected to mechanical grinding for 30 minutes, 60 minutes and 120 minutes keeping the content introduced constant. It worths to note that the increased rheology of referans KCl mud was achieved due to 9 wt% concentration of FA. Gel strength results showed a parallel trend to other rheological parameter results. 10 seconds, 1 minute and 10 minutes gel strengths of the fluid remained constant with different ground time of FAs. However, driling mud designed with unground FA had greater gel strength values than fluids formulated with ground FAs., as can be seen in Fig.7.14B.

Although FA with different size did not have a significant effect on the rheology of the shale inhibitor mud, it produced a certain variation on the fluid loss, density and thickness of filter cake.

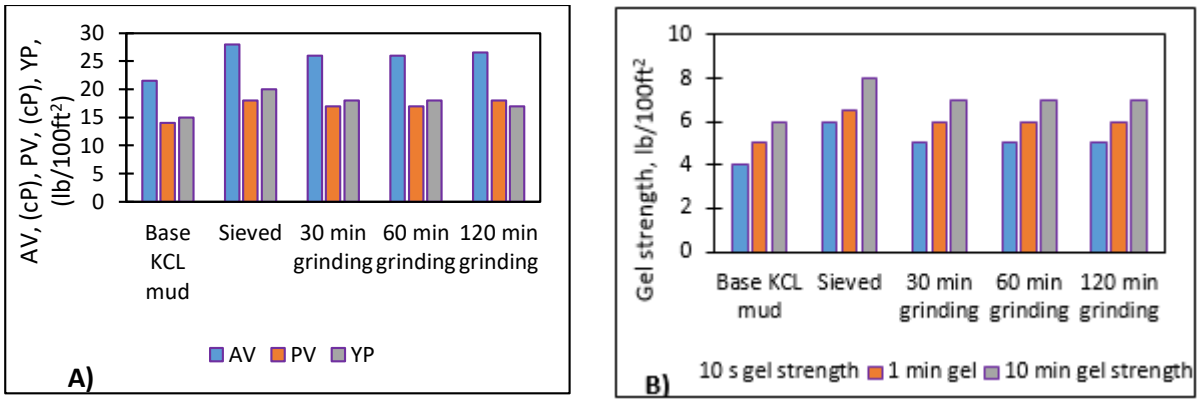

Figure 7.14. Rheological properties of shale inhibitor mud with different grinding time of FA and unground FA

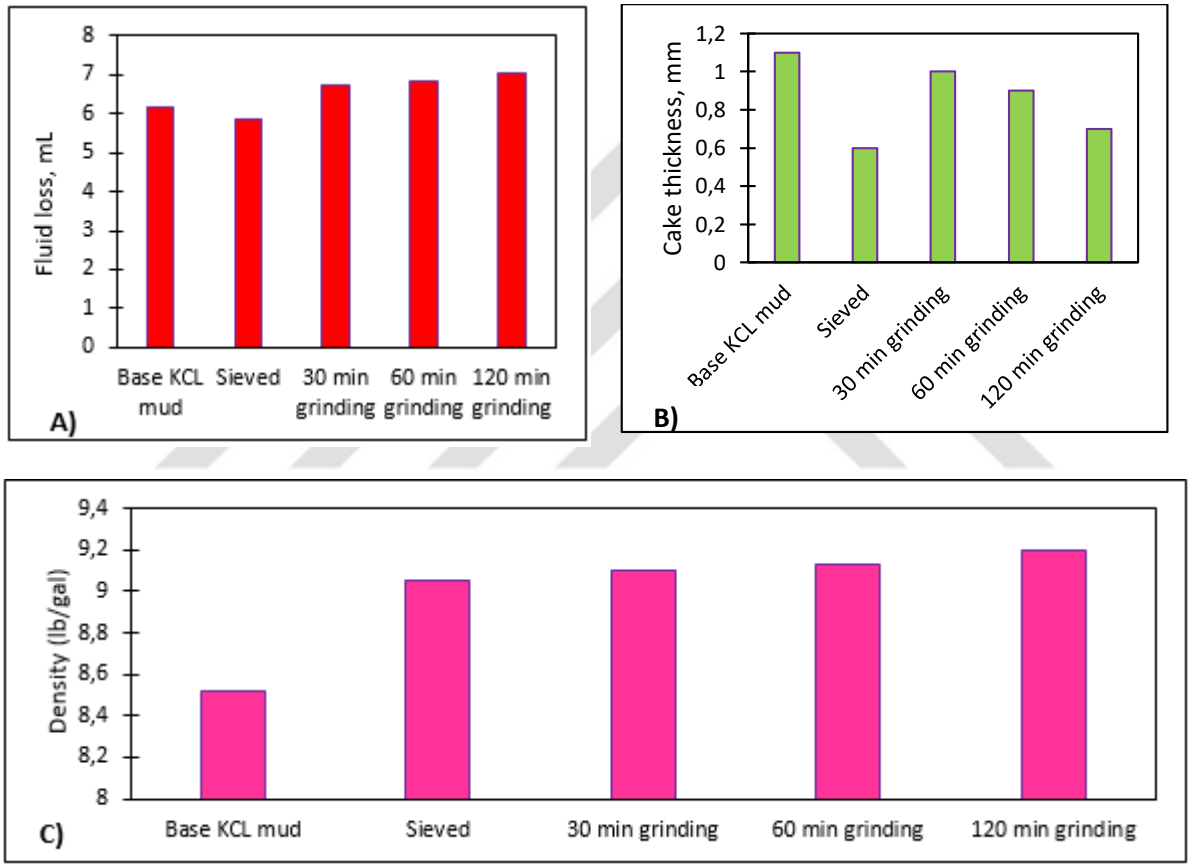

Figure 7.15. Filtration properties and density of shale inhibitor mud with different grinding time of FA and unground FA. A) Fluid loss, B) Mud cake thickness, C) Density

Figure 7.15 shows the API fluid loss, density and mud cake thickness results of shale inhibitor drilling mud formulated with 9% FA of different particle sizes obtained as a result of mechanical grinding. The results showed that as the grinding time increased, which means finer particles, the fluid loss increased. However, lower fluid loss was achieved with drilling mud formulated with unground FA compared to drilling muds with ground FAs (Fig. 7.15A). The filter cake results showed a similar trend to the filtration results. Drilling muds with FA

subjected to mechanical grinding caused to increase filter cake. However, it should be noted that when drilling muds with ground FAs were examined, it was observed that the thickness of the mud cake decreased due to the increase in the grinding time. The lowest mud cake was obtained with drilling mud formulated with unground FA compared to ground FA muds (Fig. 7.15B). Mud density test results showed that mechanical grinding of FA did not have a serious effect on the density. The mud density tended to increase slightly with the increase of the grinding time, and the highest density was obtained with the mud formulated with FA milled for 120 minutes (Figure 7.15C). The reason for this partial density increase can be attributed to the increase in particle density due to grinding.

7.5. Comparative investigation of fly ash and rice husk ash in shale inhibitor mud

Fig.7.16 shows viscosity and gel strenght of shale inhibitor mud in presence of FA and RHA.

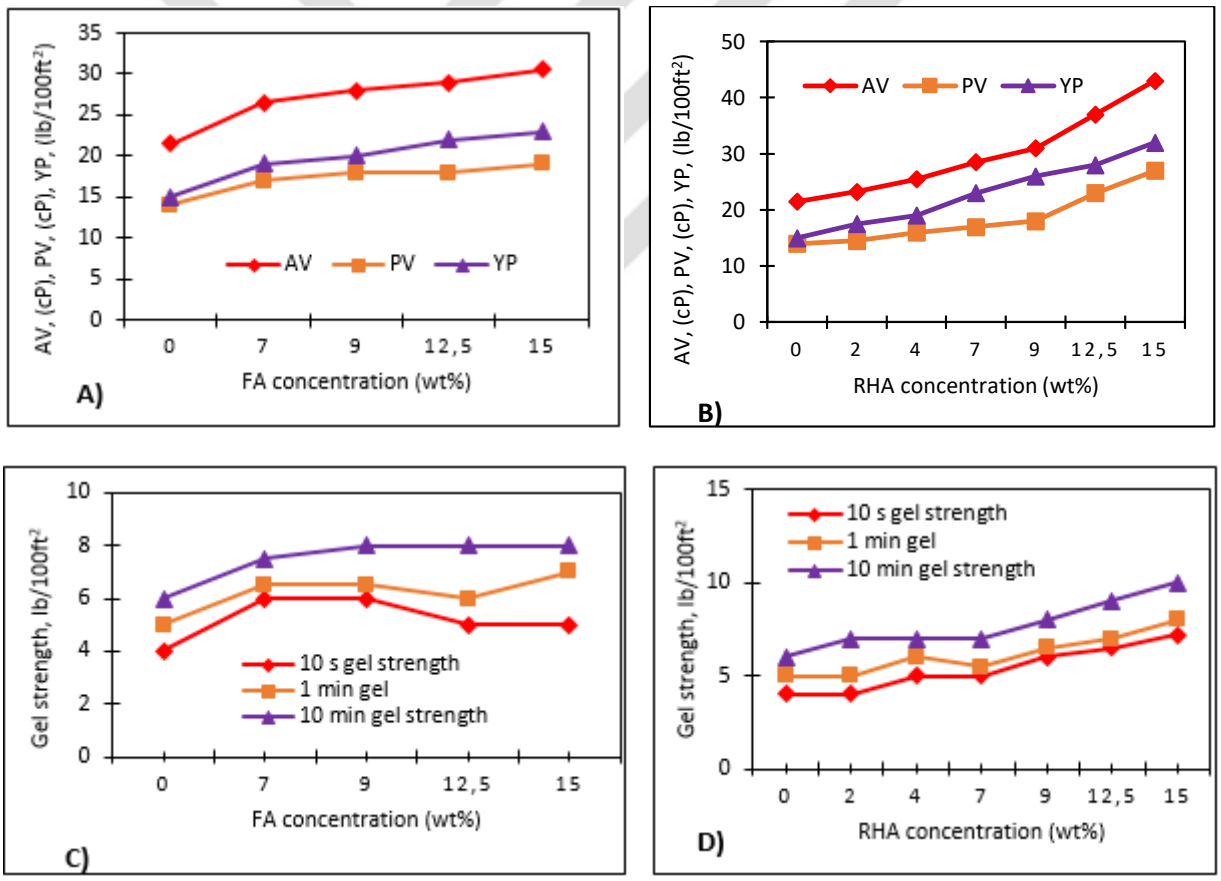

Figure 7.16. Rheological properties of shale inhibitor mud including FA and RHA, Viscosity (A) FA (B) RHA, Gel strength (C) FA (D) RHA.

The rheological parameter measurement results revealed that the shale inhibitor mud showed an increase depending on the increase in concentrations of both FA and RHA (Figure 7.16A-B). However, greater values of AV, PV, YP and gel strength were obtained in drilling muds

formulated with RHA under constant concentration. For instance, AV, PV and YP values of drilling mud formulated with 15% RHA increased by 100%, 113%, and 92%, respectively, while these parameters increased by 41%, 34%, and 35%, respectively, with 15% FA drilling mud. As can be seen from Figure 7.16C-D, under constant FA and RHA concentration, 10 seconds, 1 minute and 10 minutes gel strength of the shale inhibitor muds with RHA were slightly higher than those with FA.

Fluid loss, mud cake and density results of shale inhibitor mud formulated with different concentrations of FA and RHA were presented in Figure 7.17.

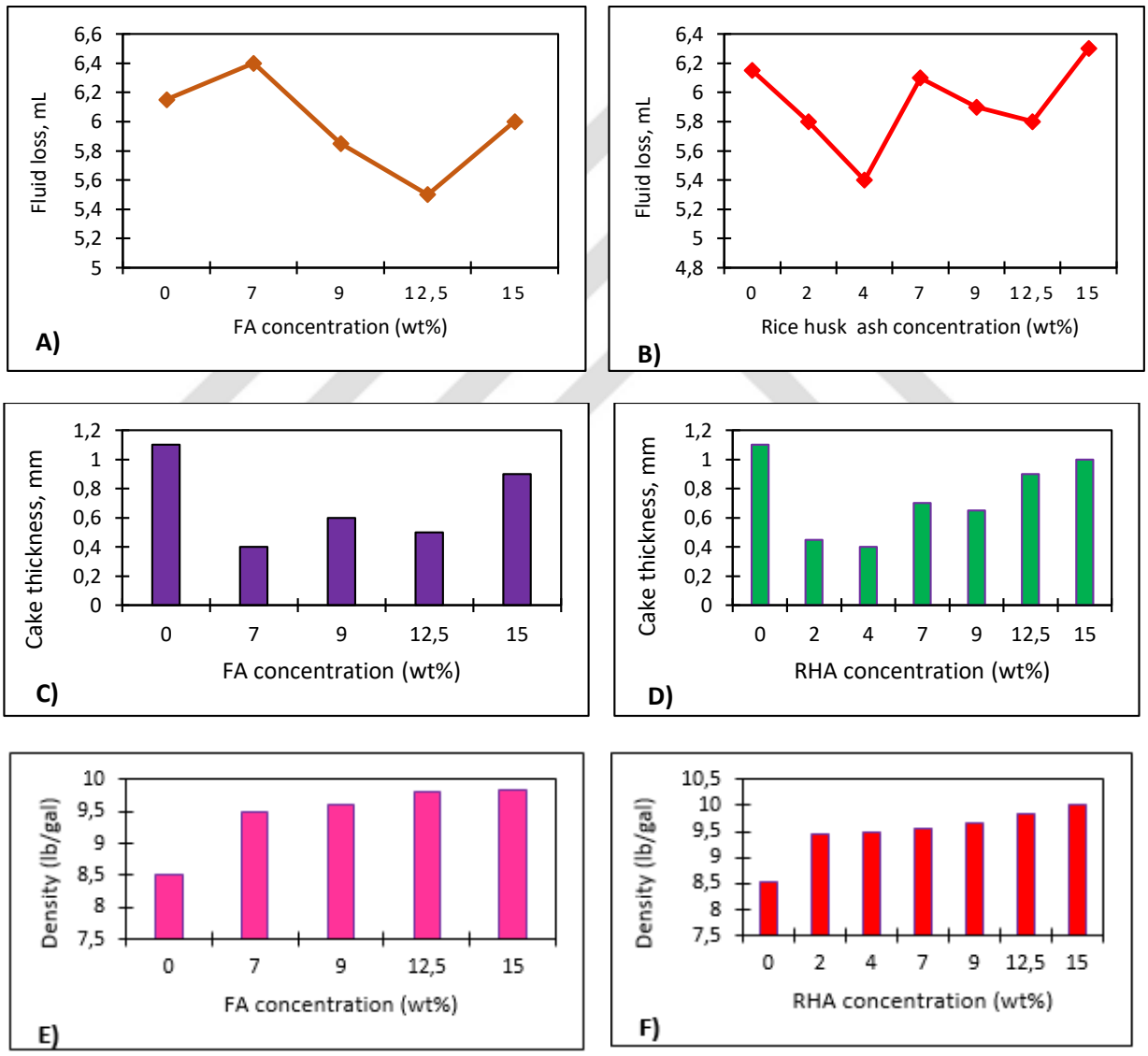

Figure 7.17. Filtration properties and density of shale inhibitor mud including FA and RHA. Fluid loss (A) FA (B) RHA, Mud cake thickness (C) FA D) RHA, Density (E) FA and (F) RHA

From Figure 7.17A-B, it can be said that there is no direct correlation between the addition of FA and RHA at different concentrations to the shale inhibitor mud and fluid loss and mud cake.

For instance, among the muds formulated with FA, the lowest fluid loss was obtained with the drilling mud formed by 12.5% FA, while the lowest fluid loss among the muds with RHA was observed with the mud formed by 4% RHA. Although there was no significant difference between the fluid loss reduction rates of these mud compared to the reference mud without FA or RHA, 12.5% FA mud reduced fluid loss by 10%, while 4% RHA mud provide to decrease by 12%. Mud cake thickness results of the muds with the lowest filtration showed that RHA was relatively more effective than FA in reducing the mud cake thickness (Figure 7.17C-D). Mud with 4% RHA reduced the cake thickness by 63%, while mud with 12.5% FA reduced the cake thickness by 54%. As can be seen from Figure 7.17E-F, under constant FA and RHA contents, higher density values were observed in muds formed by RHA, although the mud density increased for both depending on the concentration increase. This can be attributed to the fact that RHA has a higher particle density compared to FA. In addition, in fact, the lower density of the "fly ash" is mainly due to the larger, closed, gas-filled pores. Considering the rheological and filtration results as a whole, the optimum formulation was determined as 12.5% mud among the mud formulated with FA, while 4% mud was determined as the optimum formulation among the mud formulated with RHA.

7.6. Effect of bentonite, XG, CMC concentration and aging time on performance of fly ash

To analyze effect of aging time and bentonite, XG and CMC concentration on performance of FA four different mud systems were designed whose compositions were given in Table 6.6. Milestones were performed based on flowchart given in Fig.6.8 based on formulated system whose code can be seen in Table 6.7.

7.6.1. Rheology and filtration test results of bentonite concentration and aging time

Bentonite amount and aging time play a crucial role on performance of BFA in bentonite mud. Fig.7.18 shows rheological properties of optimum concentration of FA, which is 4 wt% with aging time and increasing bentonite concentration. From Fig.7.18A, it is clear that in API bentonite mud, which is bentonite concentration is 6 wt%, performance of FA increased with the increasing aging time. AV, PV and YP of the API mud increased by 4%, 14%, 3%, respectively, with the addition of 4 wt% cocentration of FA for 24 hours aging time. For 48 hours aging time AV, PV and YP of the mud increased by 9%, 7%, 11%, respectively with the addition of 4 wt% concentration of FA. For 72 hours aging time AV and YP of the mud increased by 41%, 81%, respectively with the addition of 4 wt% concentration of FA, no change

was observed in PV. When bentonite amount increased from 6 wt% to 8 wt% under same condition it was found that increasing bentonite concentration also enhanced performance of FA, which was given in Fig.7.18B. For 24 hours AV, PV and YP of mud containing 8 wt% bentonite increased by 83%, 46%, 118%, respectively with the addition of 4 wt% concentration of FA. For 48 hours aging time, the AV and YP of mud containing 8 wt% bentonite increased by 85% and 166%, respectively. And, no change was observed in PV. For 72 hours aging time AV, PV and YP of mud containing 8 wt% bentonite increased by 82%, 34%, 127%, respectively. Analyzing these results, it was found that 8 wt% bentonite aging for 48 hours condition shows the optimum properties.

Fig.7.18C-D shows that 10 seconds, 1 minute and 10 minutes gel strengths increases with the increasing aging time. Also, it should be noted that increasing bentonite concentration further increased the gel strengths. Moreover, increasing bentonite concentration (8 wt%) in presence of 4 wt% concentration of FA decreased tixotropy of the mud under same aging time compared to the mud containing lower bentonite concentration (6 wt%).

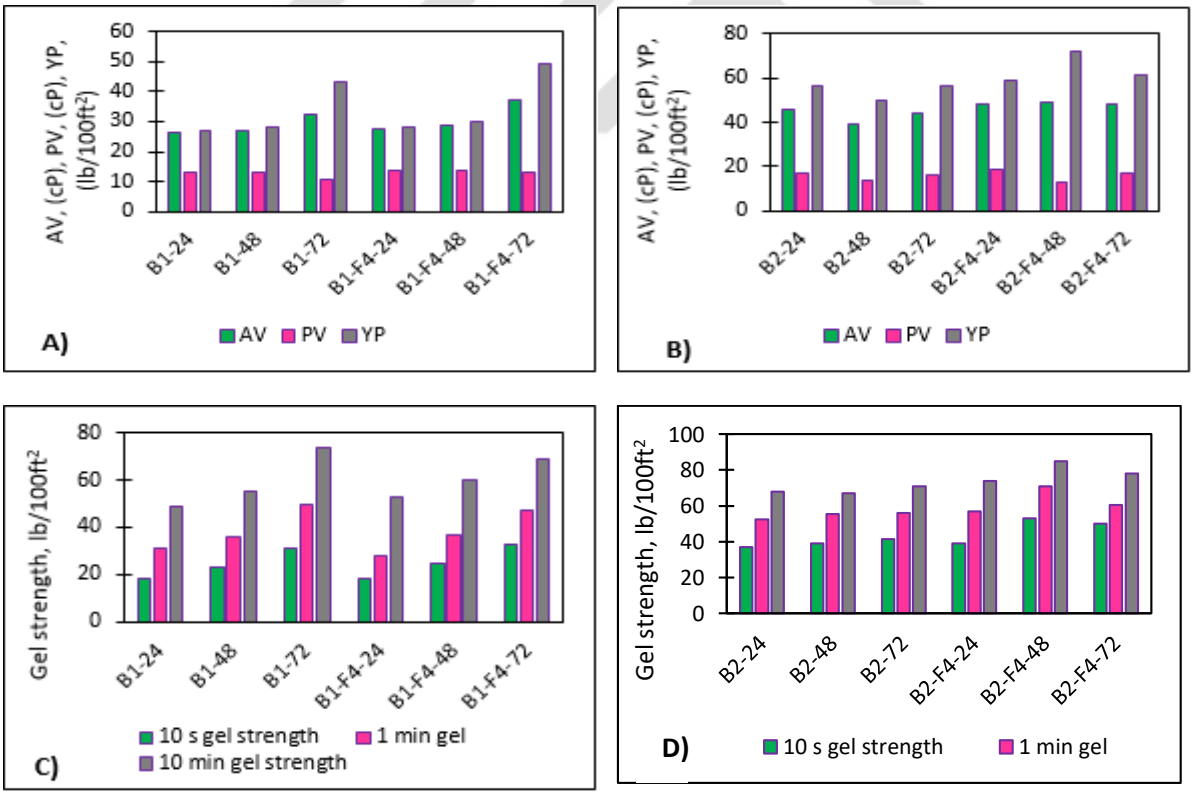

Figure 7.18. Rheological properties of optimum concentration of FA with aging time and increasing bentonite concentration.

From Fig.7.19A-B, it was seen that increasing aging time decreased filtration of both bentonite muds, 6 wt% and 8 wt% concentrations. Addition of 4 wt% concentration of FA into the muds

provided further reduction in fluid loss with increasing aging time. It should be noted that increasing bentonite also improved performance of FA in terms of filtration properties. The lowest fluid loss was achieved with 8 wt% bentonite under 72 hours aging time. Fig.7.19C showed that increasing aging time caused thicker mud cake in mud containing lower bentonite concentration, 6 wt%. However, aging in presence of 4 wt% concentration of FA provided thinner mud cake compared to 4 wt% concentration of FA free mud under same aging time. It worths to note that increasing aging time even in presence of 4 wt% concentration of FA caused to increase mud cake. On the other hand, increasing aging time decreased cake thickness of mud containing 8 wt% bentonite concentration. Cake thickness further decreased with the addition of 4 concentration of FA under increasing aging time (Fig.7.19D). To sum up, analysis results showed that mud containing 8 wt% bentonite concentration with 72 hours aging time had optimum properties among the others.

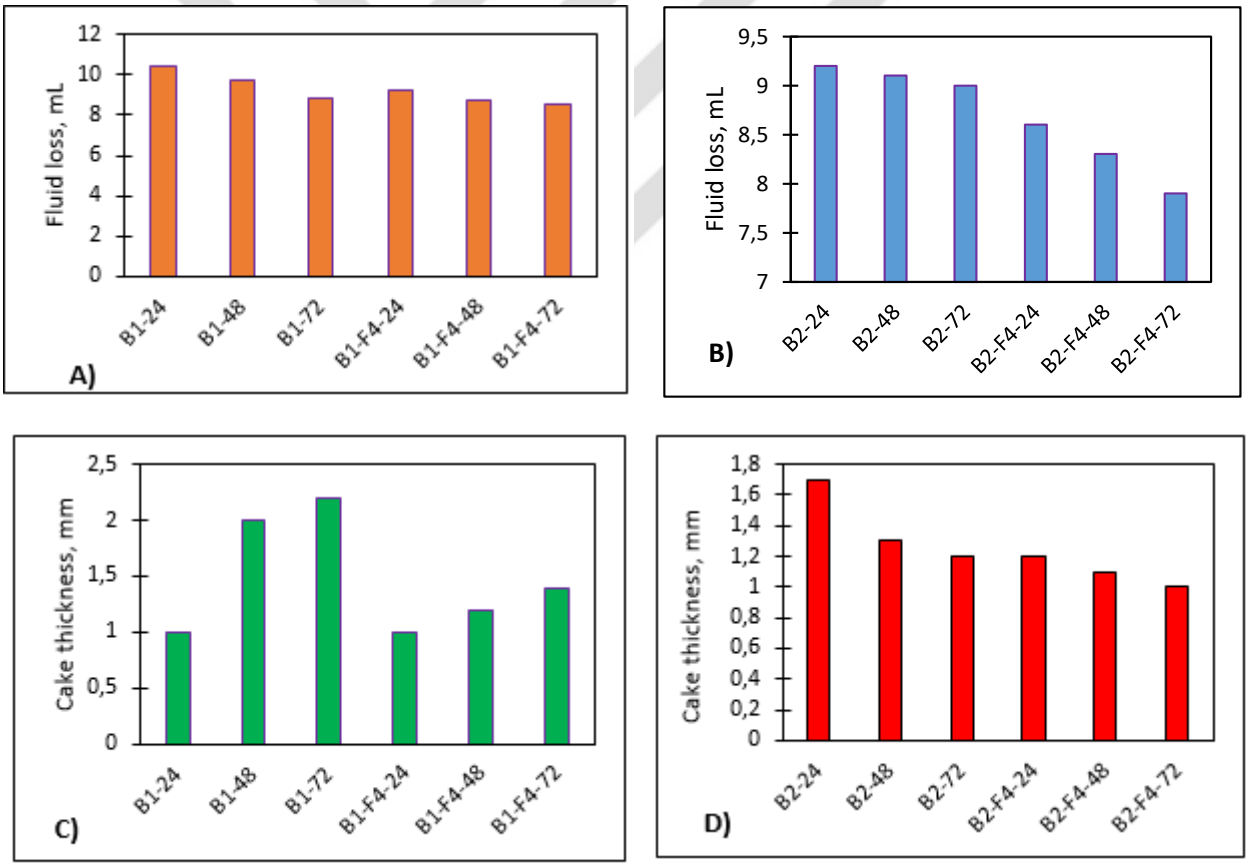

Figure 7.19. Filtration properties of optimum concentration of FA with aging time and increasing bentonite concentration.

7.6.2. Rheology and filtration test results of increasing XG and CMC concentration

Fig.7.20 demonstrates rheological properties of optimum concentration of FA, which is 4 wt%, with increasing XG and CMC concentration. From Fig.7.20A, B, it can be said that both AV and YP of bentonite mud with additive enhanced with the increasing XG concentration whereas only AV of the mud improved with increasing CMC concentration in presence of 4 wt% concentration of FA. However, increasing concentration of both XG and CMC caused an increase in PV of the mud. While AV, PV and YP increased by 20%, 14% and 26%, respectively with the increasing concentration of XG, AV increased by 9% with the increasing concentration of CMC. Increasing XG concentration also improved gel strength of the mud, as can be seen in Fig.7.20C. It provided to decrease the tixotropy by 35%. It should be noted that even increasing bentonite concentration and longer aging time didn't reduce the tixotropy of the mud. While 10 seconds, 1 minute and 10 minutes gel strengthes increased with the increasing concentration of CMC, it caused an increase in tixotropy on the mud (Fig.7.20D).

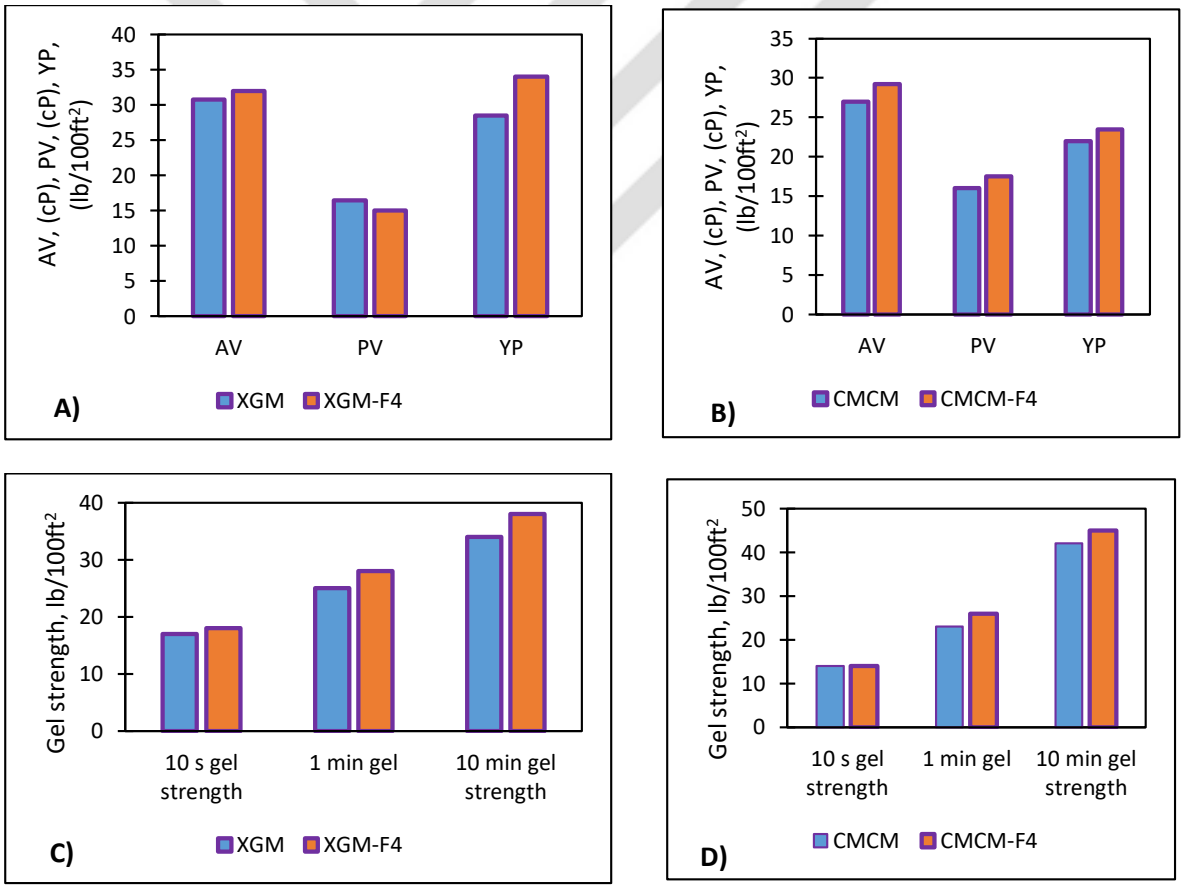

Figure 7.20. Rheological properties of optimum concentration of FA with increasing XG and CMC concentration.

Fig.7.21 presents the filtration properties of the mud with optimum concentration of FA with increasing XG and CMC concentration. While increasing XG concentration had negligible

effect of fluid loss, the fluid loss decreased with the increasing concentration of CMC, as can be seen in Fig.7.21A-B. On the other hand, From Fig.7.21C-D, it can be said that increasing concentration of both XG and CMC improved cake thickness of the mud. While mud cake thickness decreased by 10% with the increasing concentration of XG, the mud cake thickness decreased by 20% with the increasing concentration of CMC.

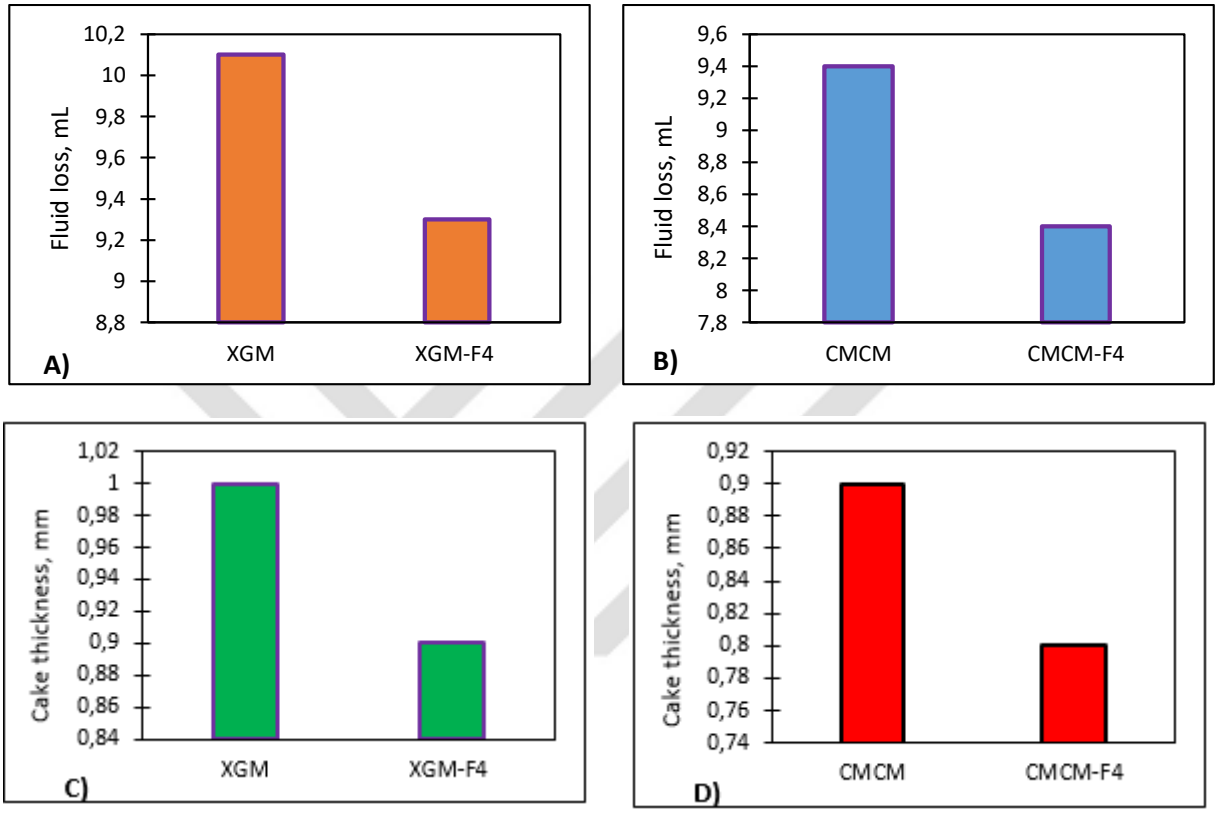

Figure 7.21. Filtration properties of optimum concentration of FA with increasing XG and CMC concentration.

7.7. Analysis of the role of fly ash in differential pressure pipe sticking

Differential sticking measurement was made with Fann Model 21,150 Differential Sticking Tester in Fig.6.17a by adding raw, sieved and ground FA with stirred media mill given in Fig.6.9 in different concentrations to the mud, whose composition is given in the Table 6.9. Subsequently, sticking coefficient and the torque values required to free drill string of the mud systems formed were calculated using Eq.6.8. Obtained results were presented below.

Fig.7.22 shows effect of raw BFA on sticking coefficient and torque of barite-weighted drilling fluid. As can be seen from the figure, sticking coefficient decreased from 0.06 to 0.045 for 0.25 wt%. Concentration more than 0.25 wt% caused an increase on the sticking coefficient. Similarly, torque value required to free stuck pipe decreased from 60 (lb-in) 45 (lb-in) for 0.25

wt% content of FA. With the introduction concentration of more than 0.25 wt%, torque started to increase.

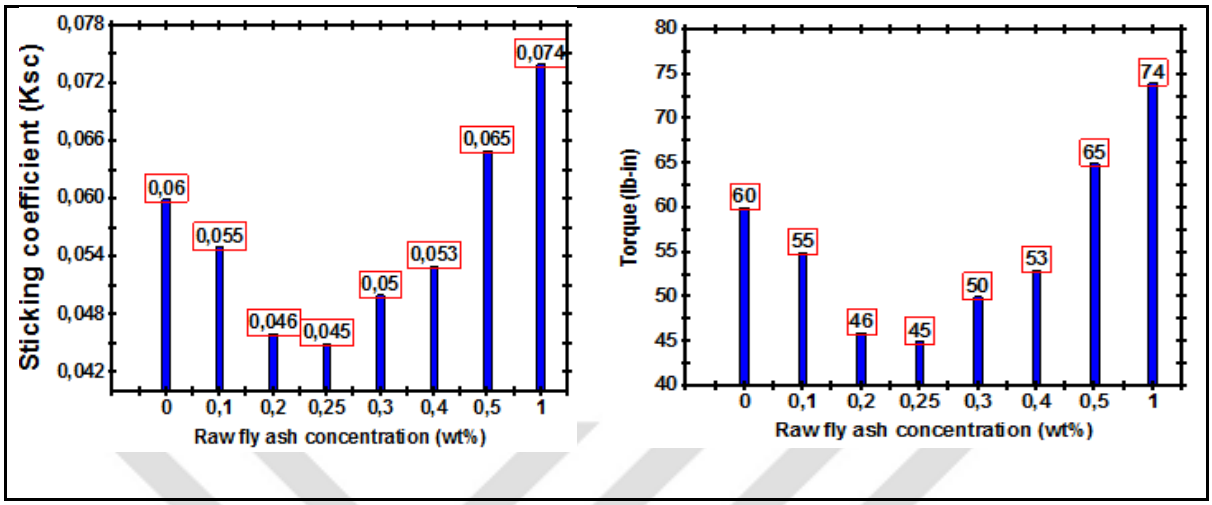

Figure 7.22. Variation of sticking coefficient and torque of the drilling mud with the increasing concentration of raw FA (Yalman et al., 2022b)

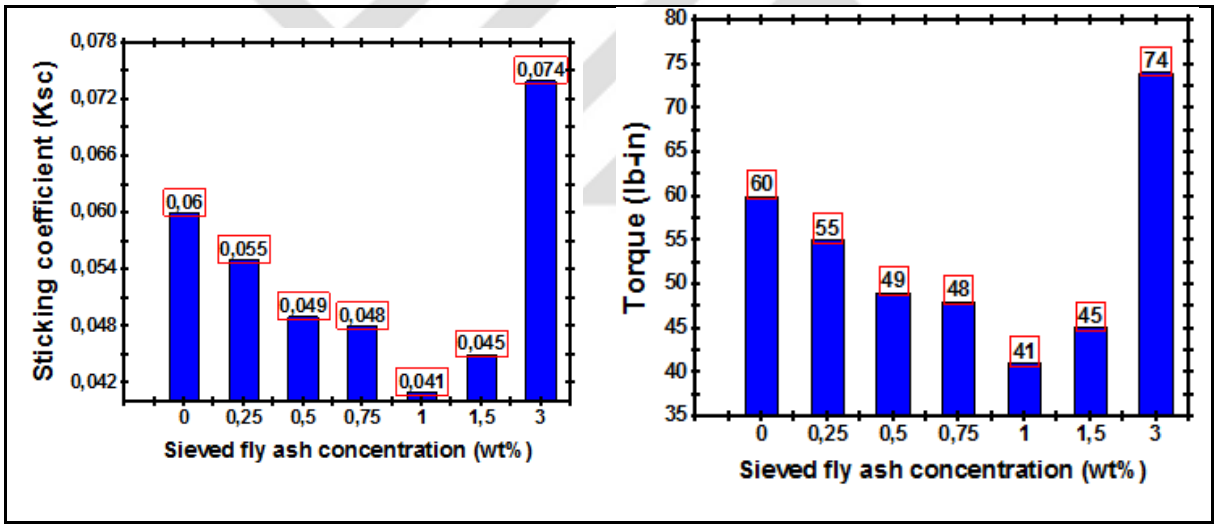

Figure 7.23. Variation of sticking coefficient and torque of the drilling mud with the increasing concentration of sieved FA (Yalman et al., 2022b)

Fig.7.23 shows effect of sieved FA on sticking coefficient of drilling fluid. Similar trend was observed as effect of raw FA. The sticking coefficient decreased up to 1.0 wt% FA. However, the sticking coefficient increased with the FA more than 1.0 wt% concentration of FA. Torque value of the fluid decreased from 60 (lb-in) to 41 (lb-in) with the employment of the 1.0 wt% content of sieved FA.

Fig.7.24 shows effect of ground FA on the sticking coefficient and torque of drilling mud. Sticking coefficient and torque of the barite weighted drilling fluid decreased from 0.06 to 0.033

and 60 (lb-in) to 33 (lb-in), respectively with the employment of 0.3 wt% concentration of the ground FA. Employment of more than 0.3 wt% concentration yielded an increasing on the sticking coefficient and torque values.

Comparative results of the drilling fluid with raw, sieved and ground FA were given in Fig.7.25 for a better understanding of the effect of different particle size of FA on differential sticking tendency of the drilling fluid. From the figure, it is clear that drilling fluid incorporated with ground FA exhibited better results than those of drilling fluid with the FA both in raw and sieved form. The lowest sticking coefficient and torque value was obtained with drilling fluid blended with ground FA, followed by sieved and raw FA.

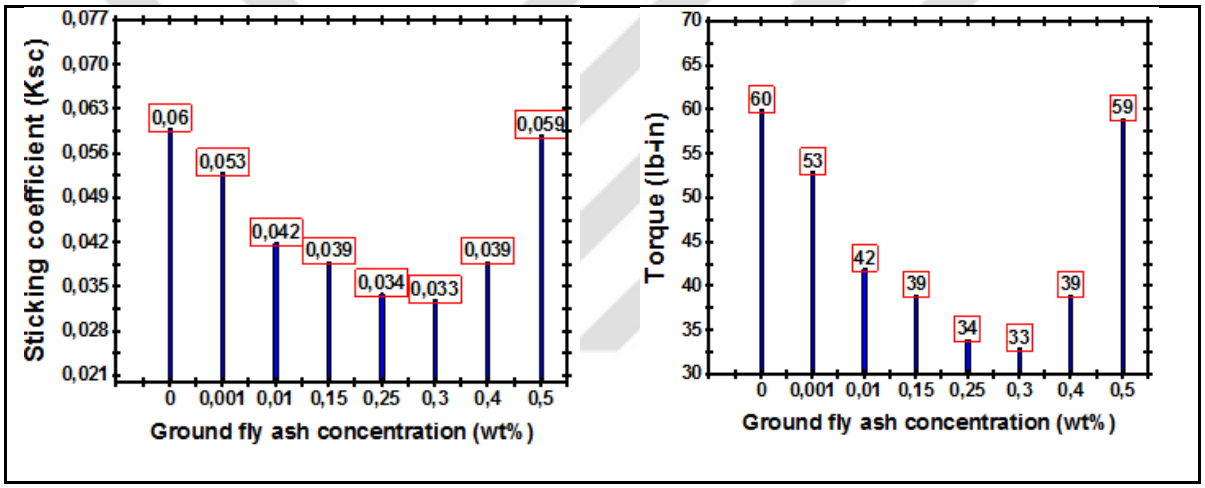

Figure 7.24 Variation of sticking coefficient and torque of the drilling mud with the increasing concentration of ground FA (Yalman et al., 2022b)

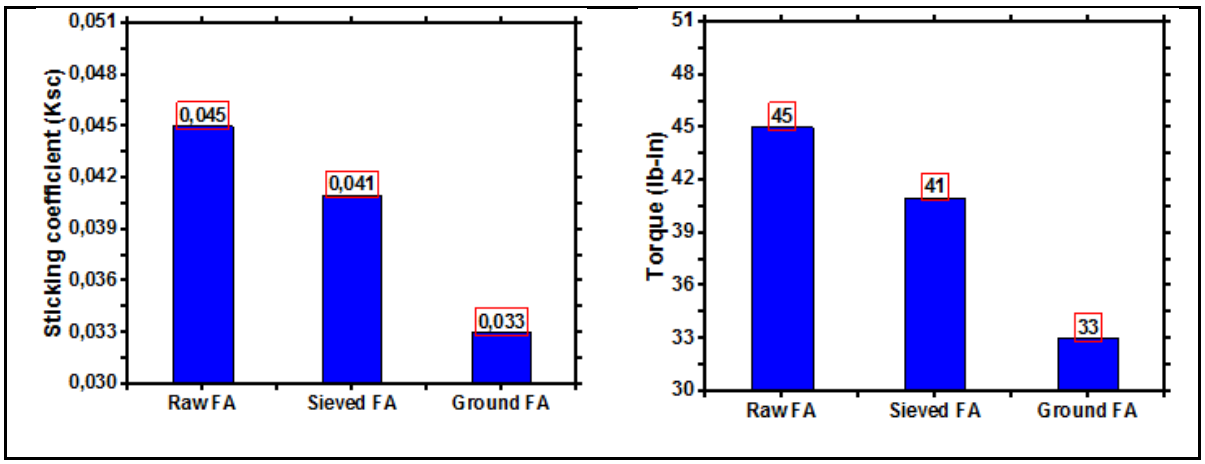

Figure 7.25. Variation of sticking coefficient and torque of the drilling mud with the different particle size of FA (Yalman et al., 2022b)

In addition, rheological and filtration properties of the samples were measured at room temperature. Table 12.1-12.3 given in Appendix-B shows the results of the drilling fluid formulated with raw FA, sieved FA and ground FA, respectively.

7.8. The role of rice husk ash in assessment of flow behaviour of bentonite mud with additives and wellbore hydraulics

Performance of RHA in drilling fluid was assessed based on the bentonite mud with additives (XG and CMC) whose composition can be seen in Table 6.8. RHA with various concentration (2 wt%, 4wt%, 7 wt%, 9 wt%, 12.5 wt% and 15 wt%) introduced to the drilling fluid. Milestone given in Fig.6.9 were followed in the evaluation performance of RHA. Observed results were given in below.

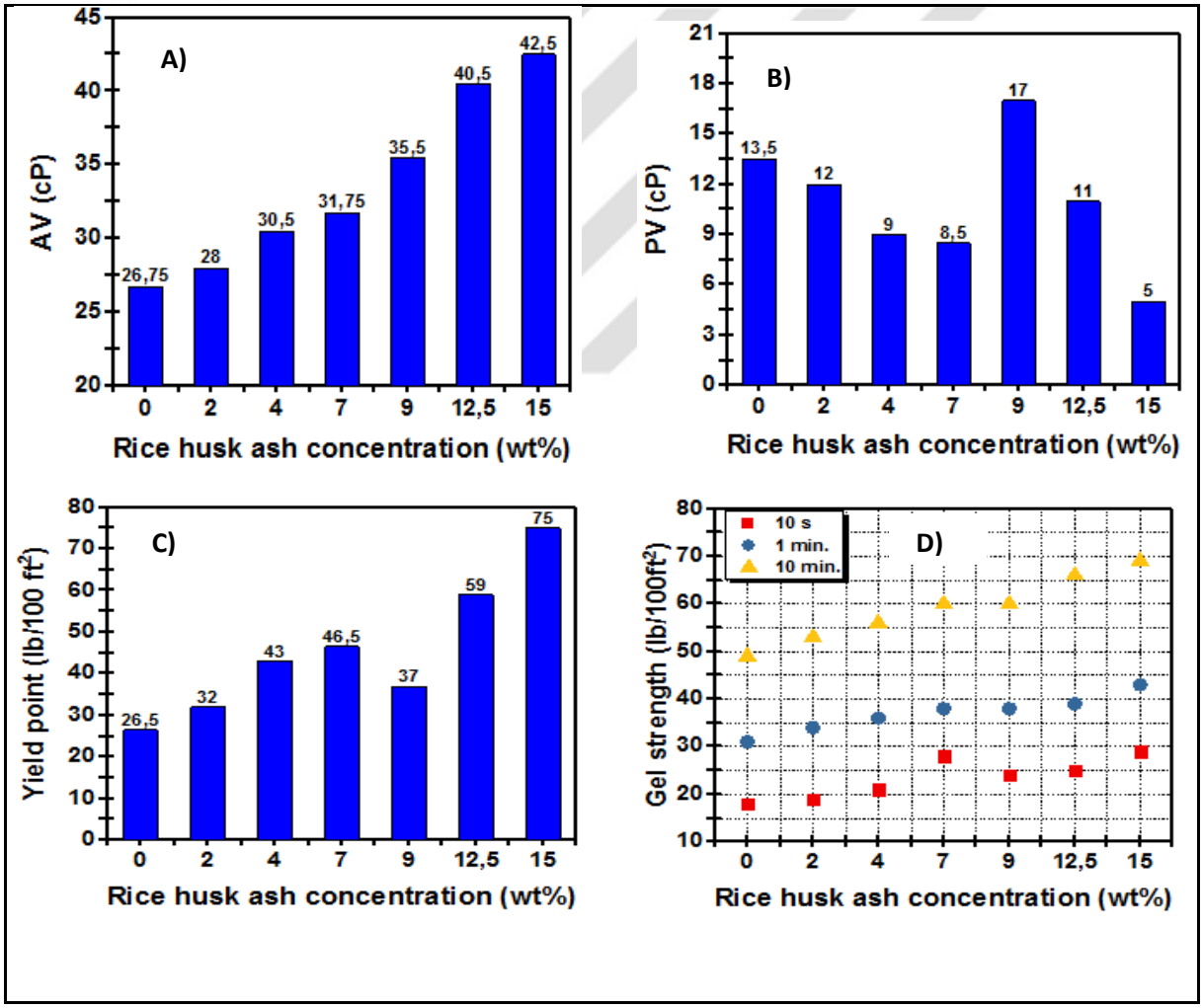

Figure 7.26. Rheological properties of bentonite mud with additive including RHA (Yalman et al., 2021b).

Stable trend was observed with the increasing concentration of RHA with respect to rheology. AV and YP of bentonite mud with additive increased constantly with the increasing concentration of RHA (Fig.7.26A, C). Highest AV and YP magnitude were obtained with the

driling fluid blended with 15 wt% concentration of RHA compared to driling fluid with the other concentration of RHA and reference fluid. In contrast, PV decreased up to 7.0 wt% concentration of RHA (Fig.7.26B). While the highest PV was obtained with 9.0 wt% RHA, lowest PV was seen when 15.0 wt% content of RHA was added to the drilling fluid. Fig.7.26D shows that the 10 sec., 1 min. and 10 min gel strength increased constantly with the increasing concentration of RHA. Whereas the highest tixotropy was obtained with 7.0 wt% concentration of RHA, the lowest tixotropy was observed with 15.0 wt% content of RHA.

Performance of RHA was also evaluated based on cutting carrying index, minimum annular velocity needed for the well cleaning efficiently and flow behaviour index of the fluid. Results calculated by Eq.6.1 and Eq.6.2 were given in Table 7.1.

Results show that hydraulic performance of driling fluid improved with the employment of RHA. Better performance was achived for each concentration of RHA compared to reference fluid without RHA. It worths to be noted that the optimum hydraulic performance was obtained with the driling fluid with 15 wt% concentration of RHA. Cutting carrying index of the reference fluid increased from 3.183 to 54.700 with the employment of the 15 wt% concentration of RHA. Moreover, minimum annular velocity needed for the well cleaning efficiently and flow behaviour index of the fluid decreased from 31.412 ft/min to 1.828 ft/min and from 0.419 to 0.087, respectively.

Table 7.1. CCI, Va and n of water based bentonite mud with additive at different RHA concentrations (Yalman et al., 2021b).

Concentration of RHA (wt%)	CCI	Va	n
0	3.183	31.412	0.419
2	5.516	18.126	0.347
4	13.855	7.217	0.230
7	17.103	5.846	0.207
9	5.258	19.015	0.394
12.5	22.101	4.5245	0.210
15	54.700	1.828	0.087

Fig.7.27 show density results of the drilling fluid blended with the various concentration of RHA. From the figure, it is seen that the density of bentonite mud with additive increased with the increasing concentration of RHA, as expected, since the solid mass in the liquid increased.

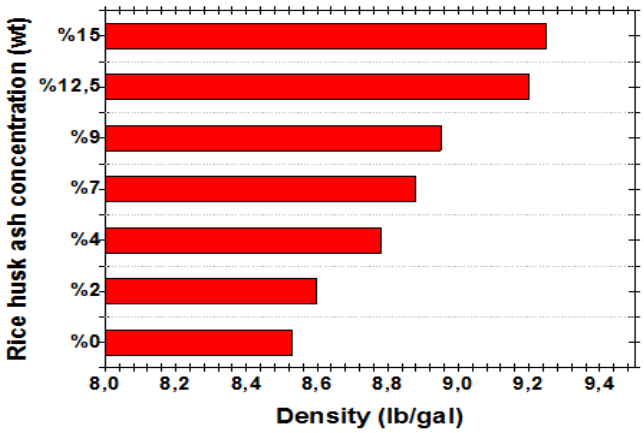

Figure 7.27. Density of bentonite mud with additive including RHA

7.9. The possibility of fly ash and rice husk ash as substitutes in portland cement based slurries

Portland cement slurry was prepared in ambient conditions according to API standards as a reference slurry in the development of cement slurry. In this context, distilled water was put into the cement blender and then cement powder was added and mixed at low speed for 15 seconds and then mixed at high speed for 35 seconds. Portland cement composition used in the thesis was given in Table 6.10.

Cement slurry and drilling fluid mixing (compatibility) tests: For the compatibility test, firstly, the mixing process of cement powder and drilling mud was carried out. In this context, drilling mud, the composition of which is given in Table 6.2, was added to the portland cement slurry prepared at the rate of 5% and 10% by weight of cement. Thereby, cement-drilling mud hybride slurry was formulated by stirring the slurry with a cement mixer at 400 rpm for 30 seconds. Thus, total weight of the hybride slurry prepared and the weight of the reference cement slurry, which does not contain drilling fluid, were kept constant, and this allowed the results to be evaluated carefully. For the cement part milestone given in Fig.6.12 was performed and results were given in below.

7.9.1. Experimental investigation on partial replacement of cement with fly ash and rice husk ash at ambient conditions

7.9.1.1. Density measurement results

The cement has been replaced by FA accordingly in the range of 0% (without FA), 10%, 15%, 20%, % 30%, 40% by weight of cement. The symbols of P1, P1F-10, P1F-15, P1F-20, P1F30 refer to neat portland cement slurry (replacement is 0%, reference sample), replacement of cement with FA in 10%, 15%, 20%, 30%, by weight of cement, respectively. P1F30R15 refers

to replacement 30% cement by FA and 15% by RHA. Explanation of the codes of the formulated samples was given in Table 6.11. Results showed that as replacement of cement by FA increased, the density of P1 decreased, in Fig.7.28A. The reason for the decrease in density can be attributed to the fact that the particle density of FA is lower than that of portland cement. From Fig.7.28B, it was seen that the further replacement of cement by RHA decreased density of P1F30 sample.

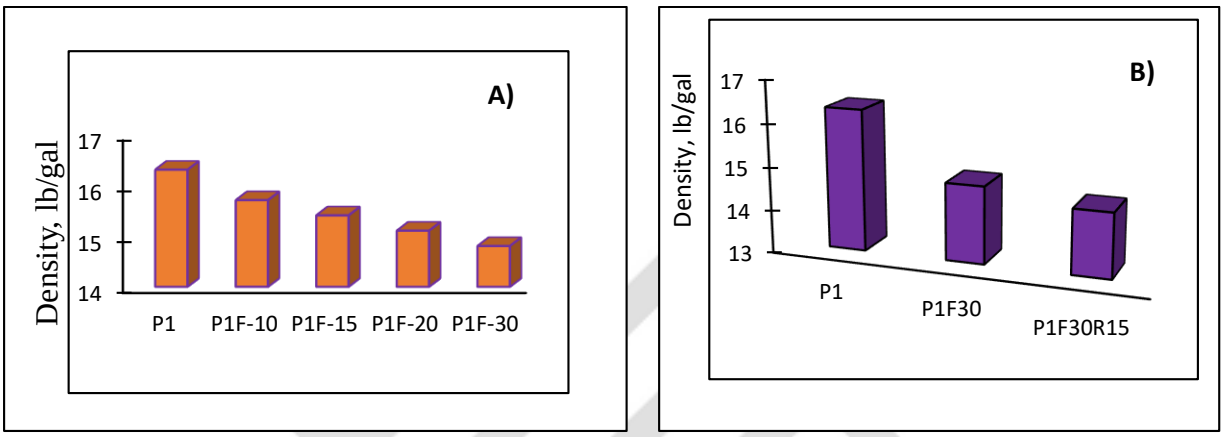

Figure 7.28. Density of portland cement and cement replacement by FA and RHA slurries

7.9.1.2. Rheology results

Cement viscosity parameter plays a very important role in the pumping process. Provided that the cement requirement is met, low-viscosity cement is easier to pump as it requires less energy in the pumping process, and this can contribute to the reduction of the cost of the cementing operation. The shear stress of slurry increased with the replacement of cement by FA, as it is shown in Fig.7.29A. The lowest shear stress was obtained in the slurry with 30% displacement compared to the slurries in which 10%, 15% and 20% of the cement weight was replaced by FA. From Fig.7.29B, it was observed that replacement of 30% cement by FA and 15% by RHA lead to achieve lower shear stresses than neat cement slurry until 350 1/s rotation speed.

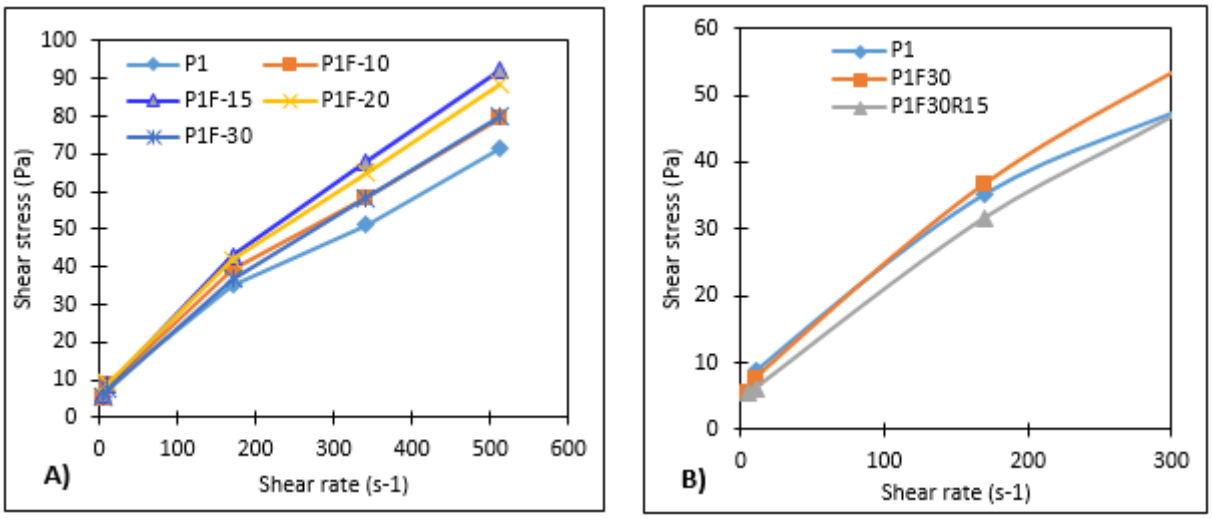

Figure 7.29. Rheological properties of portland cement and cement replacement by FA and RHA slurries

Retention of the water phase of the cement is very important in terms of performing its functions. The loss of the water phase of the cement may increase the risk of cracks and channels in the cement. Fig.7.30A showed that the fluid loss of cement slurry decreased with the increasing percentage of replace cement by FA. Also, P1F30R15 sample showed the lower fluid loss than P1F30 and P1 samples, as it is shown in Fig.7.30B.

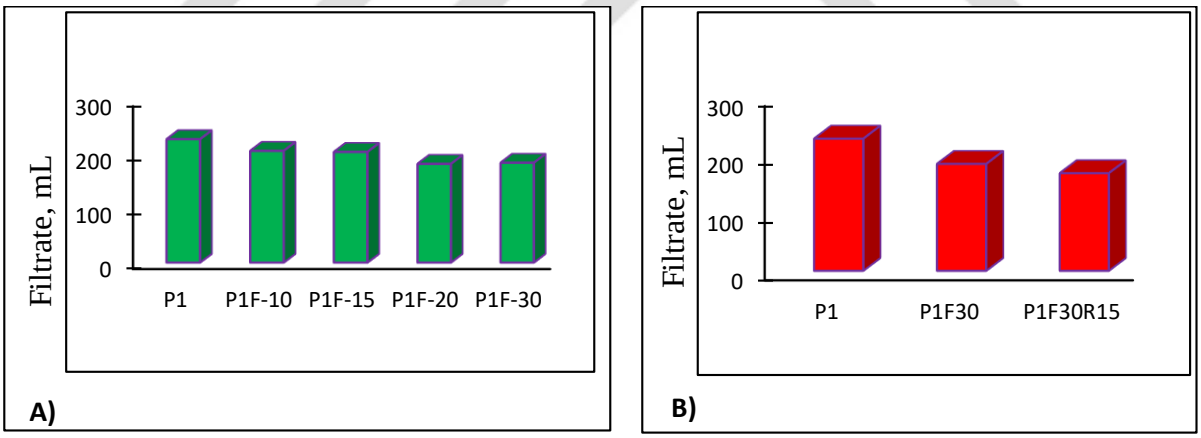

Figure 7.30. Filtration properties of portland cement and cement replacement by FA and RHA slurries

7.9.2. Experimental investigation on cement slurry and mud mixing tests at ambient conditions

7.9.2.1. Density results

Contamination of cement slurry with drilling fluid is one of the main cause of cementing failures in well drilling. In order to analyze this, firstly, portland cement slurries were prepared and mixed with drilling mud at 0%, 5% and 10% by weight of cement. Composition of the drilling fluid was given in Table 6.12 and properties of the drilling mud that is added to slurries

at the ambient conditions and elevated temperature are shown in Table 7.2 and Table 7.3, respectively. The codes P1M-5 and P1M-10 refer to mud contamination 5%, 10% by weight of cement for neat cement, respectively. Also, the codes P1F30M-5, P1F30M-10 refer replace of %30 cement by FA with 5% mud contamination and replace of 30% cement by FA with 10% mud contamination. Fig.7.31 shows that the increasing concentration of mud contamination decreases the density of neat cement slurry, P1F30 and P1F30R15 samples. It was observed that as amount of mud contamination increased the density of these slurries decreased. The density of P1 sample was higher than P1F30 and P1F30R15 samples for the same ratio of drilling mud contamination. The lowest density was obtained in P1F30R15 sample.

Table 7.2. Drilling fluid properties at ambient condition

Parameters		**Values**
Dial reading ((θ)	600	32
	300	22
	200	15
	100	10
	6	3
	3	2
Gel strength at 10 s		3
Gel strength at 10 min.		3
Apparent Viscosity, cP		16
Plastic Viscosity, cP		10
Yield Point, lb/100ft^2		12
Cake Thickness, mm		0.5
Filtrate ml/30min		7
Density, ppg		8.8

Table 7.3. Viscometer Readings at elevated temperatures

Temperatures (°F)		85	140	175
Dial Reading (θ)	600	26	17	14
	300	17	11.5	10
	200	14	9	8
	100	10	7	6
	60	6	5.5	5
	30	4.5	4	3.8
	6	3.5	2.5	2.25
	3	2.5	2	2
	10 sec gel st.	4	3	3
	1 min gel st.	4	3	3.5
	10 min gel st.	4	3.5	4

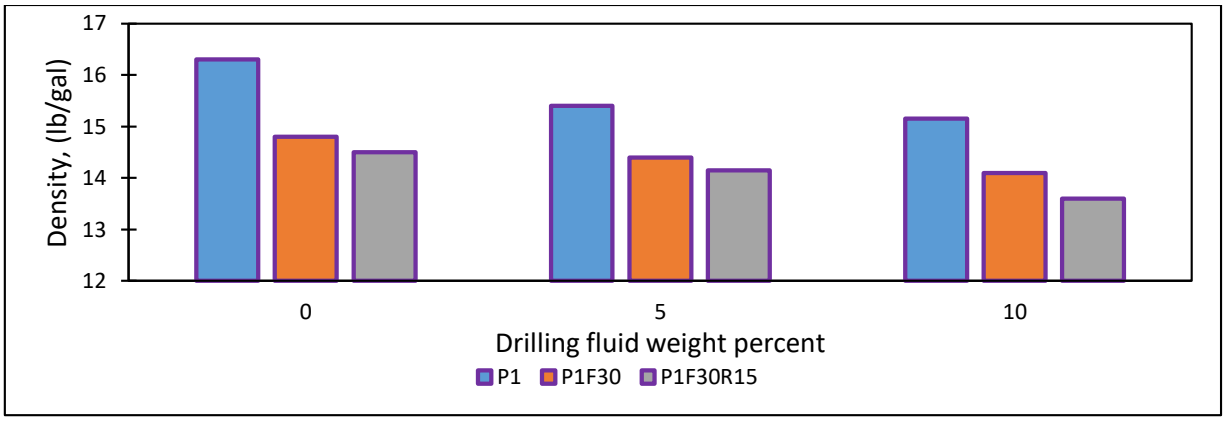

Figure 7.31. Density of Portland cement and cement replacement by FA and RHA slurries with various dosages of water based drilling mud

7.9.2.2. Rheology test results

The shear stress of neat portland cement slurry decreased with the increasing dosage of drilling mud (Fig.7.32A) while it is observed that the shear stress of replace 30% cement by FA generally increased, slightly (Fig.7.32B). On the other hand, the increasing mud contamination increased the fluid loss of both P1 and P1F30 samples. As can be seen in Fig.7.32C, the increasing concentration of mud contamination decreased shear stressess values of P1F30R15 sample for each rotation speed.

7.9.2.3. Fluid loss test results

From the Fig.7.33, it is clear that addition of mud in to slurries increased their fluid loss. Replacement 30% cement by FA had lower filtrate volme than neat cement slurry for same mud contamination. The filtrate volume of P1F30R15 sample was lower than both P1 and P1F30 samples for each amount of mud contamination and it was followed by 30% cement replacement by FA and neat cement.

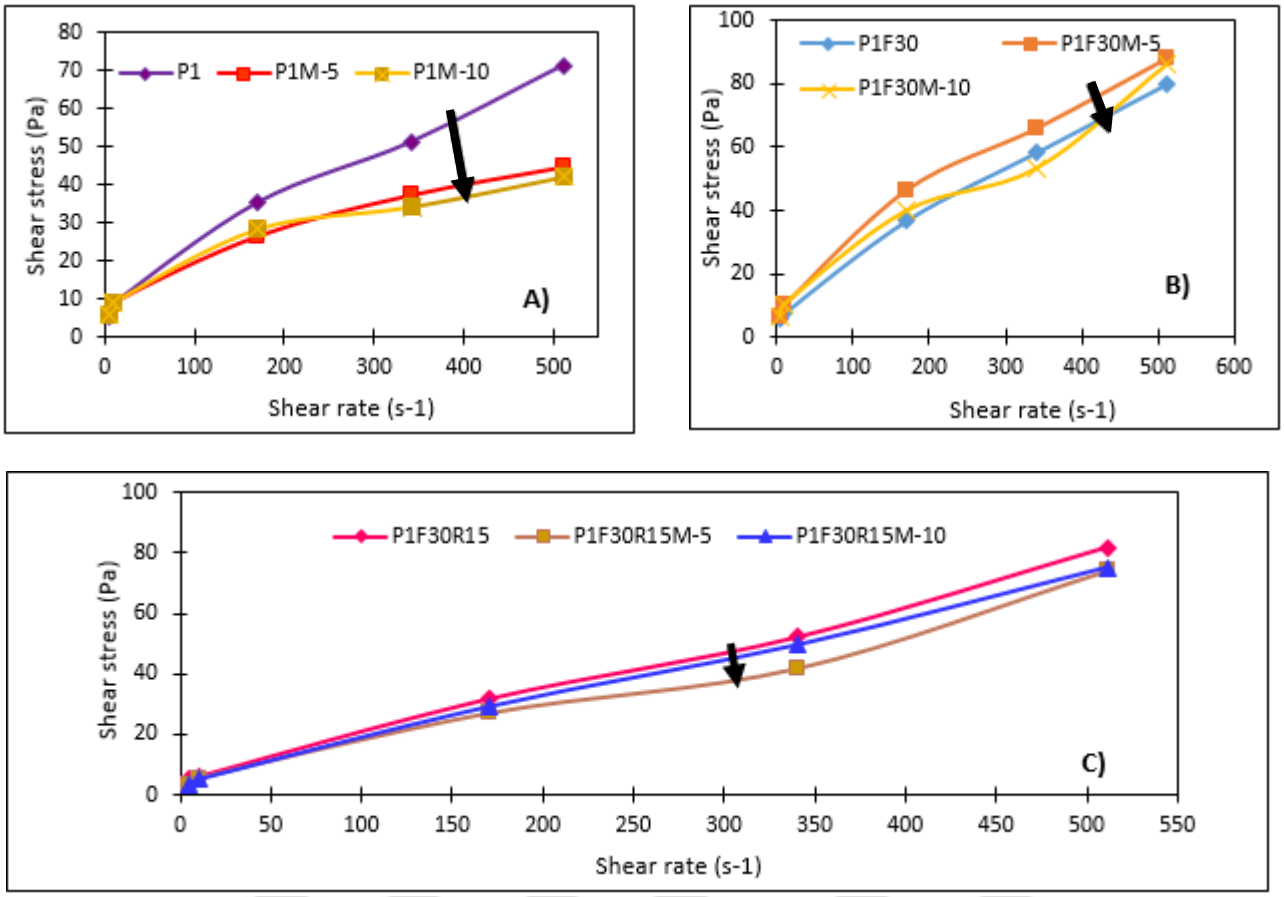

Figure 7.32. Rheological properties of portland cement and cement replacement by FA and RHA slurries with various dosages of water based drilling mud at ambient conditions.

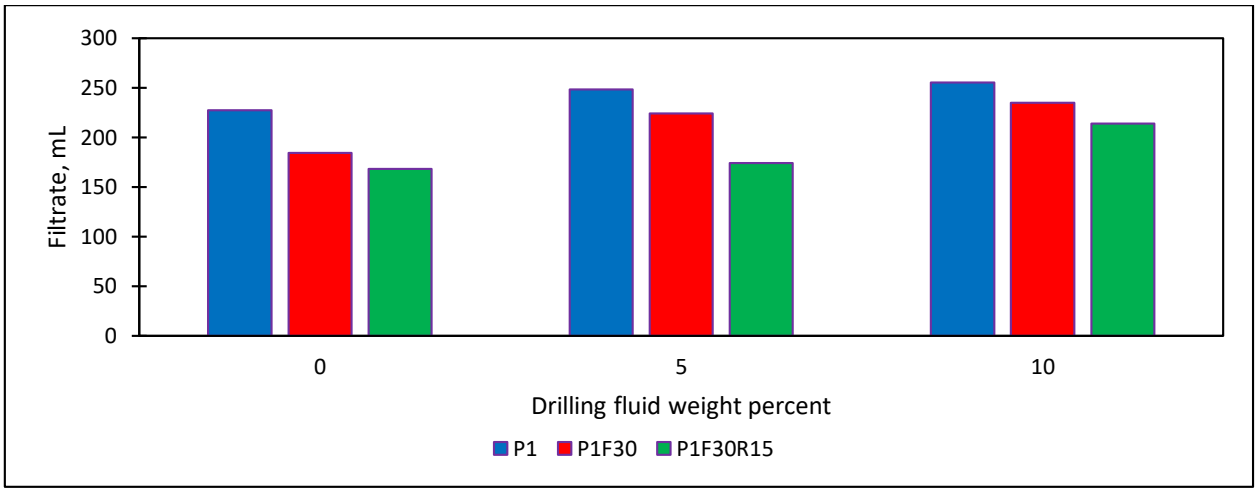

Figure 7.33. Filtration properties of portland cement and cement replacement by FA and RHA slurries with various dosages of water based drilling mud at elevated temperatures

7.9.3. Investigation of role of particle size of fly ash in cement

P1F30-S, P1F30G-1, P1F30G-2 refer to cement replacement by 30% sieved FA, 30%-30 min ground FA and 30%-120 min ground FA, respectively. Explanation of the code of the formulated samples can be seen in Table 6.11. As it is seen in Fig.7.34A, the density of cement without FA was higher than the density of slurry with 30% cement replacement by FA for sieved and ground type. As grinding duration increased the density of slurry increased. This indicate that as particle size of FA to be used in cement decreases the density of slurry increases. This can be attributed to the increase in particle density due to particle size reduction results from increasing grinding time. Particle density of the ashes was determined by the pycnometer method used liquid was alcohol. For each type of FA, measurement was identified three times and the average values were recorded. Particle density results obtained with pycnometer were given in Table 7.4. Pycnometer results reveal that as grinding time increases, particle density increases. However, the main reason for these results can be clearly determined by Scanning Electron Microscope (SEM) analysis. The SEM analysis was performed with EOL 8600 Superprobe type microscope and images were given in Fig.12.8 in Appendix A. The images were taken under same magnification value. As can be seen, as the grinding time increases, the particle size of FA decreases. In addition, the particles form a more compact structure and the space between particles decreases. Therefore, particle density increases. Results show that as particle size increases the shear stresses also increase. Fig.7.34B showed that slurry formulated by replacing 30% of the cement with FA grinded for 120 minutes had the highest viscosiy. It was followed by slurry formulated by FA grinded for 30 minutes and sieved (unground). Also the lowest fluid loss was observed when the %30 cement was replaced by sieved FA, as it is seen that from Fig.7.34C.

Table 7.4. Particle density results obtained from pycnometer

Samples	Particle density (g/cm^3)
Raw FA	1.68
30 min. grinding FA	2.05
60 min. grinding FA	2.17
120 min. grinding FA	2.28

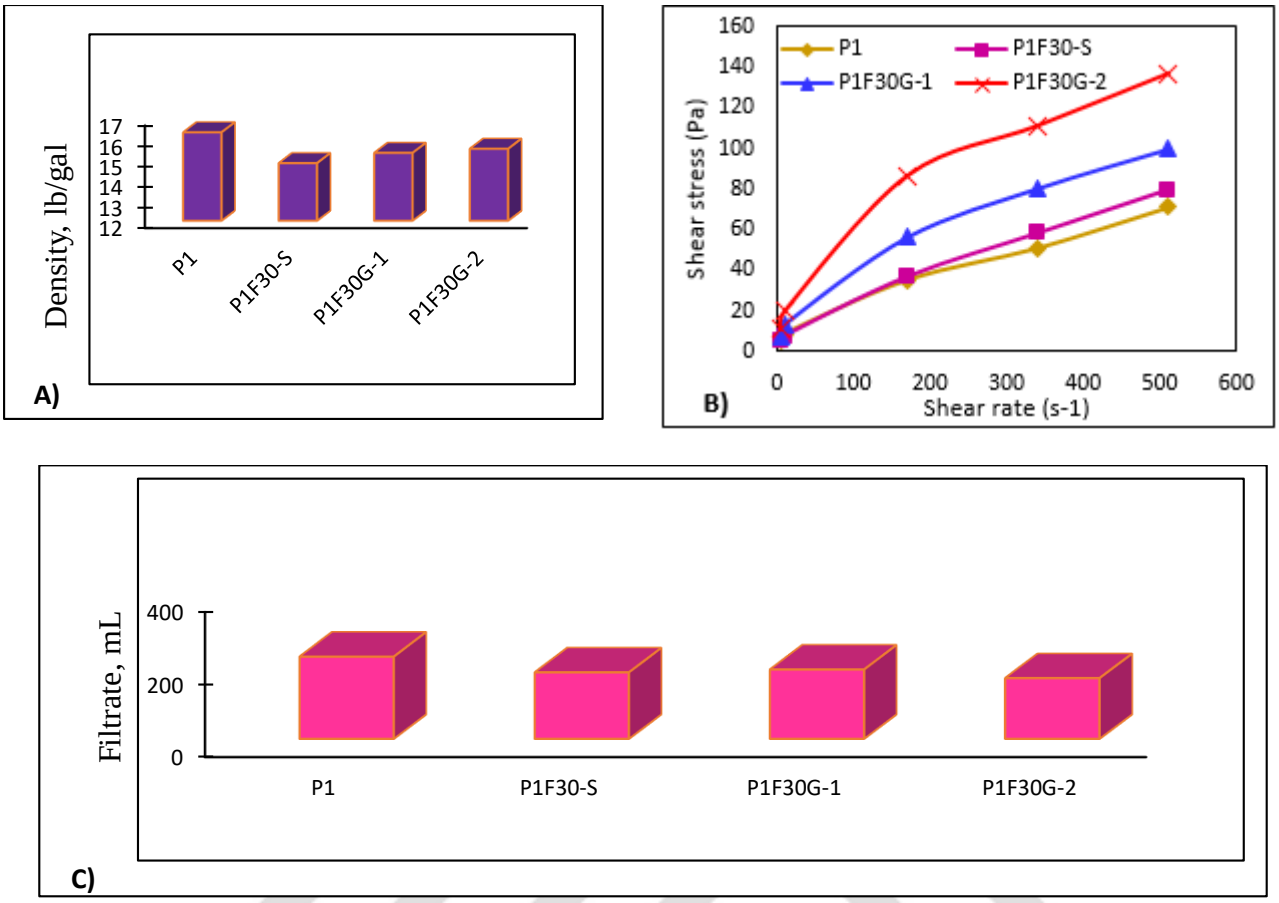

Figure 7.34. Rheological and filtration properties of portland cement and cement replacement by fly sieved FA, 30 min ground FA and 60 min ground FA. A) Density, B) Rheology, C) Filtration

7.9.4. Experimental investigation on partial replacement of cement with fly ash and rice husk ash at elevated temperature

Results reveal that rheology profile of the cement slurries highly affected by increasing temperature. While shear stresses of the portland cement experienced increased values under increasing temperature, shear stress of the developed slurry (P1F30R15) exhibited an reduced rheology profile with the increasing temperature. This indicates that while resistance to flow of the portland cement slurries increased when it exposed to increased temperature, resistance to flow of the developed slurry decreases under same conditions. As shown in Fig.7.35A, slurry without FA or RHA (P1) exhibited increased shear streesses at each rotation speeds with the increasing temperature. On the other hand, magnitude of the shear stress of the slurry that replacing cement by 10% BFA in terms of weight of cement decreased with the increasing temperature at each shear rate, as can be seen in Fig.7.35B.

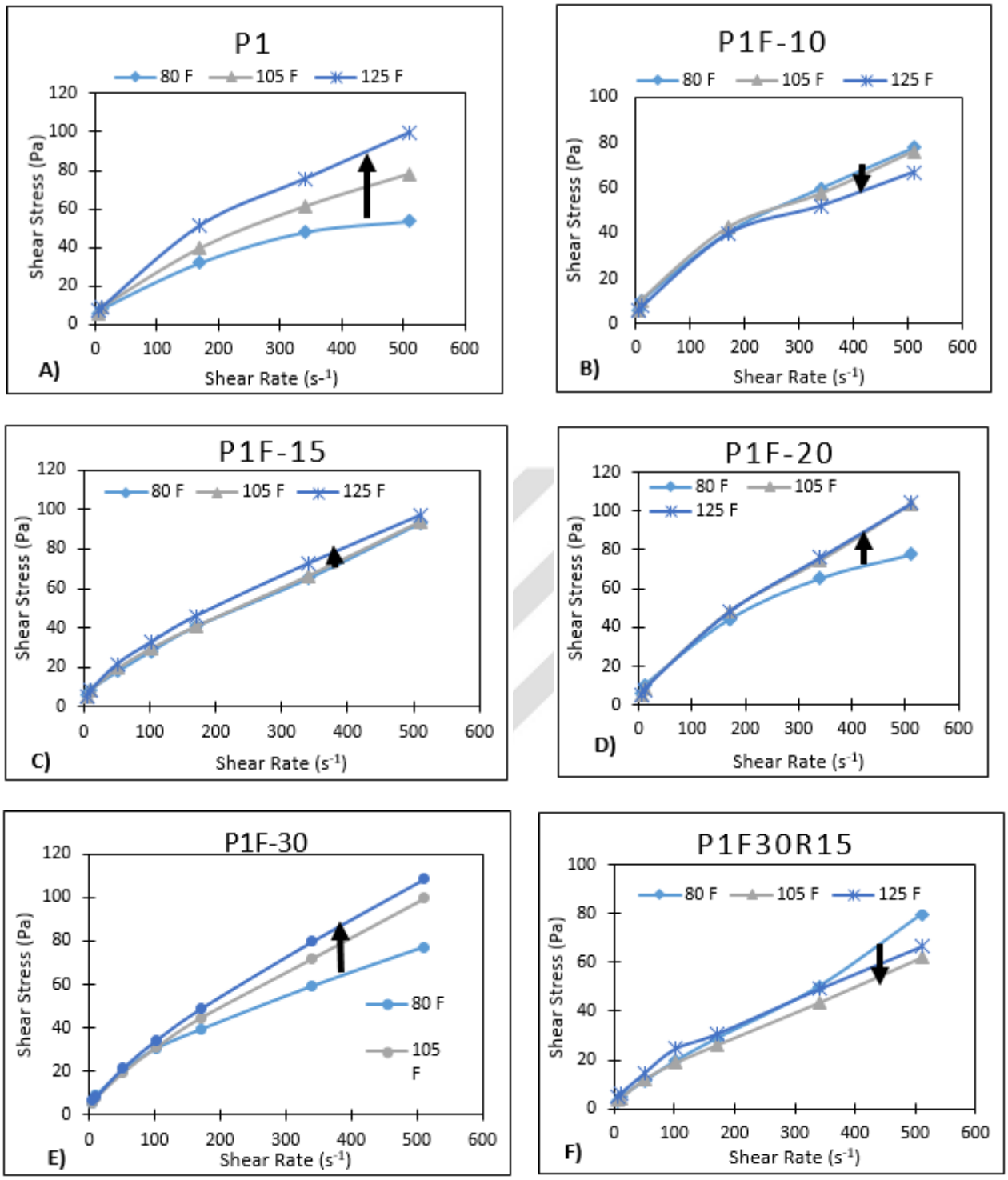

Figure 7.35. Rheological properties of neat portland cement and cement slurry replaced by FA and RHA at elevated temperatures

Samples replacing cement by 15%, 20%, 30% FA and neat cement slurry without FA had higher shear stress at each shear rate with the increasing temperature, as it can be seen from Fig.7.35C, Fig.7.35D, Fig.7.35E. However, P1F30R15 sample had lower viscosity than both P1F30 and

P1 sample. It was found that the rheological properties of slurry that replaced cement by 30% FA and 15% RHA continued to improve at higher temperatures, as shown in Fig.7.35F.

7.9.5. Experimental investigation on partial replacement of cement with fly ash and rice husk ash in presence of water based drilling mud at elevated temperature

Portland cement slurries also may suffer from loss of pumpability (increase in viscosity) when contaminated with water based drilling mud under increasing temperature.

Fig.7.36A and Fig.7.36B demonstrated that portland cement slurries contaminated with water based drilling mud became progressively more viscous as the level of temperature increases under both 5 wt% drilling mud and 10 wt% drilling mud. When these figures were compared with the neat portland cement slurry without mud contamination (Fig.7.35A), it is seen that shear stress of portland cement slurry decreases when it exposed to 5 wt% and 10 wt% drilling mud contamination. On the other hand, Fig.7.36C and Fig. 7.36D indicated that rheology measurements proved that slurry replaced cement by 30% in terms of weight exhibited better contamination resistance compared to portland cement slurries. It had lower viscosity at each shear rate, when it contaminated 5% and 10% drilling mud by weight of cement under elevated temparature. In a real case scenario when mud contamination occurs, unlike portland cement, which suffers from may become too viscous to pump, these slurries remains pumpable. In a real field scenario, the increase in viscosity causes by temperature during cement placement could lead to serious operational problems including high pumping pressure to place the cement slurry behind casing and associated unwanted fracturing of the geological formation. From Fig.7.36E and Fig.7.36F, it can be said that the temperature enhanced behavior of P1F30R15 sample. Its viscosity decreased with the increasing temperature when contamibated both 5% drilling mud and 10% drilling mud. Also, this slurry exhibited better mud contamination resistance then P1F30 and P1 samples.

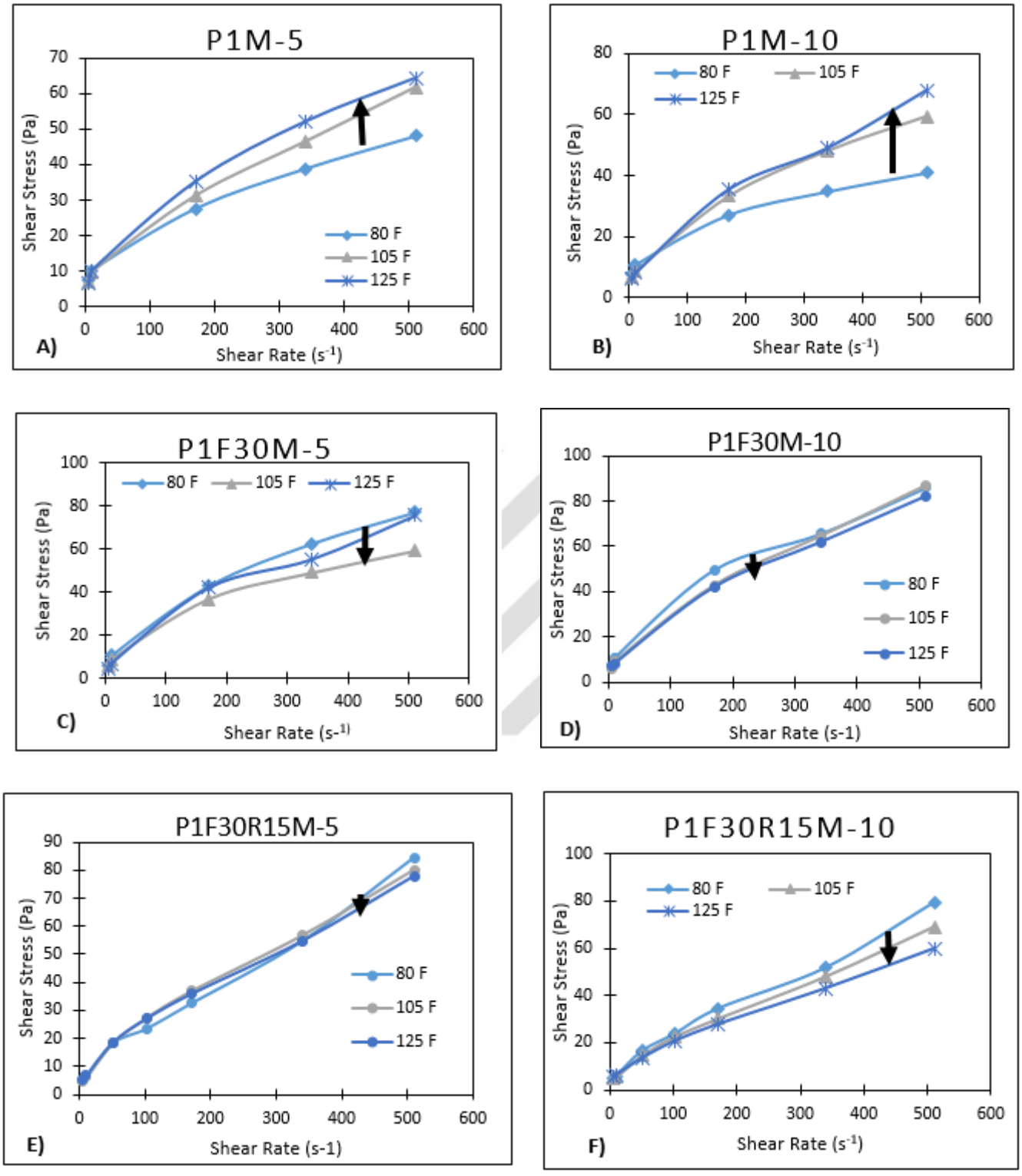

Figure 7.36. Rheological properties of portland cement and cement replacement by FA and RHA slurries with various dosages of water based drilling mud at elevated temperatures

7.9.6. Experimental investigation on partial replacement of cement with fly ash and rice husk ash at constant temperature in presence and absence of water based drilling mud

When the behavior of these slurries analyzed at the same temperature, R1F30R15 showed lower shear stress up to about 150 s^{-1} shear rate than both P1 and P1F30. Beyond which, P1 starts to have higher value than P1F30R15 at 80 ºF temperature, as shown in Fig.7.37A. Same trends was observed both at 105 ºF and 125 ºF temperature, in Fig.7.37B and Fig.7.37C. However, P1F30R15 shows lowest viscosity until about 200 s^{-1} at 105 ºF temperature. Also, P1F30 has lower viscosity than P1 up to 50 s^{-1}.

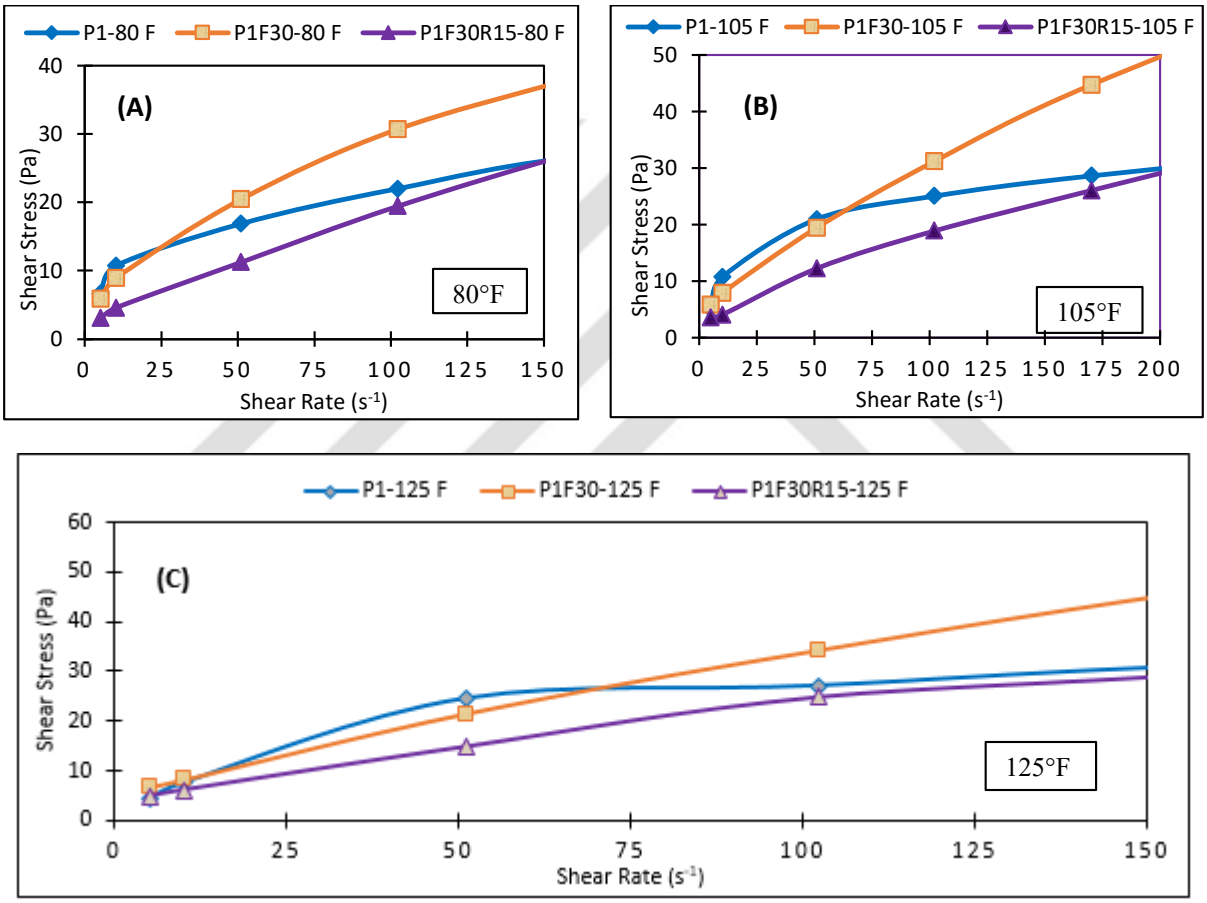

Figure 7.37. Rheological properties of portland cement and cement replacement by FA and RHA slurries at constant temperatures A) 80 ºF, B) 105 ºF, C) 125 ºF.

Results reveal that mud contamination has a significant effect on rheology profile of cement slurry. Shear stress of the slurries increases with the increasing mud contamination at the constant shear rate compared to slurry without mud contamination for both portland cement and developed slurries. This indicates that resistance to flow of the slurries experienced a reduction when they exposed to mud contamination. However, viscosity of the developed slurry Results obtained showed that both P1F30 and P1F30R15 had lower viscosity than P1 and

P1F30R15 had the lowest shear stress than among these samples up to 20 1/s rotation speeds when these slurries exposured to 5 wt% mud contamination by weight of cement at 80 ºF temperature, as shown in Fig.7.38A. At high shear rates P1F30 and P1F30R15 showed higher viscosity than P1 at this temperature. From Fig.7.38B and Fig.7.38C, it can be said that same trend was also seen at 105 ºF and 125 ºF temperatures.

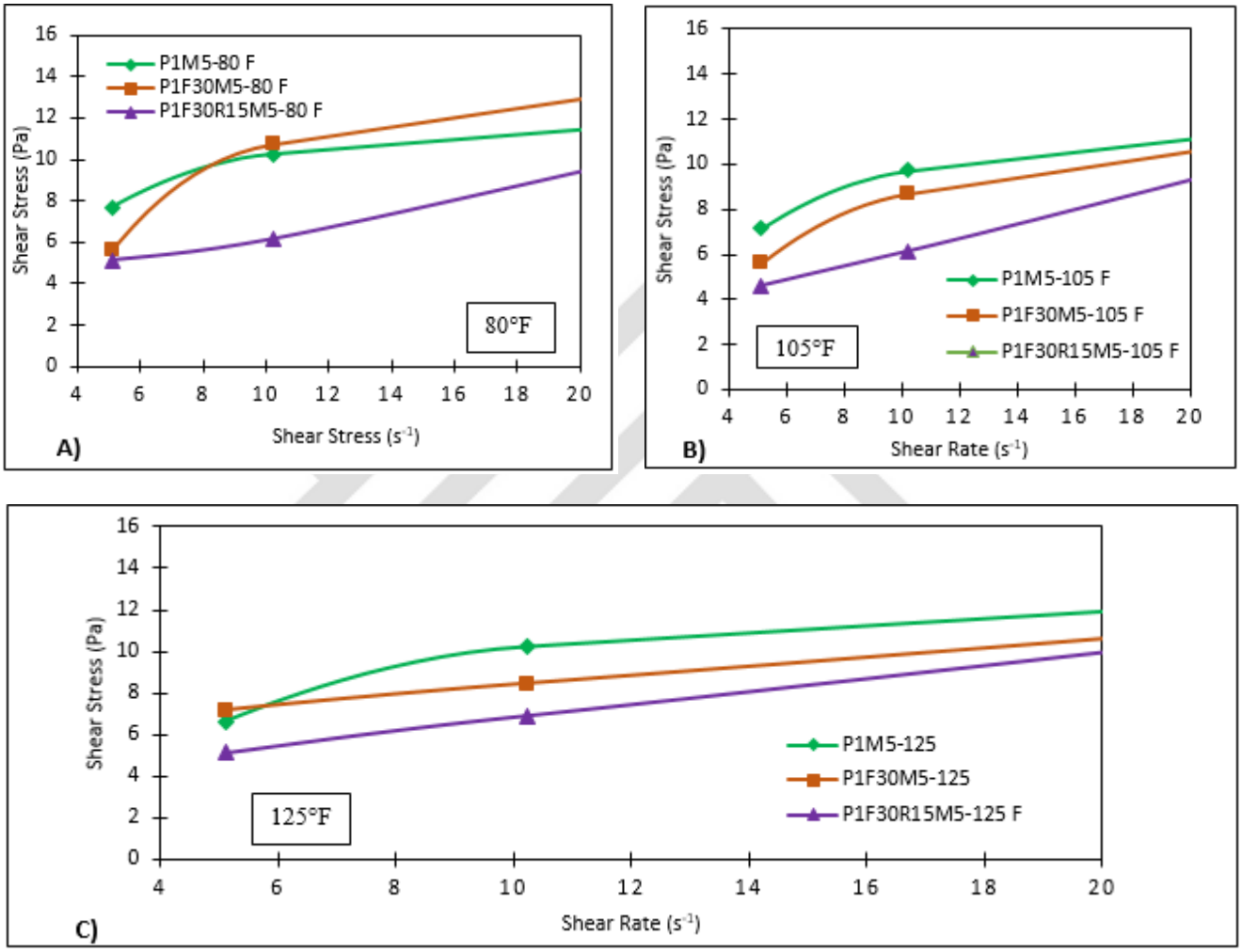

Figure 7.38. Rheological properties of Portland cement and cement replacement by FA and RHA slurries with 5% water based drilling mud at constant temperatures A) 80 ºF, B) 105 ºF, C) 125 ºF.

In case P1F30R15 exposure to 10% mud contamination by weight of cement showed better performance compared to case under 5% mud contamination for all temperature studied. It has lower shear stress than P1 up to about 50 s^{-1} when exposure to %10 mud contamination at 80 ºF temperature, as shown in Fig.7.39A. Fig.7.39B indicated that P1F30R15 continoud to show better performance with the increasing temperature until about 350 s^{-1} totation speed it showed the lowest viscosity under 10% mud contamination at 105 ºF temperature. Also it had lower

viscosity than both P1 and P1F30 sample until more than 500 s^{-1} rotation speed under 10% mud contamination at 125 °F temperature, as it is given in Fig.7.39C.

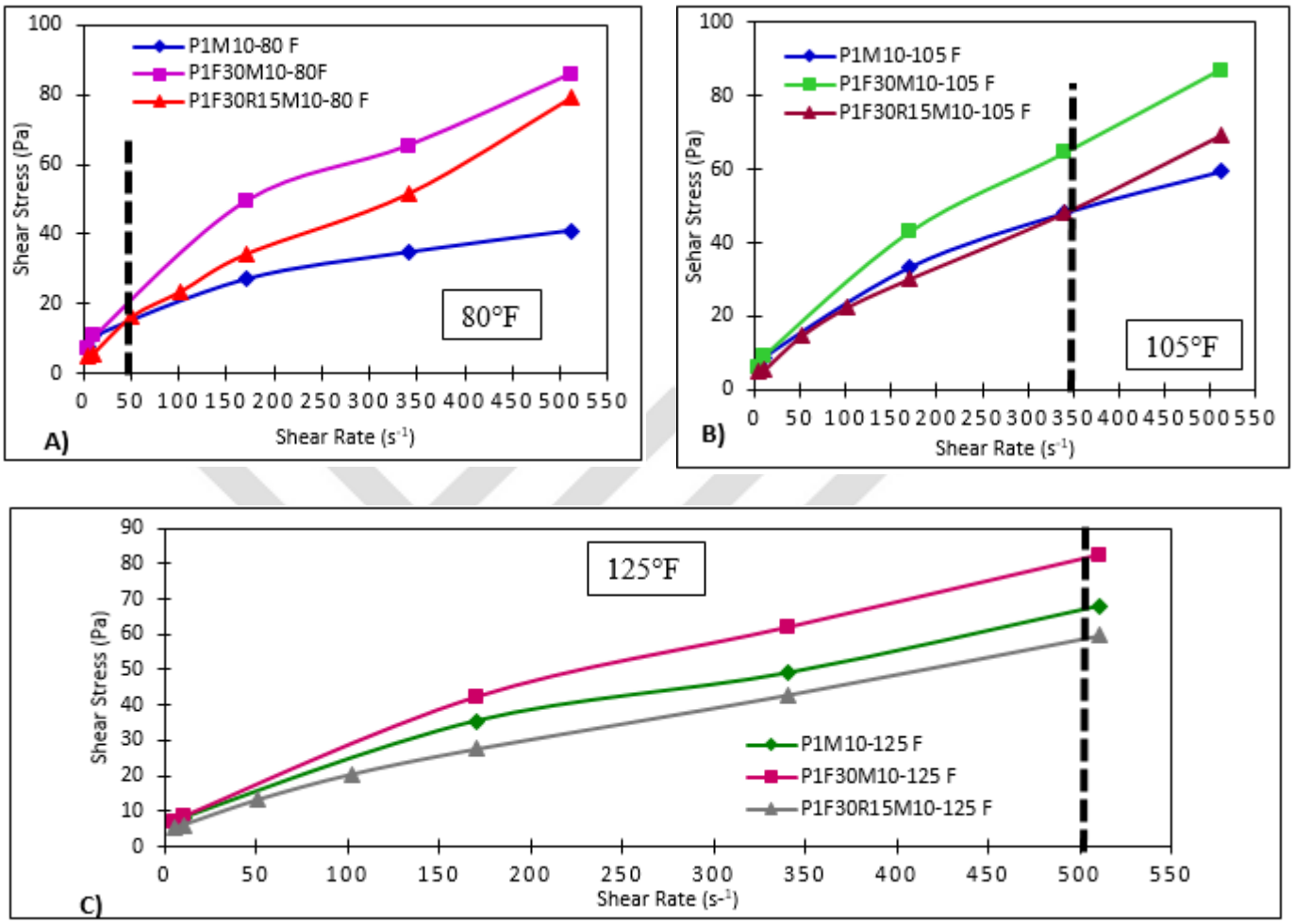

Figure 7.39. Rheological properties of portland cement and cement replacement by FA and RHA slurries with 10% water based drilling mud at constant temperatures A) 80 °F, B) 105 °F, C) 125 °F.

7.10. Mud to cement conversion portland cement and geopolymer

7.10.1. Effect of finess of fly ash on geopolymer

From Fig.7.40, it is clear that finess of FA has a great effect on geopolymer characterics. Fig.7.40A showed as grinding time for FA increased density of geopolymer increased. This is due to the increasing particle density as the grinding time increases. From Fig.7.40B,it can be seen that the geopolymer including FA milled for 120 minutes showed the lowest rheology than those of geopolymer prepared using FA milled for both 30 minutes and 60 minutes also sieved. Same trend was observed also for filtration. Geopolymer prepared using FA milled for 120

minutes had lowest fluid loss than the other geopolymer slurries, which is shown in Fig. 7.40C. Therefore, FA milled for 120 minutes was used to prepare optimized geopolymer.

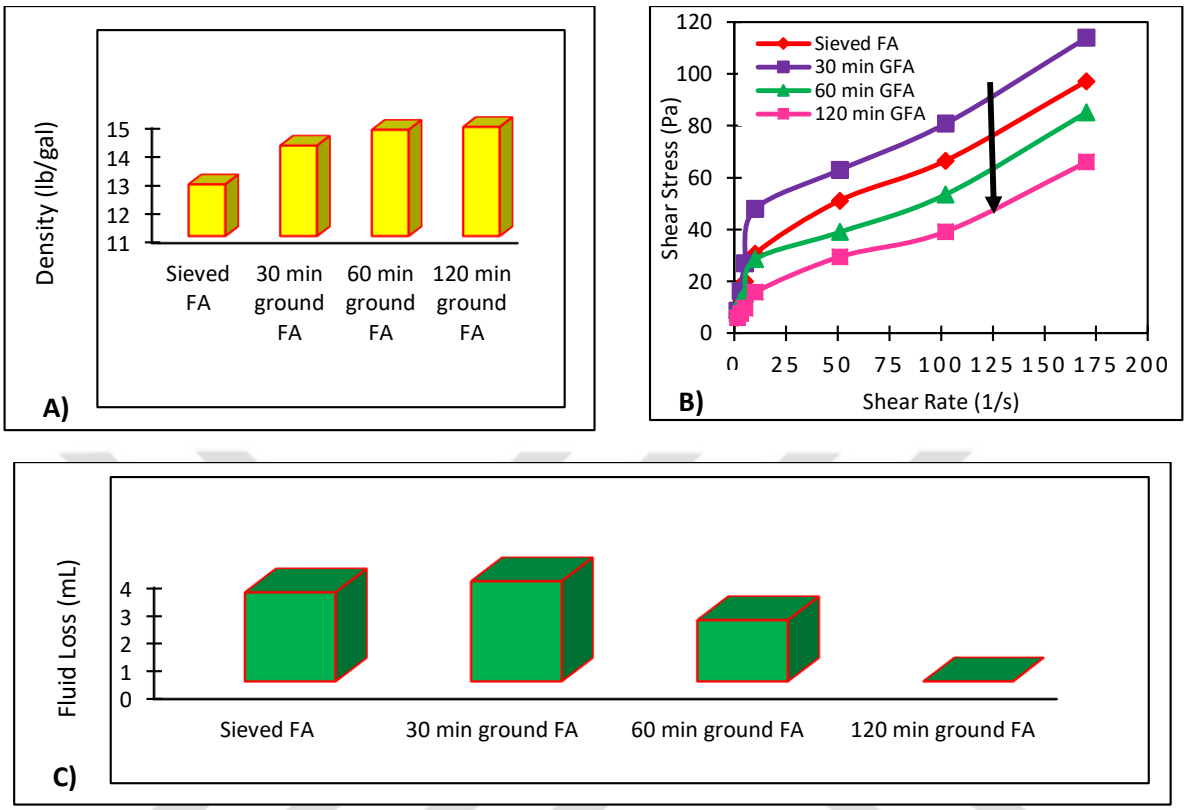

Figure 7.40. Behavior of FA with different grinding time and unground (sieved) on geopolymer. A) Density, B) Viscosity, C) Filtration

7.10.2. Effect of liquid/solid ratio on geopolymer

Liquid/solid (L/S) ratio also plays a key role on geopolymer characterictics. Different 45/55, 42.5/57.5, 47.5/52.5 and 50/50 liquid/solid ratios were anayzed to determine optimum ratio. FA milled for 120 minutes was used in all geopolymer with those ratios. Fig.7.41 demonstrated geopolymer characteristic prepared with different L/S ratios. Geopolymer prepared with 50/50 L/S ratio showed the lowest density (Fig.7.41A) and viscosity than those of geopolymers prepared with 45/55, 42.5/57.5, 47.5/52.5 L/S ratios (Fig.7.41B). All geopolymer prepared with sieved or ground FA also with different L/S ratios had very low fluid loss compared to the portland cement base slurry. Geopolymer prepared with 50/50 L/S ratio had slightly higher fluid loss than geopolymer with 45/55, 42.5/57.5 L/S ratios (Fig.7.41C). Since viscosity difference was greater than fluid loss, 50/50 L/S ratio was determined as optimum ratio.

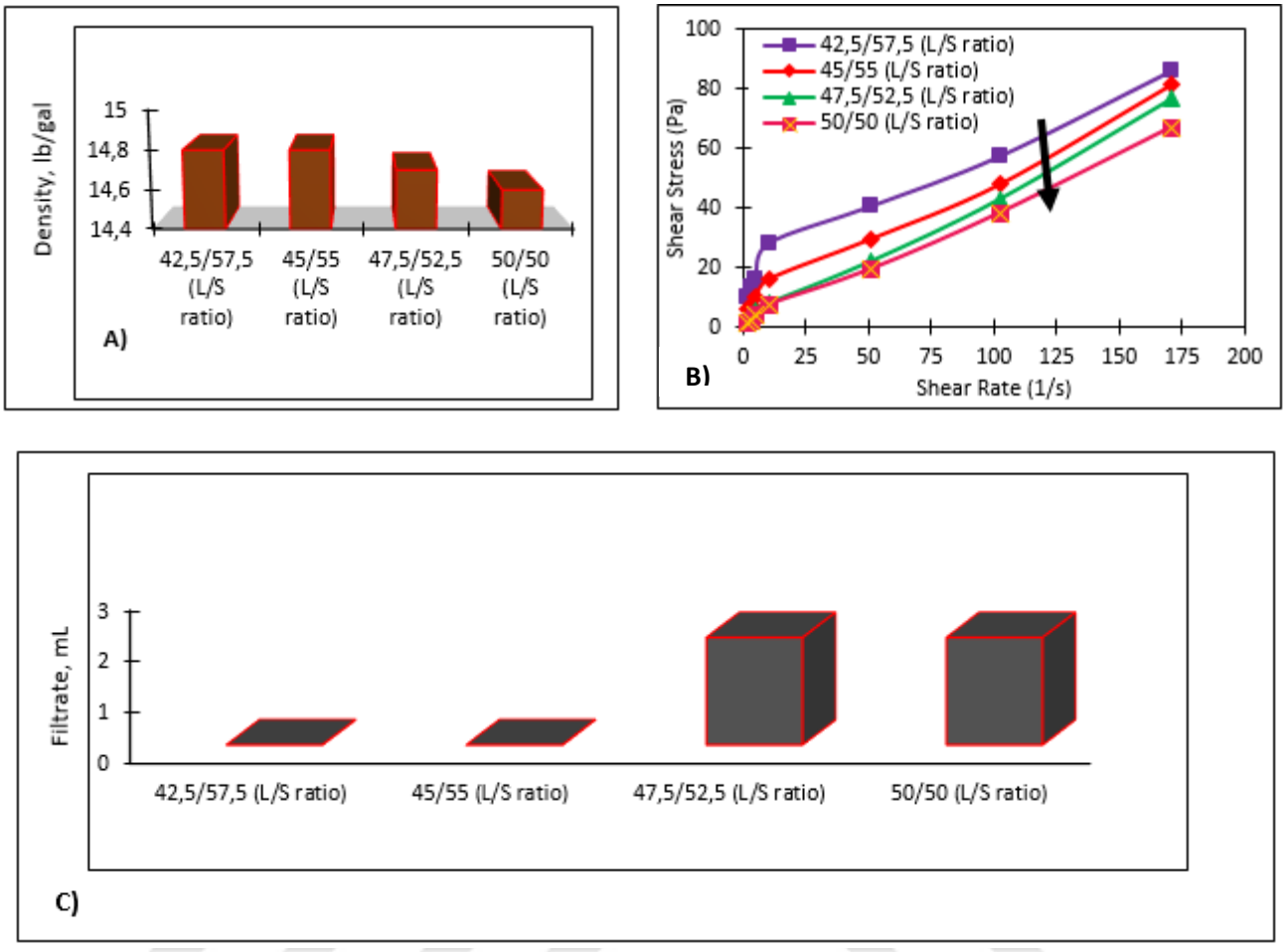

Figure 7.41. Behavior of different L/S ratio on geopolymer with 120 min. ground FA. A) Density, B) Viscosity, C) Filtration

7.10.3. Behavior of geopolymer hybrid and cement slurry at ambient and elevated temperature

The portland cement base slurry became more viscous with progressive water based mud contamination (Fig.7.42B). However, it is obvious that water based mud contamination had the opposite effect on geopolymer slurries, with viscosity decreasing as the admixture of WBM is increased, as shown in Fig.7.42A. While neat geopolymer was too viscous to pump, it was thus seen that forming a geopolymer hybrid, i.e. a geopolymer with WBM added to it, solved the viscosity challenge and made geopolymer slurries pumpable.

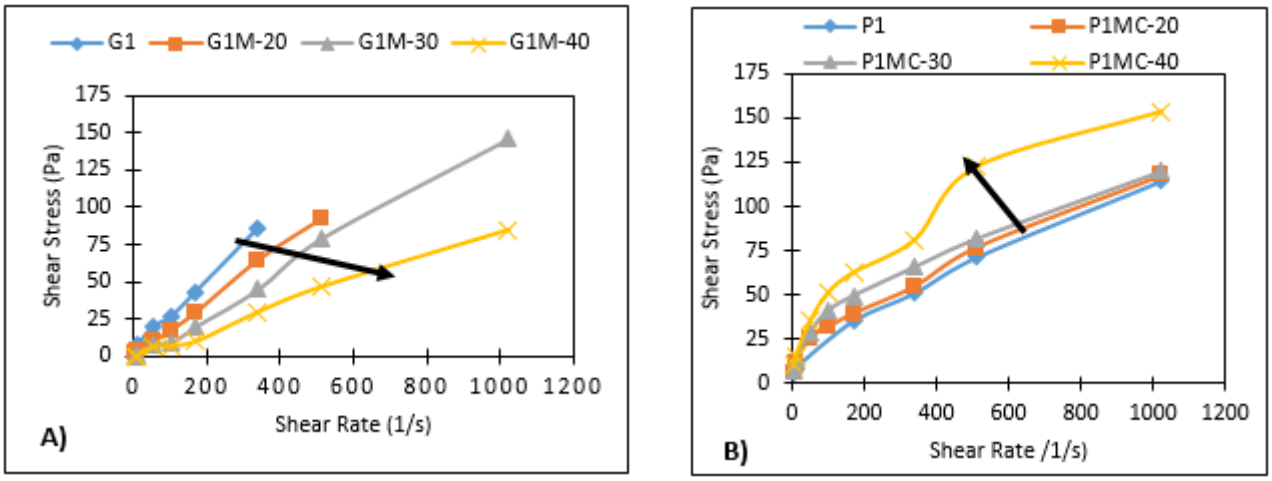

Figure 7.42. Rheological properties of (A) alkali-activated FA and (B) portland cement slurries replaced with various dosages of WBM by volume at ambient temperature.

Increasing temperature also had positive affect on gepolymer hybrids. Fig.7.43A showed that the viscosity of geopolymer hybrids decreased even at 125 ºF temperature. Nevertheless, the portland cement slurries replaced with various dosages of water based drilling fluid became more viscous with increasing temperature (Fig.7.43B).

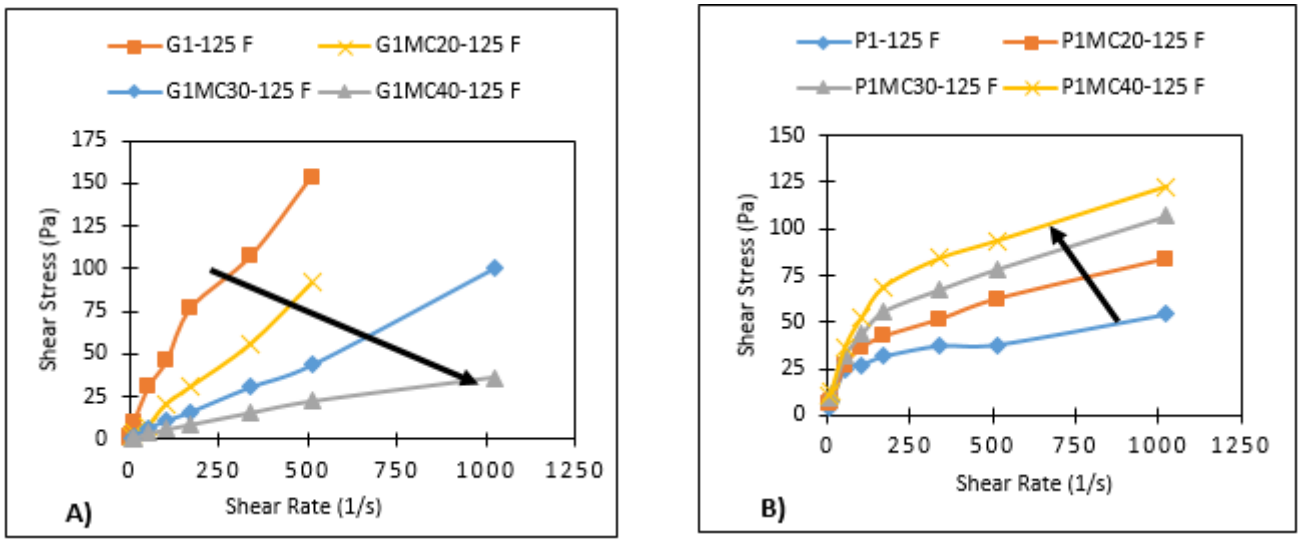

Figure 7.43. Rheological properties of (A) alkali-activated FA and (B) portland cement slurries replaced with various dosages of WBM by volume at 125 ^{o}F temperature.

Optimized geopolymer prepared with FA milled for 120 min. and 50/50 L/S ratio had lower density than neat portland cement slurry (Fig.7.44A). It is clear that fluid loss of portland cement was considerably higher then geopolymers as can be seen in Fig.7.44B.

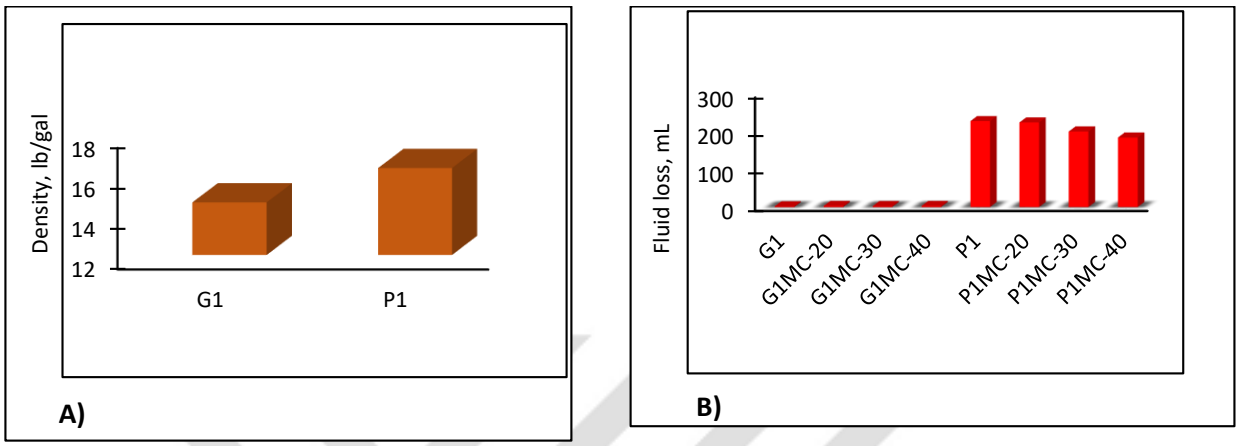

Figure 7.44. Density and filtration properties of geopolymer and portland cement slurries. A) Density of neat geopolymer and cement mud-free B) Filtration of geopolymer and cement replaced with various dosages of WBM by volume.

7.11. Effect of fly ash in shale inhibitor mud under increasing temperature

7.11.1. Rheological behvaiour of the drilling fluid at elevated temperature

After the extensive analyzing of drilling fluid system with FA and RHA at room temperature, rheology of the fluids was also studied under increasing temperatures. Reogram results of water based drilling fluid at constant temperature were given in Fig.7.45. As can be seen from the figure, increasing concentration of FA resulted in an increase in rheology profile of the fluid at the temperatures of 30 ºC, 40 ºC and 50 ºC.

Behaviour of the drilling fluid systems under increasing temperature and constant concentration of FA was given in Fig.7.46. When analyzed under constant concentration of FA it is obvious that increasing temperature decreased the rheology profile of the all fluid at constant concentration FA. An another observation is differences between the shear stress magnitudes increases with the increasing concentration of FA depending on constant temperature compared to reference fluid not containing FA. Maximum difference was obtained with the drilling fluid with 15 wt% concentration of FA.

Behaviour of the drilling fluid systems at constant 600 rpm shear rate was also investigated. As can be seen in Fig.7.47, increasing temperature caused an decrease on the shear stress magnitudes of the fluids at 600 rpm and maximum shear rate magnitudes were observed with the fluid incorporated 15 wt% FA for each temperature.

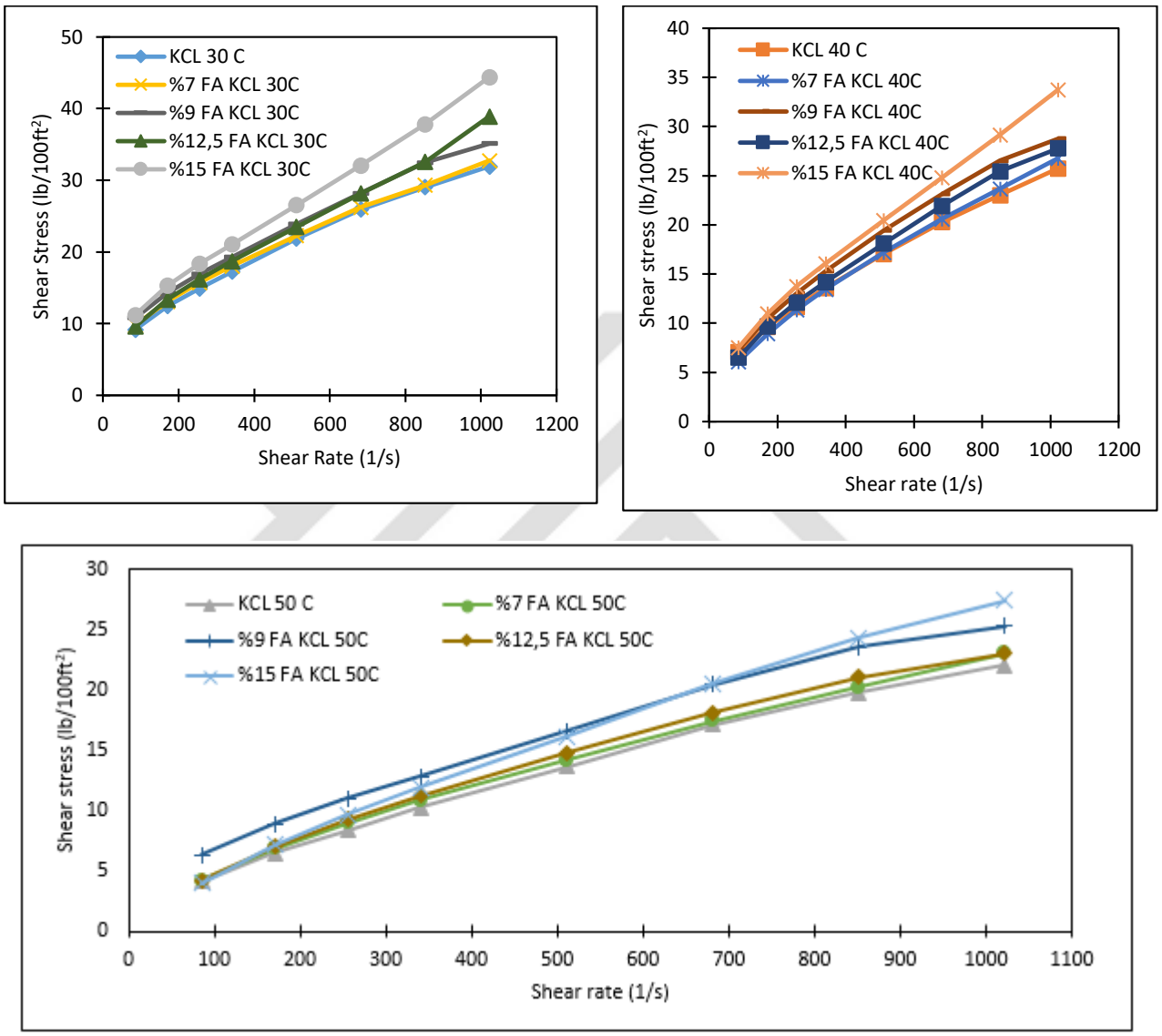

Figure 7.45. Rheology profile of water based drilling fluid with FA at constant temperature

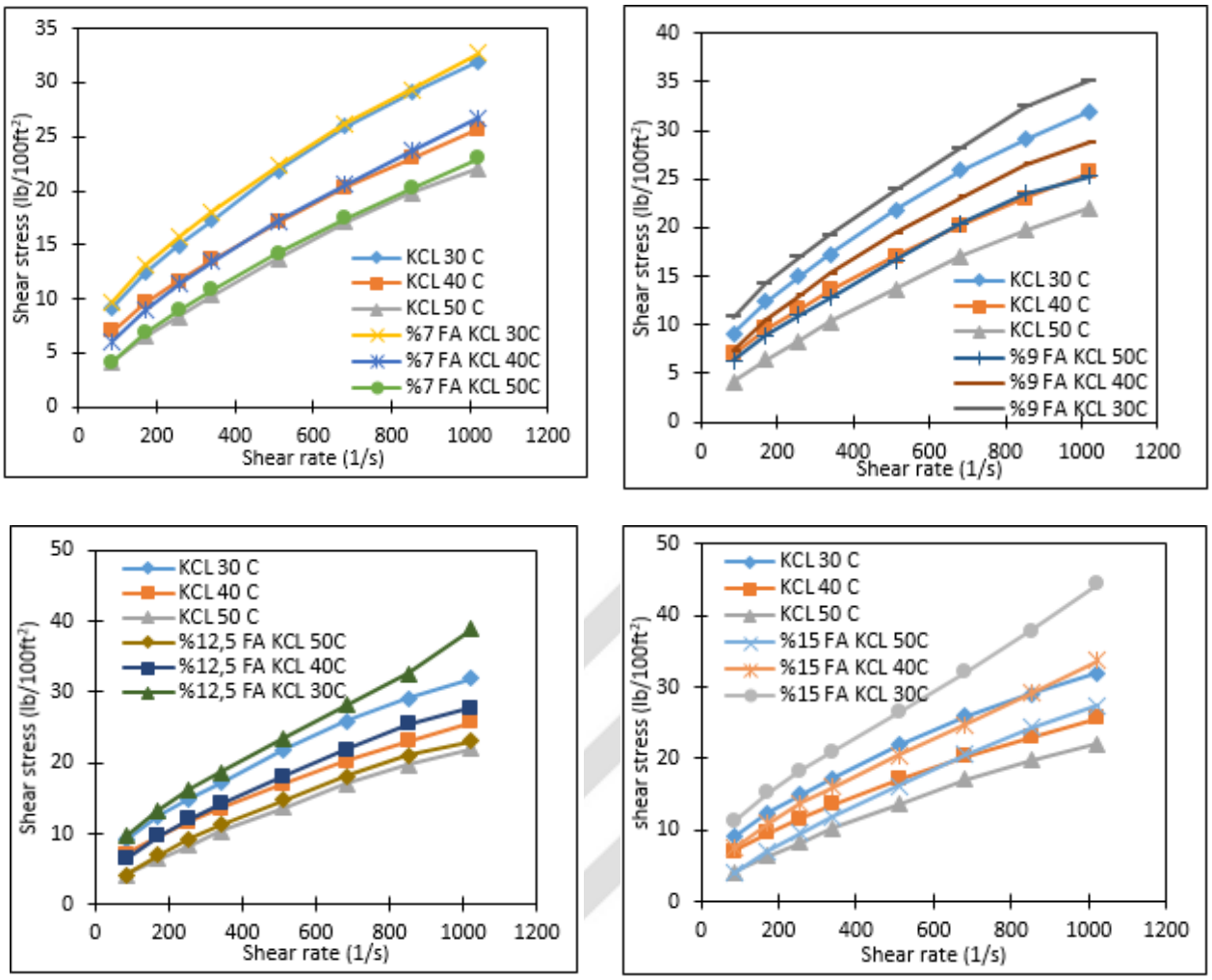

Figure 7.46. Rheology profile of water based drilling fluid with FA at increasing temperature

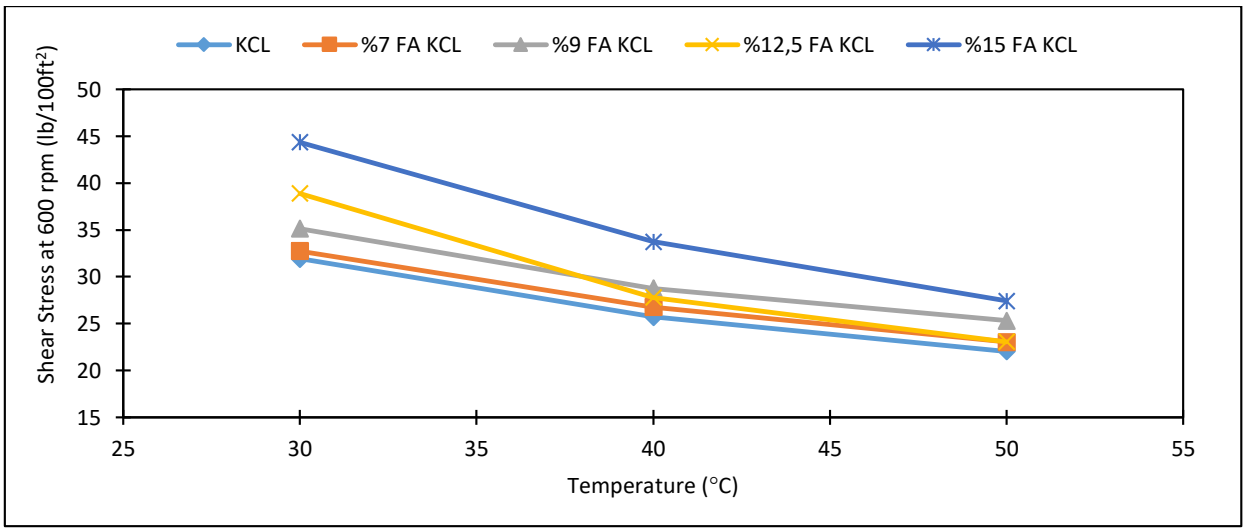

Figure 7.47. Shear stress of water based drilling fluid with FA at 600 rpm and increasing temperature

7.11.2. Hydraulic performance of drilling fluids under elevated temperature

Rheologically, performance of drilling fluids should be evaluated based on their CCI values rather than rheological parameters such as plastic viscosity and yield point. A CCI value of 1.0 is considered a adequate and effective well cleaning condition and the required minimum annular average velocities of the fluids were calculated from Equation (3.14). In the drilling industry, the average annular mud velocity (Va) is assumed to be 100 ft/min for effective cleaning of vertical and near-vertical angled wells. However, it is reported that for advanced drilling fluids produced with today's technology, the annular velocity required for effective cleaning of the same well may be even lower (Bourgoyne, 1991). Moreover, high annular velocity required for effective well cleaning means that the slurry pump is operated at higher flow rates. And this also increases the cost of drilling as it requires more energy.

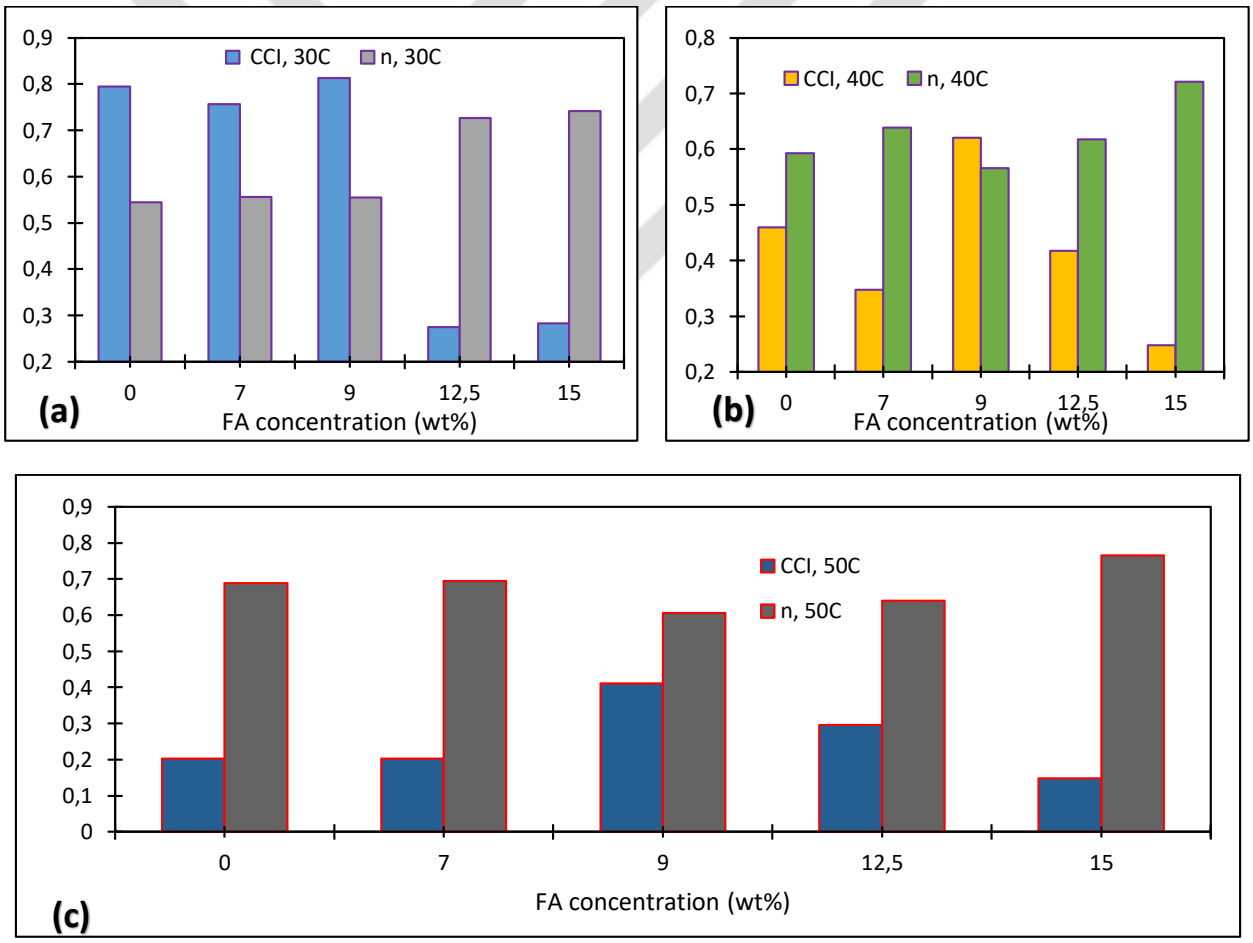

Figure 7.48. Variation of cutting carrying and flow behaviour index of water based drilling fluid at costant temperature, 30 ºC (a), 40 ºC (b), 50 ºC (c)

In Fig.7.48 can be seen results of cutting carrying and flow behaviour indexes of the fluids at constant 30°C, 40°C and 50°C temperatures. Drilling fluid system developed with 9 wt%

concentration FA had higher cutting carrying index and lower flow behaviour index compared to other systems for all revelant temperatures. Minimum annular velocity required to clean the well efficiently of the fluids at constant 30°C, 40°C and 50°C temperatures was also given in Fig.7.49. Similarly, minimum annular velocity required to clean the well efficiently was also obtained with the fluid system developed with 9 wt% concentration of FA for 30°C, 40°C and 50°C temperatures.

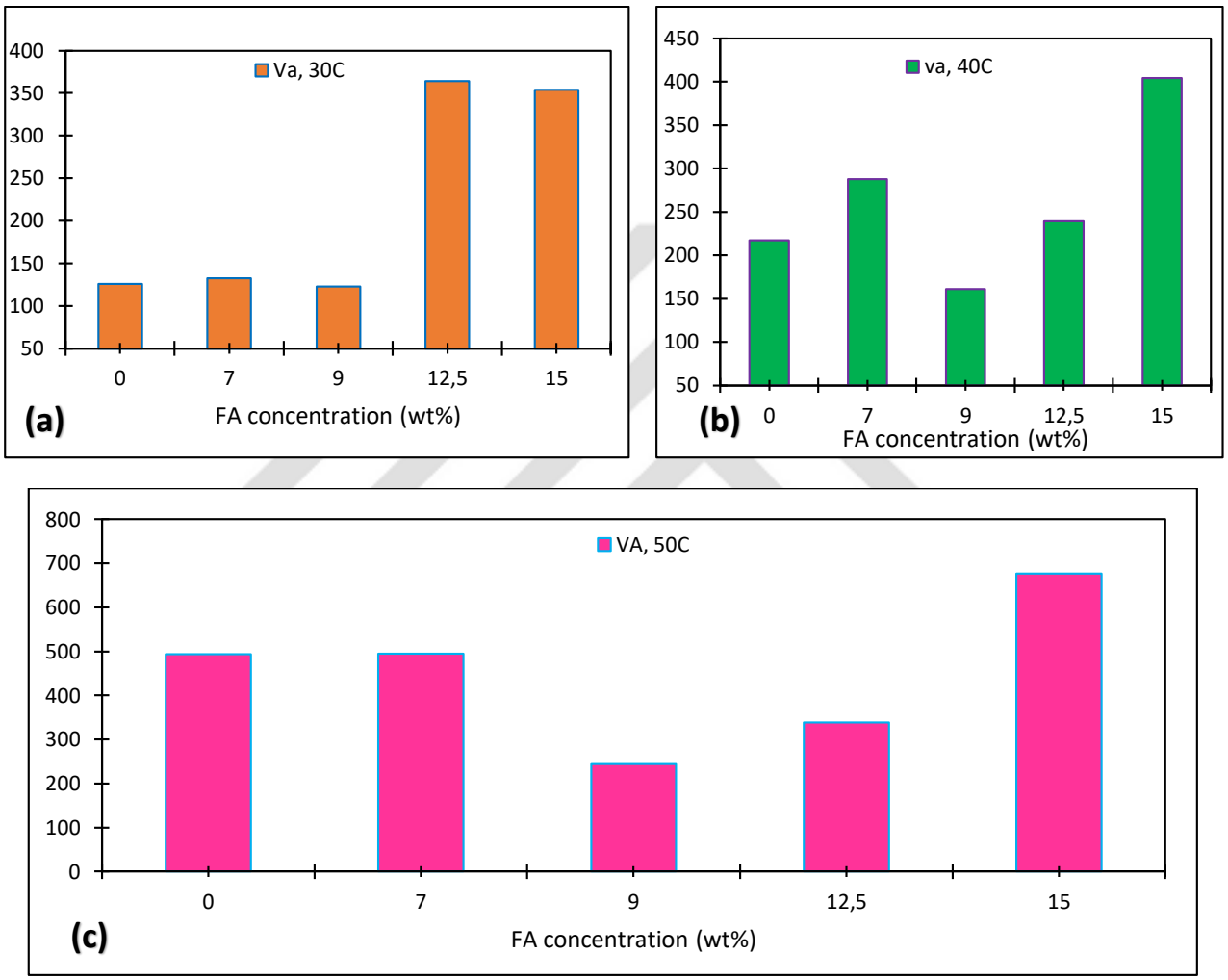

Figure 7.49. Variation of minimum annular velocity required to clean hole at at costant temperature: 30°C (a), 40°C (b), 50°C (c)

Hydraulic parameters of the fluids were also analyzed under increasing temperature. As can be seen in the Fig.7.50, temperature negatively affected to the hydraulic parameters. Cutting carrying index of each system decreased with the increasing temperature. In addition, flow behaviour index and minimum annular velocity required to clean the well efficiently of the fluids increased with the temperature. As it is well known, increasing flow behaviour index and minimum annular velocity required to clean the well yielded a negative effect on shear thinning

behaviour of the fluids and thereby may cause more pumping energy and associated cost. It should be noted that drilling fluid system developed with 9 wt% concentration of FA had the highest cutting carrying index, lowest flow behaviour index and minimum annular velocity required to clean the well.

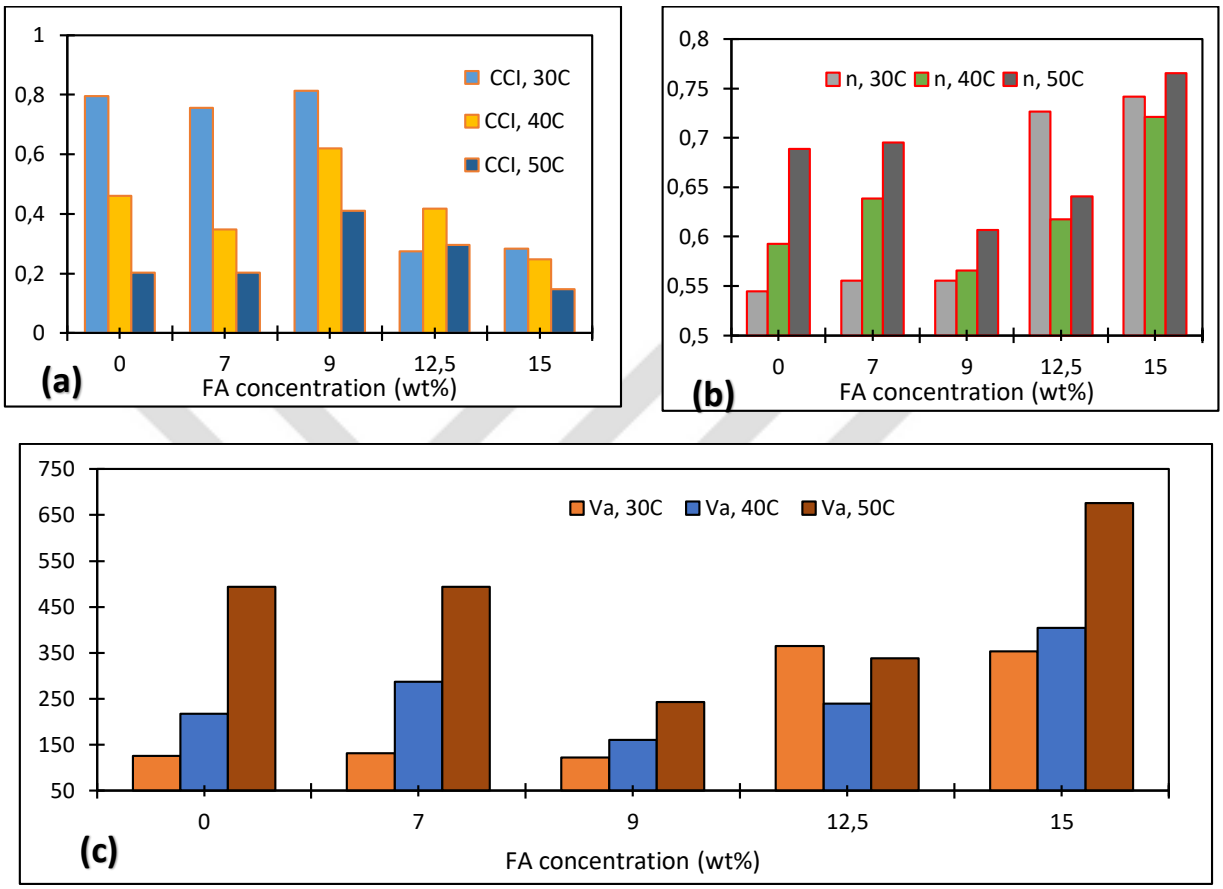

Figure 7.50. Hydrolic parameters of the water based drilling fluids under increasing temperature, cutting carrying index (a), flow behaviour index (b), minimum annular velocity required to clean the well (c)

7.12. Rheological model analysis

Rheological model mathematically relates the relationship between shear rate and shear stress of the drilling fluid. In this context, rheological model analysis plays an important role in the accurate evaluation of wellbore hydraulics. In addition, considering the proper rheological model as a basis in the calculation of the friction pressure losses of the drilling fluid affects the results considerably. Therefore, an accurate assessment of the annular flow performance of drilling fluid has an important role in reducing the risk of potential drilling problems. In determining the annular flow performance of the drilling fluid, firstly, relationship between

shear stress and shear velocity is determined mathematically. As the hydraulic system plays an active role in drilling operations, its correct design can improve rate of penetration and reduce the overall cost.

Rheological model analysis was studied to determine relationship between shear stress and shear rate of the water based drilling fluid formulated with increasing concentration of FA under increasing temperatures. In the rheological model estimation, coefficients of the models and coefficient of determination (R^2), adjusted coefficient of determination (R^2), sum of square error (SSE) and root mean square error (RMSE) parameters, which are considered in the estimation evaluation of the results, were obtained using the MATLAB curve fitting toolbox. R^2 and adjusted-R^2 can take any value between 0.0 and 1.0, and a value close to 1.0 indicates a stronger relationship between the variables. Also, when SSE and RMSE values are close to 0.0, it indicates that the model has less errors and the predicted values are closer to the real values.

Table 7.5. Results of rheological model estimation of the water based drilling fluids with the 9 wt% concentration of FA

KCL ref. Mud+%9 FA				
Temperature, °F		86	104	122
Bingham Plastic	μ_p (Pa-s)	0.0124	0.0109	0.0098
	τ_y (Pa)	4.7560	3.2670	2.6430
	SSE	1.1290	1.4370	0.8924
	RMSE	0.4339	0.4894	0.3857
	R^2	0.9908	0.9851	0.9886
	Adjusted R^2	0.9893	0.9826	0.9867
Power-Law	n	0.5103	0.5694	0.5980
	K (Pa-s^n)	0.4871	0.2686	0.1949
	SSE	0.5589	0.0834	0.2782
	RMSE	0.3052	0.1179	0.2153
	R^2	0.9955	0.9991	0.9965
	Adjusted R^2	0.9947	0.9990	0.9959
Herschel-Bulkley	m	0.6927	0.6045	0.6887
	K (Pa-s^0)	0.1184	0.2042	0.0970
	τ_y (Pa)	2.6110	0.4603	0.9017
	SSE	0.1142	0.0700	0.2065
	RMSE	0.1511	0.1184	0.2032
	R^2	0.9991	0.9993	0.9974
	Adjusted R^2	0.9987	0.9990	0.9963

In the rheological model analysis study, drilling muds were formulated with FA at 7, 9, 12.5 and 15 (wt%) concentrations, based on the mud whose composition is given in the Table 6.5.

Then, shear stress values of each drilling mud formulated at 86°F, 104°F and 122°F temperatures with a Fann model 50 SL rheometer were obtained under 8 different rotational speeds (50, 100, 150, 200, 300, 400, 500 and 600 rpm). Since 12 different shear stresses were obtained under each shear rate, the average of these values was calculated and recorded. In total, 96 shear stresses were obtained for each temperature and a total of 288 shear stress data were obtained for the 3 temperatures. The data obtained from the rheometer for each formulated drilling fluid were presented in Table 12.4-12.7 in Appendix C.

In rheological model estimation, firstly, independent variables, which are shear rates, and dependent variables, which are shear stress, files were created and named on the workspace of matlab. Afterthat, shear rate and shear stress data obtained from rheometer were recorded as x and y axis, respectively. Then the curve fitting button in the application section was activated and the x and y coordinates were selected. For the Bingham Plastic Model, first-degree polynomial function, for Power Law model first-degree power function, and for Herschel-Bulkley model second-degree power functions were selected. Then all equations coefficients and R^2, adjusted R^2, SSE and RMSE results were obtained. The statistical results for determining the rheological parameter and rheological model of the water based drilling fluid 9 wt% concentration of FA is given in Table 7.5, while estimation results of the drilling fluid formulated with 7 wt%, 12.5 wt% and 15 wt% FA concentration can be seen Table 12.8 given in Appendix C. Results show that plastic viscosity and yield point values of the samples decreased due to temperature increase. From the results, it was proved that Herschel Bulkley model provided the best estimation result compared to Power Law and Bingham Plastic models. With the Herschel Bulkley model more accurate results than the other rheological models were obtained considering R^2, adjusted R^2, SSE and RMSE values under 86°F, 104°F, 122°F temperatures.

8. NEW SCIENTIFIC ACHIEVEMENTS

In this section, new scientific results obtained as a result of experimental study and analysis were presented. Theses were listed in the results section in accordance with the order.

8.1 Thesis 1

In this thesis, a gypsum/polymer type drilling fluid system blended with 3.0 wt% content of BFA was developed. This developed mud system exhibited superior rheological and filtration properties compared to reference fluid not composed of FA. Furthermore, based on results, it

was proved that type of FA plays a crucial role on the properties of gypsum/polymer drilling fluid. From this thesis it was concluded that BFA is a promising additive in the usage of gypsum/polymer mud and it would be a welcome development when it was interpreted in proper levels.

8.2. Thesis 2

In this thesis, a novel drilling fluid system with the enhanced filtration properies was designed based on spud mud. Developed spud mud incorporated with 7 wt% concentration of BFA exhibited improved filtration properties as well as gel strength without significant variation on apparent viscosity, plastic viscosity and yield point compared to the reference fluid without FA. This developed mud system with BFA could be considered as an alternative mud system to conventional mud for reduction fluid loss of water-based bentonite muds. Moreover, from the thesis, it was proved that type of FA have a great effect on the properties of spud mud. Although the use of LFA improves the rheology of the fluid, it degrades filtration properties and filter cake thickness dramatically.

8.3. Thesis 3

In the thesis, it was proved that while grinding time of FA have no effect on the rheology of shale inhibitor mud, it exhibited a variation on the filtration. Shale inhibitor mud incorporated by 9 wt% concentration of raw FA with a mean particle size of 67.89 μm yielded greater rheological parameters than those of shale inhibitor mud formulated by ground FAs for 30, 60 and 120 minutes with the mean particle size of FA is 18.25 μm, 13.75 μm and 9.38 μm, respectively. On the other hand, it was reveal that while fluid loss of the reference shale inhibitor fluid increased, mud cake thickness of the fluid decreased with the increasing grinding time. Shale inhibitor mud incorporated with 9 wt% concentration of raw FA showed lower fluid loss and thinner mud cake than those of shale inhibitor mud blended with the ground FAs.

8.4. Thesis 4

Two different inhibitive drilling fluid systems possess improved rheological and filtration characteristics were developed based on KCl water based mud with 9 wt% concentration of FA and shale inhibitor mud with 12.5 wt% concentration of FA. Developed cost effective mud systems yields an improvement on the performance of drilling operation by increasing cutting

carrying capacity, reducing fluid loss and the possibility of stuck pipe and associated challenges.

8.5. Thesis 5

In the thesis, an improved drilling fluid was developed with 4 wt% concentration of FA and 8 wt% concentration of bentonite under 72 hours aging times based on bentonite mud with additives considering the rheological and filtration properties. It was proved that driling fluid formed by increased bentonite concentration (from 6.4 wt% to 8 wt%), incorporated with 4 wt% content of FA yielded higher rheological parameters than those of driling fluid system including increased concentration of XG (0.80 g) and CMC (1.3 g) both in absence and presence of 4 wt% concentration of FA. In addition, the developed driling fluid provided to decrease mud cake thickness and fluid loss of the reference fluid.

8.6. Thesis 6

In the thesis, a novel driling fluid system was developed with nano-sized of FA considering differential sticking. It was reveal that barite weighted bentonite driling fluid system with 0.3 wt% concentration of BFA grinded for two hours in a wet mode with a mean particle size of 272 nm decreased the sticking coefficient of driling fluid by 45%. Moreover, it was proved that differential sticking of driling fluid is greatly affected from the changing of particle size of FA. It was concluded that finer particle size and higher spesific surface area of FA has more improvement on the differential sticking tendency of driling fluid. Thereby, this developed system provides a reduction in non-productive time and associated well cost.

8.7. Thesis 7

In the thesis, an improved drilling fluid was developed with 15 wt% concentration of RHA considering rheological properties as well as cutting carrying capacity, minimum annular velocity required for effective hole cleaning and flow behaviour index. It was reveal that while apparent viscosity and yield point of the mud with 15 wt% concentration of RHA increased by 60% and 183%, respectively, thixotropy and plastic viscosity of the fluid decreased by 29% and 63%, respectively. Cutting carrying capacity of the reference drilling fluid without RHA increased from 3.183 to 54.700 in presence of 15 wt% concentration RHA. Moreover, with the developed fluid, minimum anular velocity required to clean bottom of the well efficiently and flow behaviour index of the reference fluid decreased from 31.412 to 1.828 and 0.419 to 0.087,

respectively. The designed drilling fluid posses improved hole cleaning and shear thinning behavior and also requires decreased pump power for the cleaning of the well efficently.

8.8. Thesis 8

In this thesis, possibility of using FA and RHA as substitutes in portland cement slurry was studied experimentally at ambient conditions. Based on results, it was reveal that viscosity of slurry formed by partial replacement of cement with FA in 30% and RHA in 15% by weight of cement is lower than reference slurry without replacement of the ashes up to 300 1/s rotation speed. Moreover, it was concluded that with the developed slurry fluid loss of the reference slurry decreased by 26% and density of portland cement decreased to 14.5 ppg. Developed slurry could provide a reduction on pump pressure required and possibility of cracking or channeling in the formation during pumping the cement slurry. Also, the developed slurry prevents premature gelation of the cement composition. Thereby, it can be stated that the system contributes the well cost.

8.9. Thesis 9

In this thesis, stability of the slurry formed by partial replacement of cement with FA (in 30%) and RHA (15%) was analysed experimantally against to water based inhibitive drilling fluid contamination by comparison with reference portland cement slurry at ambient conditions. It was reveal that developed slurry is more stable than than portland cement slurry under increasing mud contamination. The slurry also exhibited enhanced filtration results and shows lower fluid loss when it exposure to both 5 wt% and 10 wt% concentration of gypsum/polymer mud type contamination by comparison with reference portland cement slurry.

8.10. Thesis 10

In this thesis, effect of particle size of FA on the rheological and filtration properties of cement slurry was investigated by the mechanical grinding process to determine the optimum particle size of FA at ambient conditions. It was reveal that particle size of FA plays an important role on the properties of cement slurry. It was proved that fluid loss of the reference portland cement slurry decreased by 26% with the formulation of slurry formed by partial replacement of cement with FA (30% by weight of cement) ground for 120 minutes and mean particle size of 9.38. Moreover, slurry formed by partial replacement of cement with raw FA (30% by weight of cement) and mean particle size of 67.89 μm in exhibited lower viscosity than those of slurry

formed by partial replacement of cement with ground FAs (30% by weight of cement), for 120 minutes and 30 minutes with a mean particle size of 9.38 μm and 18.25 μm, respectively.

8.11. Thesis 11

In this thesis, flow behaviour of the slurry formed by partial replacement of cement with FA and RHA was investigated experimentally in presence and absence of water based driling fluid at elevated temperature and constant temperature by comparison with reference portland cement slurry. Developed slurry formed by partial replacement of cement with FA in 30% and RHA in 15% by weight of cement showed the superior rheology results than reference portland cement slurry both in presence and absence of drilling mud at elevated temperature. From the evaluation of results, it was proved that developed slurry yielded better mud contamination resistance than reference portland cement when it exposed to 5 wt% and 10 wt% (by weight of cement) gypsum/polymer type water based drilling fluid contamination under increasing temperatures (80-125 (°F)). In addition, it was reveal that developed slurry showed the superior rheology results up to a specific rotation speed both in presence and absence of drilling mud at constant temperature.

8.12. Thesis 12

In this thesis, a novel geopolymer hybride slurry was developed based on FA and water based drilling fluid. The developed geopolymer slurry (formed by 12 Molar NaOH (25%), Water glass (75%), 50/50 alkaline activator/120 minutes ground FA and gypsum/polymer type water based drilling fluid) showed enhanced rheolgy, filtration characteristics and higher mud contamination resistant at ambient temperature and 125 °F temperature. It was proved that as particle size of FA decreases viscosity and fluid loss of the geopolymer slurry decreases. Moreover, it was reveal that viscosity of geopolymer slurry decreases with the increasing liquid/solid ratio. The developed geopolymer not only improves its pumpability but also contributes on the enhancement of fluid loss. Also, with the forming geopolymer hybride by inroducing the mud to alkaline activated FA slurry, a recycle method was obtained for disposal of spent mud. Thus, the developed hybrid geopolymer also helps to reduce the total drilling cost.

8.13. Thesis 13

In the thesis, drilling fluid system with improved drilling performance was developed with FA under increasing temperature taking into account parameters of cutting carrying index, flow behavior index and minimum annular velocity required to clean bottom of the well efficiently. It was reveal that shale inhibitor mud incorporated with 9 wt% concentration of FA increased cutting carrying index of the reference fluid without FA from 0.794 to 0.813, from 0.459 to 0.620, from 0.202 to 0.410 under 30°C, 40°C and 50°C temperatures, respectively. In addition, with the improved driling fluid system, minimum annular velocity required to clean bottom of the well efficiently of the reference fluid decreased from 125.848 ft/min to 122.968 ft/min, from 217.536 ft/min to 161.235 ft/min, from 493.834 ft/min to 243.585 ft/min under 30°C, 40°C and 50°C temperatures, respectively. Also, developing the driling fluid system ensured to decrease flow behaviour of the index from 0.544 to 0.555, from 0.592 to 0.565, from 0.688 to 0.606 for 30°C, 40°C and 50°C temperatures, respectively. With this developed system, the performance of the drilling operation is improved and it also contributes to the reduction of the total well cost.

8.14. Thesis 14

In the thesis, rheological model analysis of the drilling fluid system with improved drilling performance was conducted to determine relationship between shear stress and shear rate mathematical under different temperatures by comparing the traditional bingham plastic, power law and herschel bulkly rheological models. Based on data obtained by measurements performed with a Fann model 50 SL rheometer, it was concluded that Herschel Bulkley model showed superior results than the Power Law and Bingham Plastic rheological models for 86°F, 104°F and 122°F temperatures. Employment of the Herschel Bulkley model in the estimation of changes of shear stress depending on shear stress which can occur during driling for 86°F, 104°F and 122°F temperatures provides more accurate assessment of well hydraulics.

9. SUMMARY

Drilling fluid and cementing are indispensable components of drilling operations. Drilling fluid plays a vital role in the success of drilling operation and represent 15 to 18% of the total cost of oil well drilling and performs many critical tasks which are essential for efficient drilling

process. Cementing is also one of the most important processes during the drilling and completion of the wells. The primary function is preventing the fluid migrations between the formations and wells to provide full zonal isolation. On the other hand, production of cement needs a large amount of energy and at the end of the cement production a significant amount CO_2 releases to atmosphere. Severe operational difficulties and huge environmental issues as well as high remedy costs could be a result of losing zonal isolation and production of cement.

As it is well known FA and RHA have been used at many industries as a useful product, although it as industrial and agriculture waste, respectively. Objective of the thesis is to investigate their utilization in drilling industry, since the usage of FA and RHA in drilling fluid and oil well cementing has not been studied comprehensively so far. To this end, an extensive experimental analysis was conducted as below:

Firstly, BFA and LFA were used in spud mud and gypsum polymer with the varying concentrations and rheological and filtration properties of the drilling fluids were investigated. At the end of this part, drilling fluid systems were developed with enhanced rheological and filtration properties for each type of the water based drilling fluid. After analyzing the results, it was found that BFA shows superior performance than LFA. Therefore, research was continued with BFA.

Secondly, FA was introduced to KCl water based mud at different concentrations. Then, optimum particle size of FA was determined based on ground for 30 minutes, 60 minutes and 120 miutes and unground of FA in shale inhibitor mud. At the end, improved KCl water based mud was designed and it was found that while particle size of have negligible effect on rheology, drilling fluid with unground FA showed better filtration resuls than that of drilling fluid with ground FA.

Thirdly, performance of FA was analyzed in bentonite mud with additive considering effect of different aging time (24, 48, 72 hours), bentonite and XG concentration It was determined that FA is more effective under increasing aging time and bentonite concentration than that of increasing XG and CMC concentration.

Forthly, differential pressure pipe sticking tendency of drilling fluid incorporated with BFA with three different forms, which are raw, sieved and grinding in wet mode for 2 hours, at the different concentrations was studied. The differential sticking is one of the most serious and common borehole instability problem faced by drilling engineer and occurs in an open hole in

case part of the drill string is pushed toward filter cake on wellbore due to overbalance pressure. Problems related to this phenomenon cost hundreds of millions dollars annually since can even cause the well to be abandoned. At the end of this part, a water based drilling fluid was designed which decreases the potential of differential pressure pipe sticking tendency.

Fifthly, performance of RHA in bentonite drilling fluid was assessed based employment of different concentration. At the end, an drilling fluid with superiour hydraulic behaviour was developed with RHA.

Sixthly, partial replacement cement with FA depending of different percentages was studied and its rheological and filtration characteristics were investigated. After the determination optimum percentage of FA, cement was partially further replaced with RHA and FA with optimum percentage found. After wards, the behavior of combined replacement of FA and RHA was analyzed under the different percentage of mud contamination since contaminated cement slurry with drilling fluids is considered one of the major cause of the well cementing failures. In this part different particle size of FA in cement slurry performance also studied based on ground and unground FA. In addition, the rheological behavior of those all the samples was further studied under increasing temperatures. At the end, it was found that cement slurry with unground FA shows better rheology than that of ground FA. At the end, an cement slurry with superiour rheological and filtration caharacteristics was designed by based on replacing cement by FA and RHA under drilling fluid contamination and elevated temperature.

Seventhly, an attempt was made for the development of a hybrid geopolymer slurry formed with FA and drilling fluid to alternative to portland cement. To this end, firstly fineness of particle size of FA (sieved, 30, 60, 120 min. ground) at the geopolymer slurry was studied by analyzing their rheology and filtration properties compared to portland cement. After the determination of optimum particle size of FA, effect of different liquid/solid ratio on geopolymer performance was investigated to determine optimum liquid/solid ratio. Results show that although filtration properties of the geopolymer slurry are better than portland cement, its viscosity higher than that of the cement slurry significantly. To solve this problem an hybrid geopolymer slurry was developed by the usage of different percentage of drilling fluid. Behavior of hybrid geopolymer and cement slurries was studied both at ambient and elevated temperatures. At the end, an hybride geopolymer with superiour rheological and filtration properties was developed under elevated temperature.

Eighthly, performance of FA based on cutting carrying index, flow behaviour index and minimum annular velocity required to clean the well efficiently was analyzed in shale inhibitor mud under increasing temperature. At the end, a drilling fluid system with improved hydraulic performance was developed under increasing temperature.

Lastly, rheological model analysis of the drilling fluid system was conducted to determine relationship between shear stress and shear rate mathematical under different temperatures by comparing the rheological models of Bingham Plastic, Power Law and Herschel Bulkley. At the end, Herschel Bulkley showed superior results than the Bingham Plastic and Power Law rheological model under increasing temperature.

In conclusion, in the thesis, different types of drilling fluids with improved hydraulic performance were developed with FA, which is a large amount of industrial waste, and RHA, which also constitutes a large amount of agricultural waste at ambient and elevated temperature. In addition, cement slurry and hybride geopolymer slurry with improved rheological and filtration properties were designed by partially changing the amount of cement with FA and RHA and completely replacement of cement by FA, respectively to reduce and eliminate cement amount needed. Lastly, for a better understanding rheological behaviour of drilling fluids and their wellbore hydraulic performance rheological model analysis was performed. Consequently, an alternative method was developed for the recycling of FA and RHA, as well as contributing to the reduction of drilling costs and environmental problems with the drilling mud and cement slurries developed in this thesis. Also, with the rheological model analysis more accurate assessment of well hydraulic was achieved. It worths to be noted that the new comprehensive findings obtained in this thesis can be used as a guide for future studies.

10. REFERENCES

Ahmaruzzaman, M. (2010). A review on the utilization of fly ash. Progress in energy and combustion science, 36(3), 327-363.

American Petroleum Institute (API). 10B Recommended Practice for Testing Oil Well Cements and Cement Additives; American Petroleum Institute: Washington, DC, USA, 1997.

American Petroleum Institute. Recommended Practice for Field Testing of Water -Based Drilling Fluids, 3rd ed. 2003; American Petroleum Institute: Washington, DC.

Amoco Production Company, (1994). Drilling Fluids Manual. six ed., pp. 426.

ASTM standard specification for coal fly ash and raw or calcined natural pozzolan for use in concrete (C618-05). In: Annual book of ASTM standards, concrete and aggregates, vol. 04.02. American Society for Testing Materials; 2005.

Avci, E., Szabo, T., & Federer, G. (2019). The Rheological Performance of Fly Ash in Inhibitive Water-Based Drilling Fluids. Petroleum & Coal, 61(6).

Azar, J. J. and Samuel, G. R. (2007). Drilling engineering. PennWell boks.

Barman, P. C., Kairi, R. R., Das, A., & Islam, R. (2016). An overview of non-newtonian fluid. International Journal of Applied Science and Engineering, 4(2), 97-101.

Barnes, H. A., Hutton, J. F. And Walters, K., (1989). An introduction to rheology. Vol. 3. Elsevier.

Blissett, R. S., & Rowson, N. A. (2012). A review of the multi-component utilisation of coal fly ash. Fuel, 97, 1-23.

Bourgoyne A.T., Chevenert M.E., Millheim K.K., Young F.S. 1991. Applied Drilling Engineering. Richardson, Teksas, ABD.

Buggenhout, J., Brijs, K., Celus, I., & Delcour, J. A. (2013). The breakage susceptibility of raw and parboiled rice: A review. Journal of Food Engineering, 117(3), 304-315.

Caenn, R., H. C. Darley, and G. R. Gray. 2011. Composition and properties of drilling and completion fluids. 6 th ed. USA. Gulf professional publishing.

Carbon brief, chatham house. https://www.carbonbrief.org/qa-why-cement-emissions-matter-for-climate-change

Cong, P., & Cheng, Y. (2021). Advances in geopolymer materials: A comprehensive review. Journal of Traffic and Transportation Engineering (English Edition).

Davidovits, J. (1989). Geopolymers and geopolymeric materials. Journal of thermal analysis, 35(2), 429-441.

Davidovits, J. (1991). Geopolymers: inorganic polymeric new materials. Journal of Thermal Analysis and calorimetry, 37(8), 1633-1656.

Davidovits, J. (1994, October). Properties of geopolymer cements. In First international conference on alkaline cements and concretes (Vol. 1, pp. 131-149). Kiev State Technical University, Ukraine: Scientific Research Institute on Binders and Materials.

Fernandes, I. J., Calheiro, D., Kieling, A. G., Moraes, C. A., Rocha, T. L., Brehm, F. A., & Modolo, R. C. (2016). Characterization of rice husk ash produced using different biomass combustion techniques for energy. Fuel, 165, 351-359.

Forum of civil engineering (2017). Production of fly ash, access date: 26.03.2022, https://www.civilengineeringforum.me/production-fly-ash/.

Guillot, D. (1990). 4 Rheology of well cement slurries. In Developments in Petroleum Science (Vol. 28, pp. 4-1). Elsevier.

Hewlett, P., & Liska, M. (Eds.). (2019). Lea's chemistry of cement and concrete. Butterworth-Heinemann.

IEA. (2018). Low-Carbon Transition in the Cement Industry. IEA. https://iea.blob.core.windows.net/assets/cbaa3da1-fd61-4c2a-8719-31538f59b54f/TechnologyRoadmapLowCarbonTransitionintheCementIndustry.pdf

Joshi, R. C., & Lohita, R. P. (1997). Fly ash in concrete: production, properties and uses (Vol. 2). CRC Press.

Khodja, M., Khodja-Saber, M., Canselier, J. P., Cohaut, N., & Bergaya, F. (2010). Drilling fluid technology: performances and environmental considerations. Products and services; from R&D to final solutions, 227-256.

Kieling AG. Influência da segregação no desempenho de cinzas de casca dearroz como pozolanas e material adsorvente. MSc dissertation, Universidadedo Vale do Rio dos Sinos, UNISINOS, São Leopoldo, RS, Brazil; 2009 [inPortuguese]

Korsch, M., & Walther, W. (2015). Peri-implantitis associated with type of cement: a retrospective analysis of different types of cement and their clinical correlation to the peri-implant tissue. Clinical implant dentistry and related research, 17, e434-e443.

Kumar, S., Sangwan, P., Dhankhar, R. M. V., & Bidra, S. (2013). Utilization of rice husk and their ash: A review. Res. J. Chem. Env. Sci, 1(5), 126-129.

Malhotra, V. M. (1993). Fly ash, slag, silica fume, and rice husk ash in concrete: A review. Concrete International, 15(4), 23-28.

Malhotra, V. M. (1999). Making concrete" greener" with fly ash. Concrete international, 21(5), 61-66.

Masi, G., Rickard, W. D., Vickers, L., Bignozzi, M. C., & Van Riessen, A. (2014). A comparison between different foaming methods for the synthesis of light weight geopolymers. Ceramics International, 40(9), 13891-13902.

Medeiros-Junior, R. A., & Lima, M. G. (2016). Electrical resistivity of unsaturated concrete using different types of cement. Construction and Building Materials, 107, 11-16.

Moayedi, H., Aghel, B., Nguyen, H., & Rashid, A. S. A. (2019). Applications of rice husk ash as green and sustainable biomass. Journal of Cleaner Production, 237, 117851.

Morrison, R. E., Minnick, L. J., & Purdy Jr, E. J. (1970). A review of ash specifications. Information Circular, (8488), 3.

Motorwala, A., Shah, V., Kammula, R., Nannapaneni, P. & Raijiwala, D. (2008). ‘‘Alkali Activated Fly-Ash Based Geopolymer Concrete,’’.

Neupane, G., & Donahoe, R. J. (2013). Leachability of elements in alkaline and acidic coal fly ash samples during batch and column leaching tests. Fuel, 104, 758-770.

Nyale, S. M., Eze, C. P., Akinyeye, R. O., Gitari, W. M., Akinyemi, S. A., Fatoba, O. O., & Petrik, L. F. (2014). The leaching behaviour and geochemical fractionation of trace elements in hydraulically disposed weathered coal fly ash. Journal of Environmental Science and Health, Part A, 49(2), 233-242.

Ofite, 300 LPLT Filter Press Instruction Manual. (2013). Manual No. 207128.

Pacheco-Torgal, F., Moura, D., Ding, Y., & Jalali, S. (2011). Composition, strength and workability of alkali-activated metakaolin based mortars. Construction and Building Materials, 25(9), 3732-3745.

Pikłowska, A. (2017). Cement slurries used in drilling–types, properties, application. World Scientific News, 76, 149-165.

Pode, R. (2016). Potential applications of rice husk ash waste from rice husk biomass power plant. Renewable and Sustainable Energy Reviews, 53, 1468-1485.

Prasara-A, J., & Gheewala, S. H. (2017). Sustainable utilization of rice husk ash from power plants: A review. Journal of cleaner production, 167, 1020-1028.

Rabia, H., (2001). Well Engineering & Construction, Entrac Consulting.

Schramm, G. (1994). A practical approach to rheology and rheometry (pp. 20-25). Karlsruhe: Haake.

Smith, D.K. (1990). Cementing, SPE Monograph, **4**, Richardson, Texas, ABD.

Soltani, N., Bahrami, A., Pech-Canul, M. I., & González, L. A. (2015). Review on the physicochemical treatments of rice husk for production of advanced materials. Chemical engineering journal, 264, 899-935.

Statista. (2014). ‘‘United states and world cement production in 2010 and 2013.’’ Online. Available: http://www.statista.com/statistics/219343/cementproduction-worldwide/ Swanepoel.

Van Oss, H. G., & Padovani, A. C. (2003). Cement manufacture and the environment part II: environmental challenges and opportunities. Journal of Industrial ecology, 7(1), 93-126.

Yahya, Z., Abdullah, M. M. A. B., Hussin, K., Ismail, K. N., Razak, R. A., & Sandu, A. V. (2015). Effect of solids-to-liquids, Na2SiO3-to-NaOH and curing temperature on the palm oil boiler ash (Si+ Ca) geopolymerisation system. Materials, 8(5), 2227-2242.

Yalman, E., Depci, T., Federer-Kovacs, G., & Al Khalaf, H. (2021b). A New Eco-Friendly and Low Cost Additive in Water-Based Drilling Fluids. Rudarsko-geološko-naftni zbornik, 36(5), 1-12.

Yalman, E., Federer, G., & Depci, T. (2021a). Cost Analysis of Inhibitive Drilling Fluids. International Journal of Energy Studies, 6(2), 149-168.

Yalman, E., Federer-Kovacs, G., Depci, T., Al Khalaf, H., Aylikci, V., & Aydin, M. G. (2022a). Development of novel inhibitive water-based drilling muds for oil and gas field applications. Journal of Petroleum Science and Engineering, 210, 109907.

Yalman. E., Federer, G., Depci. T. (2022b). Development of Water-Based Drilling Fluid in Mitigation of Differential Sticking Tendency. Rudarsko-geološko-naftni zbornik (The Mining-Geology-Petroleum Engineering Bulletin), 58(2).

Yalman. E., Federer-Kovacs. G., Depci. T. (2021c). Effect of Two Types of Fly Ash on Rheological and Filtration Properties of Water-Based Drilling Mud. Natural and Engineering Sciences. 6(3), 223-236.

Yao, Z. T., Ji, X. S., Sarker, P. K., Tang, J. H., Ge, L. Q., Xia, M. S., & Xi, Y. Q. (2015). A comprehensive review on the applications of coal fly ash. Earth-Science Reviews, 141, 105-121

Zhuang, X. Y., Chen, L., Komarneni, S., Zhou, C. H., Tong, D. S., Yang, H. M., & Wang, H. (2016). Fly ash-based geopolymer: clean production, properties and applications. Journal of Cleaner Production, 125, 253-267.

11. LIST OF RELATED PUBLICATIONS AND PRESENTATIONS

11.1 Journal articles

1. Avcı, E., 2018. Effect of Salinity on Flow Properties of Drilling Fluids: An Experimental Approach. Petroleum and Coal 60(2): 232-235. Slovakia.

2. Avcı, E. (2018). An Artificial Neural Network Approach for the prediction of Water-Based Drilling Fluid Rheological Behaviour. International Advanced Researches and Engineering Journal, 2(2), 124-131. Turkey.

3. Avcı, E., Szabo, T., Federer, G., (2019). The rheological performance of fly ash in inhibitive water-based drilling fluids. Petroleum and Coal 61(6): 1307-1313. Slovakia.

4. Fliss, M., Szabo, T., Avci, E., (2019). Effect of micro-sized fly ash on the rheological and filtration properties of water-based muds. Petroleum and Coal 61(6): 1361-1364. Slovakia.

5. Avci, E., Mert, B. A. (2019). The Rheology and Performance of Geothermal Spring Water-Based Drilling Fluids. Geofluids.

6. Yücel, A., Sezer, S., Birhanlı, E., Ekinci, T., Yalman, E., & Depci, T. (2020). Synthesis and characterization of whitlockite from sea urchin skeleton and investigation of antibacterial activity. Ceramics International.

7. Yalman. E., Federer-Kovacs. G., Depci. T. (2021). Effect of Two Types of Fly Ash on Rheological and Filtration Properties of Water-Based Drilling Mud. Natural and Engineering Sciences. 6(3), 223-236.

8. Yalman, E., Federer. G., Depci. T. (2021). Cost Analysis of Inhibitive Drilling Fluids. International Journal of Energy Studies. 6(2), 149-168.

9. Yalman, E., Depci, T., Federer-Kovacs. G., & Al Khalaf. H. (2021). A New Eco-Friendly and Low Cost Additive in Water-Based Drilling Fluids. Rudarsko-geološko-naftni zbornik. 36(5), 1-12.

10. Yalman. E., Federer, G., Depci. T. (2022). Development of Water-Based Drilling Fluid in Mitigation of Differential Sticking Tendency. Rudarsko-geološko-naftni zbornik (The Mining-Geology-Petroleum Engineering Bulletin).

11. Yalman, E., Federer-Kovacs, G., Depci, T., Al Khalaf, H., Aylikci, V., Aydin, M. G. (2022). Development of novel inhibitive water-based drilling muds for oil and gas field applications. Journal of Petroleum Science and Engineering, 210, 109907.

12. Yalman, E., Federer-Kovacs, G., Depci, T. (2022). A New Insight into Formulation Approach for Water Based Drilling Fluids. Petroleum and Coal.

11.2. Book Chapter

1. Federer-Kovacs, G., Al Khalaf, H., Yalman E., Al-Haj Mohammed, N. Depci, T. Reasons and resolutions of trapped annular pressure. ENGINEERING AND ARCHITECTURE SCIENCES Theory, Current Researches and New Trends 2021, Stamparija IVPE.

11.3. Proceedings of international conferences

1. Avcı, E., Mert, B.A. (2016). An Experimental Investigation of the Rheological Properties of the Geothermal Water Based Drilling Muds, International Conference on Engineering and Natural Sciences, Sarajevo/Bosna and Herzegovina.

2. Mert, B.A., Avcı, E. (2016). The Development of Well Information System Using Gis: A Case Study of the Bati Raman Oil Field in Turkey, International Conference on Engineering and Natural Sciences, Sarajevo/Bosna and Herzegovina.

3. Mert, B.A., Avcı, E. (2017). Evaluation of the Environmental Impact of Geothermal Drilling Mud Wastes, International Congress on New Trends in Science, Engineering and Technology, Barcelona/Spain.

4. Mert, B.A., Avcı, E. (2017). Experimental Investigation of the Influence of Polymer Additives on Flow Properties of the Water-Based Bentonite Mud, International Multidisciplinary Congress of Eurasian, Rome/Italy.

5. Mert, B.A., Avcı, E. (2017). Reflections of the Legal Regulations on Geothermal Activities in Turkey, International Multidisciplinary Congress of Eurasian, Rome/Italy.

6. Avcı, E. (2017). An Experimental Investigation of the Effect of Seawater on Rheological Properties of Drilling Fluids, International Iskenderun Bay Symposium, Hatay/Turkey.

7. Avcı, E. (2017). Investigation of Shear Rate-Shear Stress Relation in Polymer Based Drilling Fluids, International Advanced Researches and Engineering Congress, Osmaniye/Turkey.

8. Avcı, E., Demir, M.H. (2017). Estimation of Shear Stress in Water-Based Drilling Fluids Using Artificial Neural Network, International Advanced Researches and Engineering Congress, Osmaniye/Turkey.
9. Duren, O., Yalman, E., Aydin, M. G., Depci, T. (2021). An Investigation of Sodium Polyacrylate Effect on Water Based Drilling Fluid, 6Th International Congress on Engineering and Technology Management.

10. Depci, T., Onal, Y., Aydemir, R., Yalman, E., Aydin, M. G. (2021). Investigation of the Biomass Properties of Algae Growing in Iskenderun Bay, International Congress on Sciences and Engineering for Sustainability.

11.4. Conference Presentations

1. Avcı, E., Mert, B.A. (2016) "An Experimental Investigation of the Rheological Properties of the Geothermal Water Based Drilling Muds", International Conference on Engineering and Natural Sciences, Sarajevo/Bosna and Herzegovina.

2. Mert, B.A., Avcı, E. (2016) "The Development of Well Information System Using Gis: A Case Study of the Bati Raman Oil Field in Turkey", International Conference on Engineering and Natural Sciences, Sarajevo/Bosna and Herzegovina.

3. Mert, B.A., Avcı, E. (2017) "Evaluation of the Environmental Impact of Geothermal Drilling Mud Wastes", International Congress on New Trends in Science, Engineering and Technology, Barcelona/Spain.

4. Mert, B.A., Avcı, E. (2017) "Experimental Investigation of the Influence of Polymer Additives on Flow Properties of the Water-Based Bentonite Mud", International Multidisciplinary Congress of Eurasian, Rome/Italy.

5. Mert, B.A., Avcı, E. (2017) "Reflections of the Legal Regulations on Geothermal Activities in Turkey" International Multidisciplinary Congress of Eurasian, Rome/Italy.

6. Avcı, E. (2017) "An Experimental Investigation of the Effect of Seawater on Rheological Properties of Drilling Fluids", International Iskenderun Bay Symposium, Hatay/Turkey.

7. Avcı, E. (2017) "Investigation of Shear Rate-Shear Stress Relation in Polymer Based Drilling Fluids", International Advanced Researches and Engineering Congress, Osmaniye/Turkey.

8. Avcı, E., Demir, M.H. (2017) "Estimation of Shear Stress in Water-Based Drilling Fluids Using Artificial Neural Network", International Advanced Researches and Engineering Congress, Osmaniye/Turkey.

9. Yalman, E., Federer, G., (2021) “Effect of fly ash on the differential sticking”, Earth science PhD forum, Miskolc, Hungary.

12. APPENDICES

12.1. Appendix A

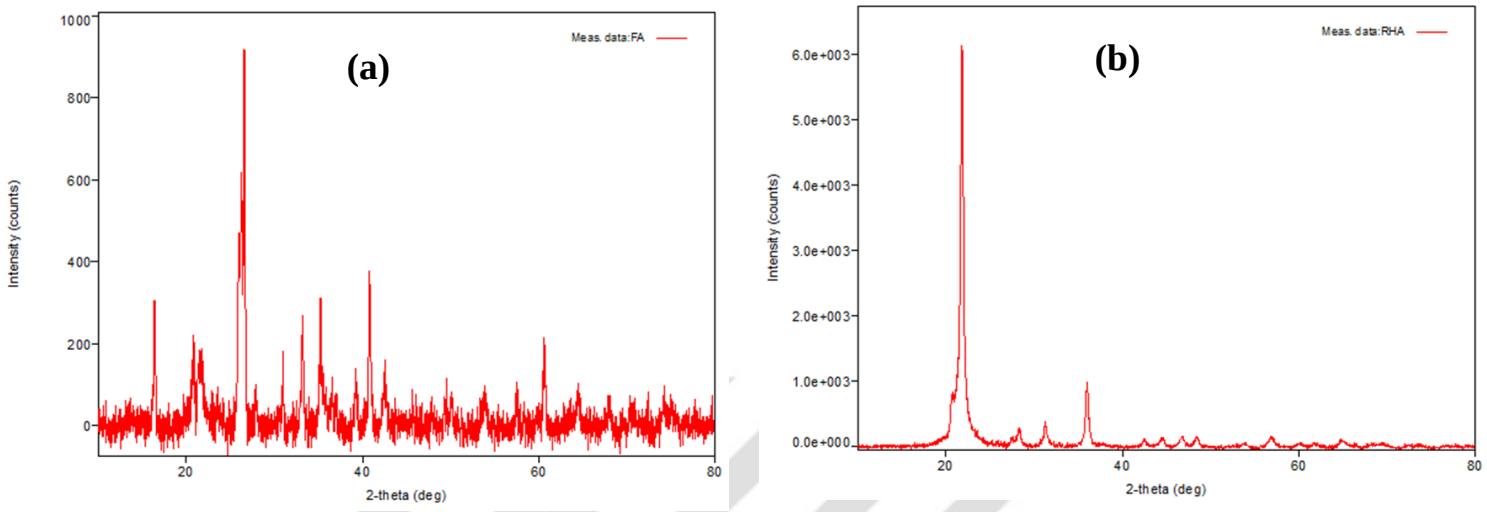

Figure 12.1. XRD pattern of BFA (a) and RHA (b). (Yalman et al., 2022a)

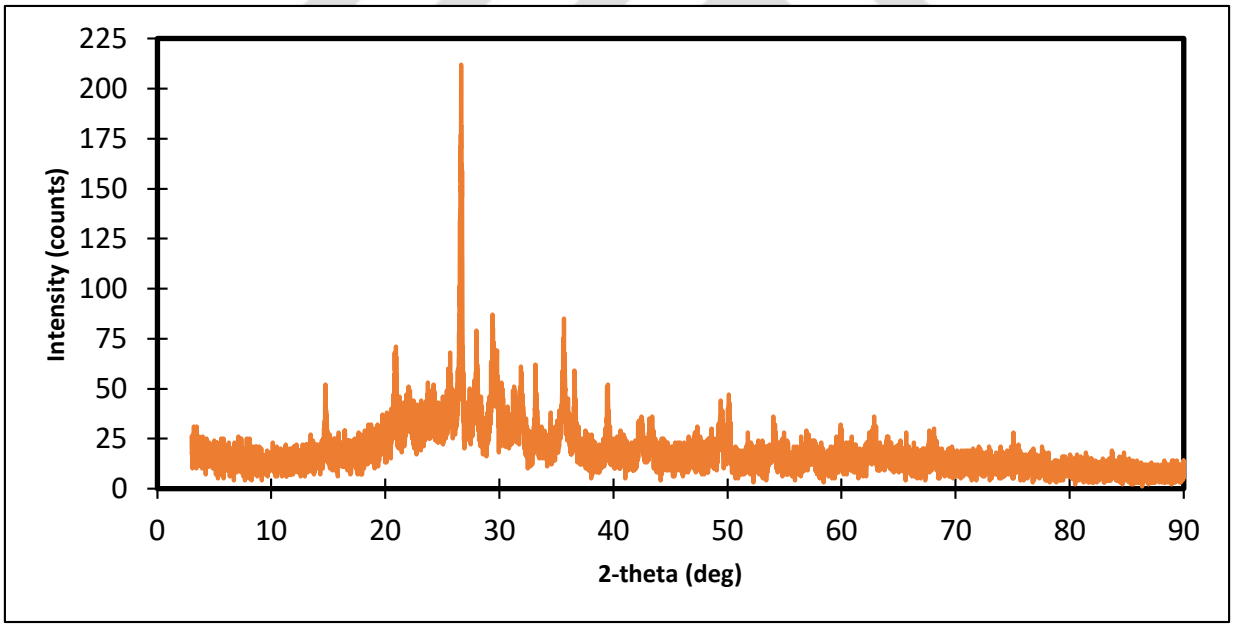

Figure 12.2. XRD pattern of LFA

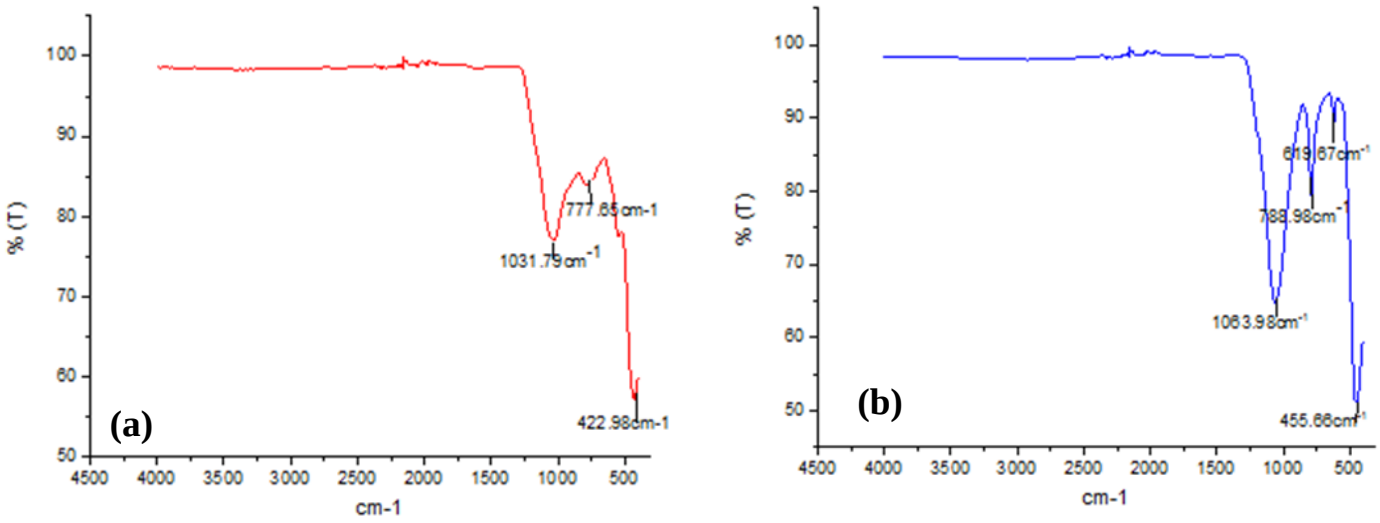

Figure 12.3. FTIR spectrum of BFA (a) and RHA (b) (Yalman et al., 2022a)

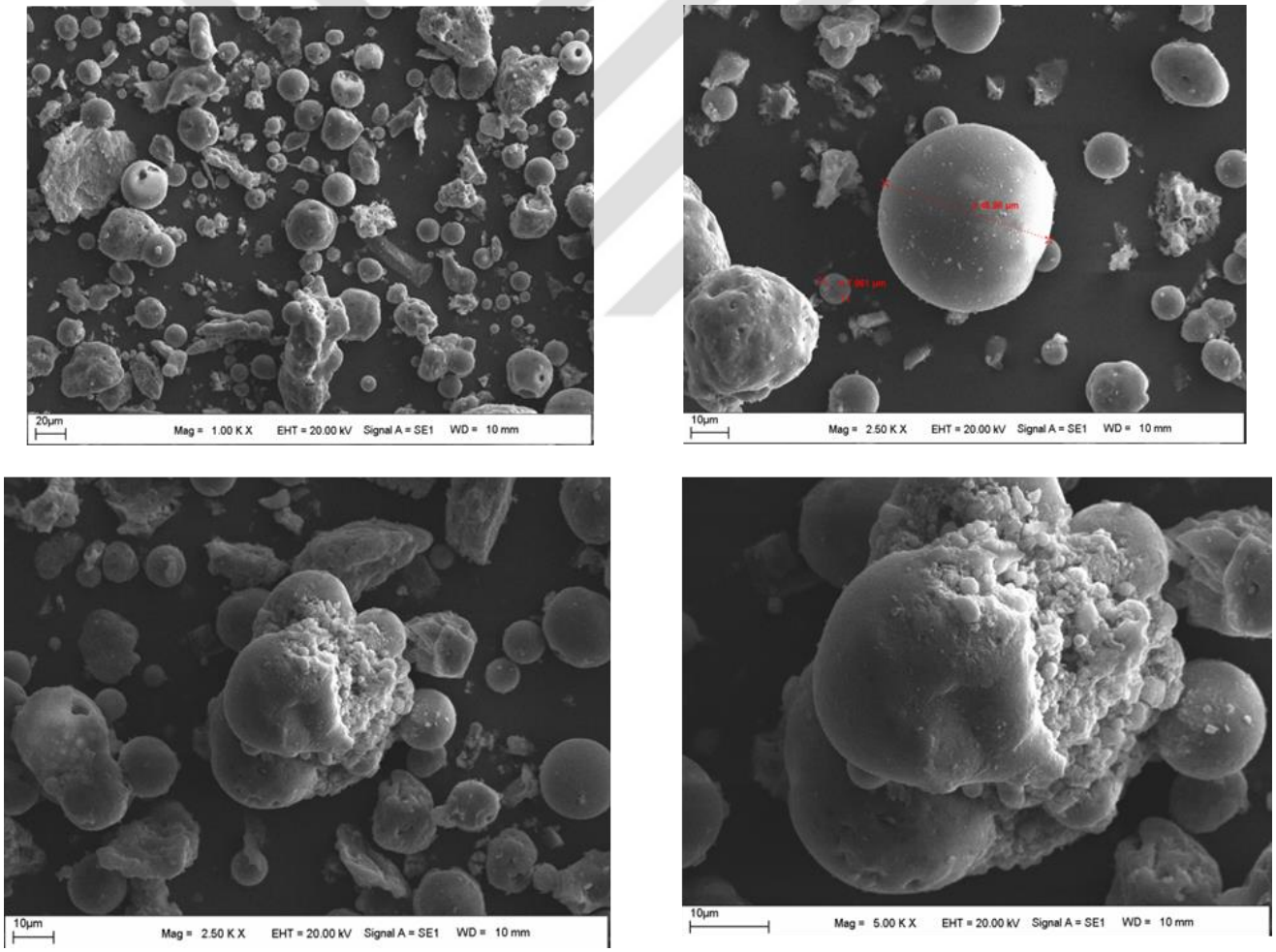

Figure 12.4. Morphology of BFA (Yalman et al., 2022a)

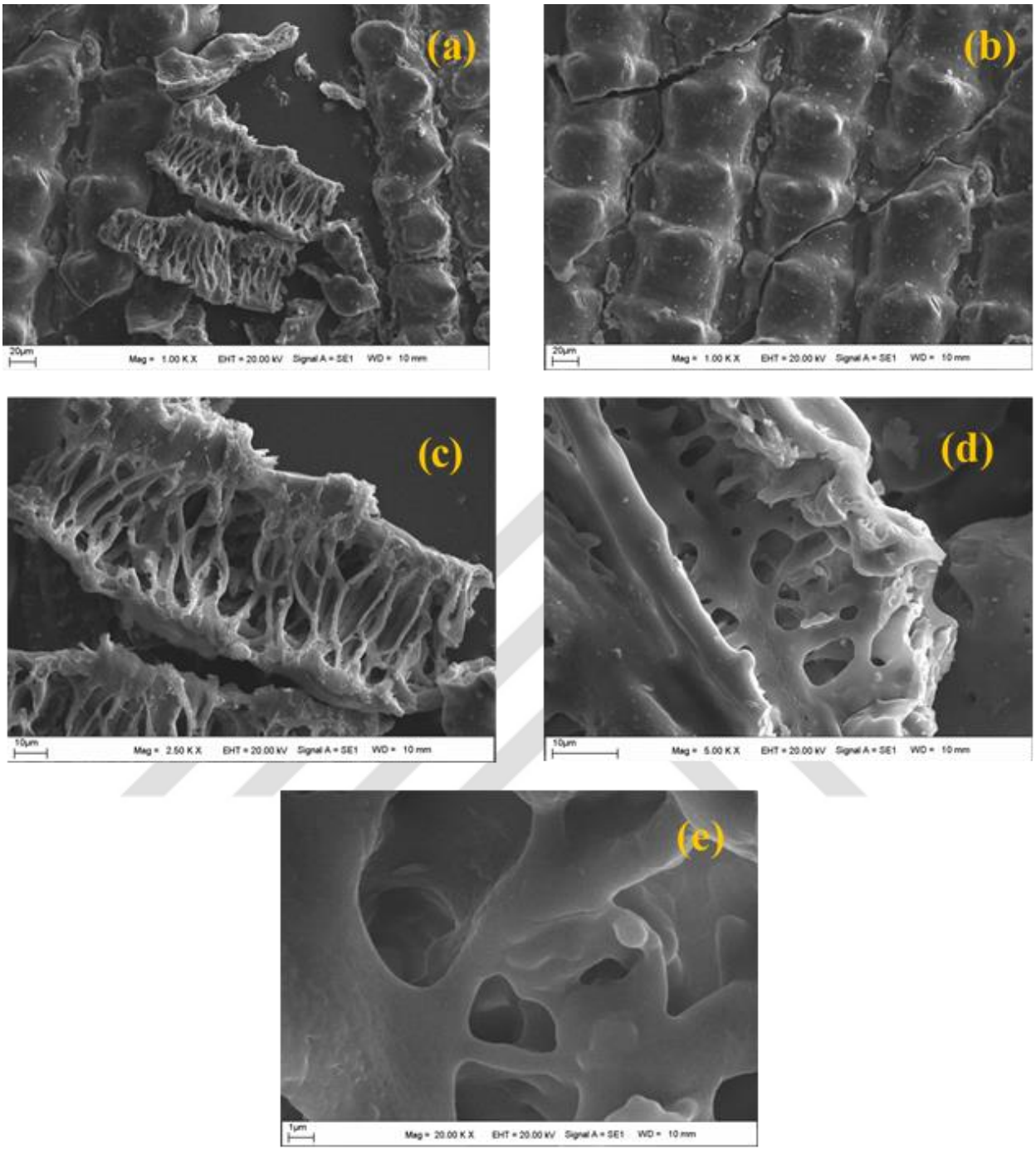

Figure 12.5. Morphology of RHA (Yalman et al., 2022a)

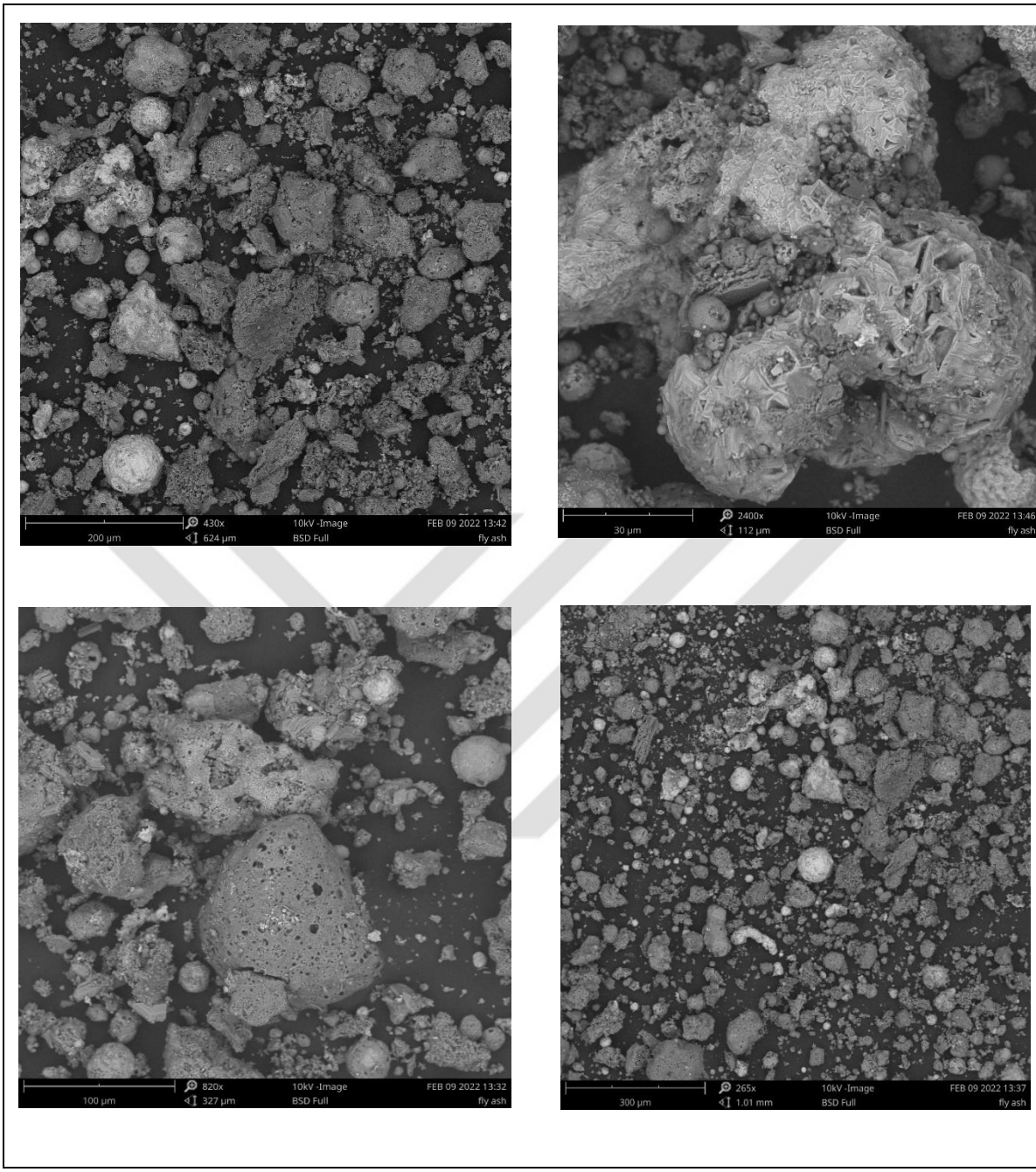

Figure 12.6. Morphology of LFA

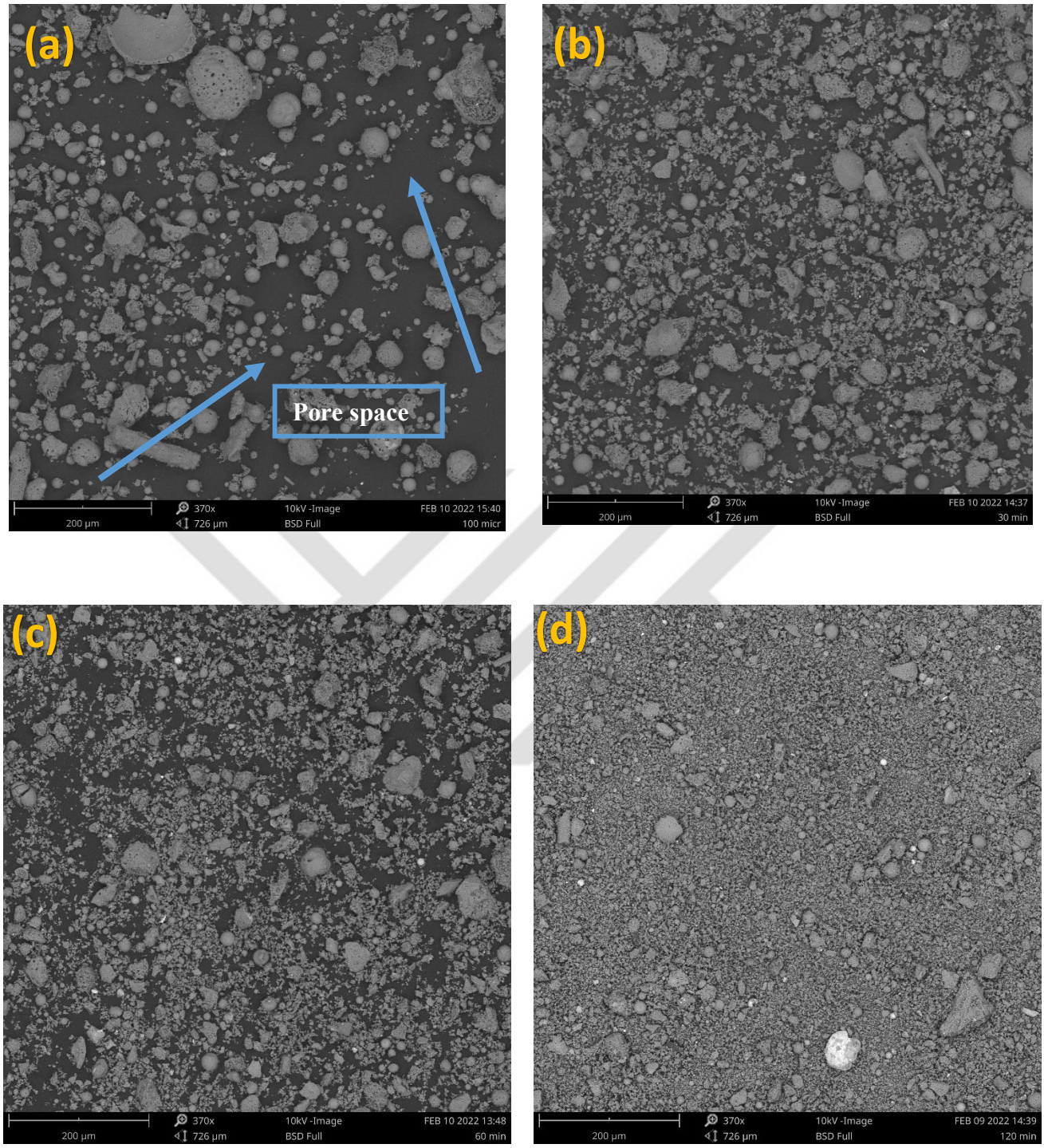

Figure 12.7. Comparison of the void volume of raw FA and ground FAs: raw fly ash (a), 30 min. ground (b), 60 min ground (c), 120 min. ground (d).

12.2. Appendix B

Table 12.1. Barite weighted bentonite drilling mud with raw FA (Yalman et al., 2022b).

Samples		Base Mud	0.1% FA	0.2% FA	0.25% FA	0.3% FA	0.4% FA	0.5% FA	1.0% FA
Dial Reading (θ)	600	52	53	54	55	56	55	57	59
	300	48	43	43	44	45	42	56	49
	200	45	38	39	40	41	37	42	45
	100	38	31	32	34	35	31	35	37
	6	27	23	26	27	25	19	21	23
	3	26	22	25	25	23	18	20	22
Apparent Viscosity (cp)		26	26.5	27	27.5	28	27.5	28.5	29.5
Plastic Viscosity (PV), cp		4	10	11	11	11	13	1	10
Yield Point (YP), lb/100 ft^2		44	33	32	33	34	29	55	39
Gel Strength, 10s,/1min,/10min (lb/100 ft^2)		29/42/60	27/39/57	27/40/58	27/40/59	29/42/60	25/37/55	31/43/61	32/45/64
Density (lb/gal)		10.2	10.2	10.2	10.2	10.2	10.2	10.2	10.2
API fluid loss (mL)	3 min.	2.5	2.4	2.4	2.3	2.8	2.6	2.6	2.7
	5 min.	3.5	3.4	3.3	3.1	3.5	3.6	3.5	3.5
	7.5 min.	4.3	4.3	4.1	4.1	4.4	4.5	4.4	4.4
	10 min.	5.2	5.1	4.9	4.9	5.2	5.3	5.3	5.3
	15 min.	6.4	6.5	6.4	6.1	6.5	6.7	6.5	6.5
	20 min.	7.6	7.6	7.4	7.3	7.6	7.8	7.7	7.5
	25 min.	8.6	8.6	8.4	8.4	8.8	8.8	8.6	8.6
	30 min.	9.6	9.5	9.3	9.2	9.6	9.8	9.6	9.4
Cake Thickness, mm		3	1.9	1.8	1.5	1.9	2	2	2.2

Table 12.2. Barite weighted bentonite drilling mud with sieved FA (Yalman et al., 2022b).

Samples		Base Mud	0.2%5 FA	0.50% FA	0.75% FA	1.0% FA	1.50% FA	3.0% FA
Dial Reading (θ)	600	52	55	56	55	55	54	55
	300	48	44	45	47	45	43	44
	200	45	39	41	41	41	38	36
	100	38	32	34	33	34	32	33
	6	27	17	19	20	21	19	20
	3	26	16	18	19	19	17	18
Apparent Viscosity (cp)		26	27.5	28	27.5	27.5	27	27.5
Plastic Viscosity (PV), cp		4	11	11	8	10	11	11
Yield Point (YP), lb/100 ft^2		44	33	34	39	35	32	33
Gel Strength, 10s,/1min,/10min (lb/100 ft^2)		29/42/60	27/40/56	29/41/60	28/40/57	26/39/56	26/38/56	26/39/57
Density (lb/gal)		10.2	10.2	10.2	10.2	10.2	10.2	10.2
API fluid loss (mL)	3 min.	2.5	2.4	2.4	2.1	2.2	2.5	2.3
	5 min.	3.5	3.3	3.3	3.4	3.5	3.5	3.4
	7.5 min.	4.3	4.3	4.3	4	4.1	4.3	4.2
	10 min.	5.2	5.1	5.1	4.8	4.9	5.2	5.1
	15 min.	6.4	6.4	6.4	6.1	6.2	6.5	6.4

	20 min.	7.6	7.4	7.4	7.2	7.3	7.6	7.5
	25 min.	8.6	8.4	8.4	8.2	8.3	8.7	8.6
	30 min.	9.6	9.4	9.4	9.1	9.2	9.4	9.3
Cake Thickness. mm		3	1.7	1.6	1.3	1	1.9	2.1

Table 12.3. Barite weighted bentonite drilling mud with ground FA (Yalman et al., 2022b).

Samples		Base Mud	0.001% FA	0.001% FA	0.15% FA	0.25% FA	0.3% FA	0.4% FA	0.5% FA
Dial Reading (θ)	600	52	52	53	53	54	55	53	54
	300	48	42	42	42	43	44	42	43
	200	45	39	39	39	39	40	38	39
	100	38	30	30	31	31	31	30	32
	6	27	18	19	19	20	20	18	19
	3	26	17	18	18	19	19	17	18
Apparent Viscosity (cp)		26	26	26.5	26.5	27	27.5	26.5	27
Plastic Viscosity (PV) cp		4	10	11	11	11	11	11	11
Yield Point (YP) lb/100 ft^2		44	32	31	31	32	33	31	32
Gel Strength, 10s,/1min,/10min (lb/100 ft^2)		29/42/60	24/37/53	25/37/54.5	24/37/54	25.5/38/57	27/39/57	25/37/55	26/38/57
Density (lb/gal)		10.2	10.2	10.2	10.2	10.2	10.2	10.2	10.2
API fluid loss (mL)	3 min.	2.5	2.6	2.5	2.4	2.5	2.8	2.7	2.5
	5 min.	3.5	3.7	3.7	3.4	3.5	3.8	3.6	3.4
	7.5 min.	4.3	4.4	4.4	4.3	4.4	4.6	4.6	4.4
	10 min.	5.2	5.3	5.3	5.2	5.2	5.4	5.4	5.2
	15 min.	6.4	6.6	6.6	6.5	6.6	6.5	6.8	6.6
	20 min.	7.6	7.8	7.8	7.6	7.8	7.8	7.9	7.7
	25 min.	8.6	8.8	8.8	8.6	8.7	8.8	9	8.8
	30 min.	9.6	9.6	9.6	9.5	9.6	9.7	9.9	9.6
Cake Thickness. mm		3	2	1.9	1	0.9	0.8	1.9	2.4

12.3. Appendix C

Table 12.4. Data obtained from rheometer for the rheological model analysis of drilling fluid with 7% FA at 86 °F, 104°F and 122°F

No	Shear rate (1/s)	Tempera ture (°C)	Shear stress (dyne/cm^2)	No	Shear rate (1/s)	Tempera ture (°C)	Shear stress (dyne/cm^2)	No	Shear rate (1/s)	Tempera ture (°C)	Shear stress (dyne/cm^2)
1	50.471314	85.1	49.274988	97	50.506311	101.84	31.000557	193	50.501311	118.04	21.466071
2	50.127995	85.280001	48.480447	98	50.008833	101.84	30.206016	194	50.022998	118.04	20.67153
3	49.991332	85.280001	47.685907	99	49.9655	101.84	29.411476	195	49.978002	118.04	20.67153
4	49.928835	85.280001	46.891366	100	49.998834	102.02	29.411476	196	50.04383	118.04	19.87699
5	49.967168	85.280001	46.891366	101	49.986333	102.02	29.411476	197	49.983001	118.22	19.87699
6	50.154661	85.280001	46.891366	102	50.017998	102.02	28.616935	198	50.008833	118.22	19.87699
7	50.072165	85.280001	46.096826	103	50.014667	102.02	28.616935	199	49.958003	118.22	19.87699
8	49.981333	85.280001	46.096826	104	50.04383	102.2	28.616935	200	50.007165	118.4	19.87699
9	50.116327	85.280001	46.096826	105	50.142159	102.2	28.616935	201	49.9605	118.4	19.87699

10	49.973836	85.280001	45.302285	106	49.975499	102.38	28.616935	202	49.902168	118.4	19.87699
11	49.923001	85.280001	45.302285	107	49.9605	102.38	28.616935	203	49.924669	118.58	19.87699
12	49.998834	85.460001	45.302285	108	50.014667	102.38	28.616935	204	50.0305	118.58	19.082449
13	101.65594	85.460001	65.165798	109	101.97425	102.38	43.713204	205	102.22925	118.58	33.384178
14	100.16266	85.460001	63.576717	110	100.051	102.38	43.713204	206	100.19099	118.58	32.589638
15	100.00101	85.460001	63.576717	111	100.10933	102.56	42.918664	207	100.00934	118.76	32.589638
16	100.026	85.460001	62.782176	112	100.10599	102.56	42.918664	208	100.04433	118.76	32.589638
17	99.972665	85.460001	62.782176	113	99.984333	102.56	42.918664	209	99.987669	118.76	32.589638
18	99.984333	85.460001	62.782176	114	100.111	102.74	42.918664	210	99.95934	118.94	32.589638
19	100.00433	85.460001	61.987636	115	99.97767	102.74	42.918664	211	100.05433	118.94	32.589638
20	99.952667	85.460001	61.987636	116	100.09599	102.92	42.124123	212	100.02266	119.12	32.589638
21	100.01266	85.460001	61.987636	117	100.00767	102.92	42.124123	213	100.016	119.3	32.589638
22	99.97767	85.639999	61.987636	118	99.969339	102.92	42.124123	214	99.952667	119.3	32.589638
23	100.026	85.639999	61.987636	119	100.10933	103.1	42.124123	215	100.00934	119.3	32.589638
24	99.937673	85.639999	61.193095	120	99.969339	103.1	42.124123	216	99.962666	119.48	32.589638
25	151.95392	85.819999	77.083905	121	151.98726	103.28	54.042231	217	152.40057	119.48	42.918664
26	150.09067	85.819999	76.289364	122	150.21733	103.28	54.836771	218	150.13066	119.66	42.918664
27	150.10399	85.819999	75.494824	123	149.984	103.46	54.836771	219	150.02733	120.02	42.918664
28	150.06067	85.819999	75.494824	124	150.02733	103.64	54.042231	220	149.964	120.2	42.918664
29	149.964	86	75.494824	125	150.004	103.64	54.836771	221	150.07399	120.2	42.918664
30	150.04067	86	75.494824	126	150.04067	103.82	54.836771	222	150.04067	120.56	42.918664
31	149.95734	86	74.700283	127	149.97734	104	54.042231	223	149.87401	120.56	42.918664
32	150.054	86.180001	74.700283	128	150.01066	104	54.042231	224	149.92733	120.92	42.918664
33	150.124	86.180001	74.700283	129	149.89401	104.18	54.042231	225	149.91401	121.1	42.918664
34	150.07399	86.180001	74.700283	130	150.014	104.36	54.042231	226	150.04067	121.28	42.918664
35	150.09067	86.360001	74.700283	131	150.04733	104.36	54.042231	227	150.01066	121.28	42.918664
36	150.07399	86.360001	74.700283	132	150.014	104.54	54.042231	228	150.054	121.46	42.918664
37	201.78526	86.360001	87.412931	133	202.11858	104.72	64.371257	229	202.45524	121.64	52.45315
38	200.07533	86.360001	86.618391	134	200.082	104.72	64.371257	230	200.10865	121.82	51.658609
39	200.082	86.539999	86.618391	135	199.94199	104.9	64.371257	231	200.13533	121.82	51.658609
40	200.04532	86.539999	86.618391	136	199.92533	105.08	64.371257	232	199.98199	122	52.45315
41	199.93201	86.539999	86.618391	137	199.96199	105.08	64.371257	233	199.90533	122.18	52.45315
42	200.03867	86.719999	85.82385	138	199.97534	105.26	64.371257	234	199.97534	122.36	51.658609
43	200.06866	86.719999	85.82385	139	199.96199	105.44	64.371257	235	199.96867	122.36	52.45315
44	200.13533	86.719999	85.82385	140	200.13533	105.44	64.371257	236	199.98866	122.54	52.45315
45	200.06532	86.719999	85.82385	141	199.96867	105.44	64.371257	237	200.03867	122.54	51.658609

46	200.05867	86.719999	85.82385	142	199.92533	105.62	64.371257	238	200.01867	122.72	51.658609
47	200.06866	86.9	85.82385	143	199.98199	105.62	64.371257	239	200.02532	122.72	51.658609
48	200.02532	86.9	85.82385	144	199.99534	105.8	64.371257	240	199.97534	122.72	51.658609
49	303.50119	86.9	108.07098	145	304.55449	105.8	82.645688	241	304.9478	122.9	68.343959
50	300.268	86.9	106.4819	146	300.29465	105.8	81.851148	242	300.43466	122.9	67.549419
51	300.06799	86.9	106.4819	147	299.988	105.98	81.851148	243	299.96133	123.08	67.549419
52	300.06799	86.9	106.4819	148	300.04132	105.98	82.645688	244	300.10134	123.08	67.549419
53	299.94133	86.9	106.4819	149	299.86134	105.98	81.851148	245	300.10134	123.08	67.549419
54	300.11466	86.9	106.4819	150	300.00133	105.98	81.851148	246	300.15466	123.26	67.549419
55	300.10134	86.9	106.4819	151	300.04132	105.98	81.851148	247	299.948	123.08	68.343959
56	299.92801	87.080001	106.4819	152	300.01467	106.16	82.645688	248	300.15466	123.26	68.343959
57	299.90133	87.080001	106.4819	153	300.06799	106.16	82.645688	249	299.94133	123.26	68.343959
58	300.00133	87.080001	106.4819	154	299.87466	106.16	82.645688	250	299.97468	123.26	68.343959
59	299.96133	87.080001	106.4819	155	300.08134	106.16	82.645688	251	299.96133	123.26	68.343959
60	300.00133	87.080001	106.4819	156	300.06799	106.16	82.645688	252	300.00133	123.26	69.1385
61	404.03051	87.080001	126.34542	157	405.35044	106.16	100.12558	253	406.11042	123.26	84.234769
62	400.27732	87.080001	125.55088	158	400.5173	106.34	98.536498	254	400.47063	123.26	83.440229
63	399.99735	87.080001	125.55088	159	399.99735	106.34	98.536498	255	400.01065	123.26	83.440229
64	399.99735	87.080001	124.75633	160	399.99735	106.34	98.536498	256	400.05732	123.26	83.440229
65	400.01065	87.080001	125.55088	161	399.99735	106.34	98.536498	257	400.03734	123.26	83.440229
66	399.97065	87.080001	125.55088	162	399.97065	106.34	98.536498	258	400.05732	123.26	83.440229
67	399.99735	87.080001	125.55088	163	399.93066	106.34	98.536498	259	400.05065	123.26	83.440229
68	399.984	87.080001	125.55088	164	399.97065	106.34	98.536498	260	399.93066	123.26	83.440229
69	399.99735	86.9	125.55088	165	399.984	106.34	98.536498	261	399.99735	123.26	83.440229
70	400.03734	87.080001	125.55088	166	399.99735	106.34	98.536498	262	399.97065	123.26	83.440229
71	400.03734	87.080001	125.55088	167	400.03734	106.34	98.536498	263	399.984	123.26	83.440229
72	399.99735	87.080001	124.75633	168	400.03734	106.34	98.536498	264	400.03734	123.08	83.440229
73	503.89985	87.080001	141.44168	169	506.05975	106.34	112.83823	265	506.48641	123.08	96.152877
74	500.28667	87.080001	140.64714	170	500.37997	106.34	112.83823	266	500.37997	123.08	96.152877
75	499.98	87.080001	140.64714	171	500.28667	106.34	112.83823	267	500.05999	123.08	96.152877
76	500.00665	87.080001	140.64714	172	499.95335	106.34	112.83823	268	499.78002	123.08	96.947417
77	499.98	87.080001	140.64714	173	499.82001	106.16	112.83823	269	500.08664	122.9	96.947417
78	500.03334	87.080001	140.64714	174	499.84666	106.16	113.63277	270	500.09999	122.9	96.947417
79	499.84666	87.080001	140.64714	175	499.82001	106.16	113.63277	271	499.92666	122.9	96.947417
80	499.92666	87.080001	139.8526	176	500.05999	106.16	113.63277	272	500.08664	122.9	96.947417
81	499.95335	87.080001	139.8526	177	500.17998	106.16	112.83823	273	500.05999	122.9	96.947417

82	499.98	87.080001	139.8526	178	500.15333	106.16	113.63277	274	499.95335	122.9	96.947417
83	500.08664	87.080001	139.8526	179	500.17998	106.16	113.63277	275	500.05999	122.9	96.947417
84	500.05999	87.080001	139.05806	180	500.09999	105.98	114.42731	276	500.00665	122.9	96.947417
85	604.3625	87.080001	155.74341	181	605.68244	105.98	127.9345	277	606.52241	122.72	109.66007
86	600.32267	87.080001	155.74341	182	600.52265	105.98	127.13996	278	600.66929	122.72	108.86552
87	600.10934	86.9	155.74341	183	599.936	105.98	127.13996	279	599.98935	122.72	109.66007
88	600.04265	87.080001	156.53795	184	599.96265	105.98	127.9345	280	600.04265	122.72	109.66007
89	600.016	86.9	156.53795	185	600.016	105.98	127.9345	281	599.936	122.54	109.66007
90	600.04265	87.080001	156.53795	186	599.88266	105.98	127.9345	282	599.936	122.54	110.45461
91	600.08264	87.080001	156.53795	187	600.016	105.98	127.9345	283	600.13599	122.54	110.45461
92	599.936	86.9	157.33249	188	600.08264	105.98	128.72904	284	599.936	122.36	110.45461
93	599.98935	86.9	157.33249	189	600.016	105.8	128.72904	285	599.98935	122.36	110.45461
94	599.98935	87.080001	157.33249	190	599.98935	105.8	128.72904	286	599.96265	122.36	111.24915
95	599.98935	86.9	157.33249	191	600.06934	105.8	128.72904	287	600.016	122.36	111.24915
96	600.016	86.9	158.12704	192	600.016	105.8	129.52358	288	599.98935	122.18	111.24915

Table 12.5. Data obtained from rheometer for the rheological model analysis of drilling fluid with 9% FA at 86 °F, 104°F and 122°F

No	Shear rate (1/s)	Temperature (°C)	Shear stress (dyne/cm^2)	No	Shear rate (1/s)	Temperature (°C)	Shear stress (dyne/cm^2)	No	Shear rate (1/s)	Temperature (°C)	Shear stress (dyne/cm^2)
1	50.27215	84.92	54.83677	97	50.68547	101.84	36.56234	193	50.19133	118.22	31.00056
2	49.923	84.92	53.24769	98	50.00383	101.84	35.7678	194	50.058	118.22	31.00056
3	49.91134	84.92	53.24769	99	49.81634	101.84	35.7678	195	50.12966	118.22	31.00056
4	50.128	84.92	52.45315	100	50.0305	101.84	34.97326	196	50.07383	118.22	30.20602
5	49.94217	84.92	51.65861	101	50.07383	101.84	34.97326	197	50.10549	118.4	31.00056
6	49.9705	84.92	51.65861	102	50.07966	102.02	34.97326	198	50.10049	118.4	30.20602
7	50.01133	84.92	51.65861	103	49.85884	102.02	34.97326	199	50.04383	118.4	30.20602
8	50.01133	85.1	50.86407	104	50.00883	102.02	34.97326	200	50.06883	118.58	30.20602
9	50.14966	85.1	50.86407	105	50.018	102.2	34.17872	201	50.07717	118.58	30.20602
10	50.0055	85.1	50.86407	106	49.87967	102.2	34.17872	202	49.92467	118.58	30.20602
11	50.16716	85.1	50.06953	107	50.02134	102.2	34.17872	203	50.10216	118.58	30.20602
12	49.943	85.1	50.06953	108	50.07883	102.38	34.17872	204	50.06883	118.76	30.20602
13	101.3926	85.1	70.72758	109	101.7193	102.38	50.86407	205	102.2992	118.76	42.91866
14	100.1443	85.1	69.93304	110	100.211	102.38	50.86407	206	100.2477	118.76	42.91866
15	100.0127	85.1	69.1385	111	100.0293	102.56	50.86407	207	100.131	118.94	42.91866
16	99.96267	85.28	69.1385	112	100.036	102.56	50.06953	208	99.90267	118.94	42.12412
17	99.99767	85.28	68.34396	113	100.086	102.74	50.06953	209	99.86767	119.12	42.91866
18	100.051	85.28	68.34396	114	100.0043	102.74	50.06953	210	100.0127	119.3	42.91866
19	100.0393	85.28	67.54942	115	99.82934	102.74	50.06953	211	99.91434	119.3	42.12412
20	100.061	85.46	67.54942	116	100.0393	102.92	50.06953	212	99.93434	119.48	42.12412

21	99.94267	85.28	67.54942	117	100.0293	102.92	50.06953	213	99.94933	119.48	42.12412
22	100.0193	85.46	67.54942	118	99.92434	103.1	50.06953	214	100.0993	119.66	42.12412
23	99.97267	85.46	67.54942	119	99.89267	103.1	50.06953	215	99.92434	119.66	42.12412
24	100.0327	85.46	66.75488	120	99.85767	103.28	50.06953	216	100.166	119.84	42.12412
25	151.4639	85.46	82.64569	121	151.7773	103.28	62.78218	217	152.0039	120.02	53.24769
26	150.0607	85.64	81.85115	122	150.174	103.46	62.78218	218	150.2073	120.02	53.24769
27	150.124	85.64	81.85115	123	149.9407	103.46	62.78218	219	150.0407	120.2	53.24769
28	150.054	85.64	81.85115	124	149.9573	103.64	62.78218	220	150.0607	120.38	52.45315
29	149.9273	85.64	81.05661	125	149.9707	103.64	62.78218	221	150.0273	120.56	52.45315
30	150.104	85.82	81.05661	126	149.9273	103.82	62.78218	222	150.054	120.56	52.45315
31	150.054	85.82	81.05661	127	149.9407	104	61.98764	223	150.074	120.74	52.45315
32	149.934	85.82	81.05661	128	149.944	104.18	61.98764	224	149.9907	120.92	52.45315
33	149.9773	85.82	80.26207	129	149.9907	104.18	61.98764	225	150.0407	121.1	52.45315
34	149.9407	86	80.26207	130	149.9573	104.36	61.98764	226	150.074	121.28	52.45315
35	150.0973	86	80.26207	131	150.0107	104.54	61.98764	227	150.004	121.46	52.45315
36	149.9907	86	80.26207	132	150.004	104.54	61.98764	228	150.0473	121.46	52.45315
37	201.2853	86	93.76926	133	201.6353	104.72	73.1112	229	202.2819	121.64	61.98764
38	200.122	86	92.97472	134	200.0387	104.72	73.1112	230	200.2553	121.82	61.98764
39	200.1087	86.18	92.97472	135	200.0587	104.9	73.1112	231	199.8987	122	61.1931
40	199.8853	86.18	92.97472	136	200.052	105.08	73.90574	232	199.9553	122	61.1931
41	200.052	86.18	92.18017	137	199.932	105.08	73.1112	233	200.122	122	61.1931
42	200.082	86.18	92.18017	138	199.912	105.26	73.1112	234	199.962	122.18	61.1931
43	200.082	86.18	92.18017	139	199.962	105.44	73.1112	235	199.962	122.36	61.1931
44	199.8853	86.36	92.18017	140	200.0653	105.44	73.1112	236	200.1387	122.36	61.1931
45	199.9253	86.36	92.18017	141	200.0687	105.62	73.1112	237	199.962	122.36	61.1931
46	200.0253	86.36	91.38563	142	200.0253	105.62	73.1112	238	199.9487	122.54	61.1931
47	199.862	86.36	91.38563	143	199.942	105.62	73.1112	239	199.9687	122.54	61.1931
48	200.0453	86.54	91.38563	144	200.0753	105.62	73.1112	240	199.9953	122.54	61.1931
49	303.0812	86.54	115.2218	145	305.0611	105.8	93.76926	241	305.6078	122.72	80.26207
50	300.3346	86.54	114.4273	146	300.3346	105.8	92.97472	242	300.3946	122.72	79.46753
51	299.948	86.54	114.4273	147	299.988	105.98	92.97472	243	300.0147	122.9	79.46753
52	300.0013	86.54	114.4273	148	300.0413	105.98	92.97472	244	300.068	122.9	79.46753
53	300.028	86.54	114.4273	149	299.988	105.98	92.97472	245	300.0147	122.9	79.46753
54	300.0413	86.54	114.4273	150	300.0013	105.98	92.97472	246	299.848	122.9	79.46753
55	300.0013	86.54	113.6328	151	299.9613	105.98	92.97472	247	299.9013	122.9	79.46753
56	299.988	86.54	114.4273	152	299.988	106.16	92.97472	248	299.9013	123.08	79.46753
57	300.0413	86.54	114.4273	153	300.068	106.16	92.97472	249	300.1147	122.9	79.46753
58	300.0413	86.54	114.4273	154	300.0013	106.16	92.97472	250	300.088	123.08	79.46753
59	300.0547	86.54	114.4273	155	300.0413	106.16	92.97472	251	300.0813	123.08	80.26207
60	299.848	86.72	114.4273	156	300.0413	106.16	92.97472	252	299.9413	123.08	79.46753
61	403.2506	86.54	135.8799	157	404.5838	106.16	111.2491	253	405.0571	123.08	97.74196
62	400.224	86.54	134.2908	158	400.2107	106.34	110.4546	254	400.4706	123.08	97.74196
63	400.0506	86.54	134.2908	159	400.0506	106.34	110.4546	255	400.0107	123.08	97.74196
64	399.9573	86.72	134.2908	160	399.8973	106.34	110.4546	256	400.0373	123.08	97.74196

65	399.984	86.54	134.2908	161	400.0373	106.34	110.4546	257	400.0506	123.08	97.74196
66	400.0373	86.54	134.2908	162	399.8707	106.16	110.4546	258	400.0506	123.08	97.74196
67	400.0573	86.54	134.2908	163	400.0573	106.34	110.4546	259	399.8973	123.08	97.74196
68	400.0707	86.54	135.0854	164	400.0573	106.34	111.2491	260	400.0573	123.08	97.74196
69	400.0573	86.54	135.0854	165	399.9707	106.34	111.2491	261	400.0373	123.08	97.74196
70	400.0973	86.54	135.8799	166	399.9307	106.34	111.2491	262	399.844	123.08	97.74196
71	400.0973	86.54	135.8799	167	399.9307	106.34	111.2491	263	400.0573	122.9	98.5365
72	399.9573	86.54	135.8799	168	399.9573	106.34	111.2491	264	399.9174	122.9	98.5365
73	504.0998	86.54	154.9489	169	504.4332	106.16	127.9345	265	505.7531	122.9	113.6328
74	500.1	86.72	153.3598	170	500.1	106.16	126.3454	266	500.2333	122.9	112.0437
75	500.1	86.72	152.5653	171	500.06	106.16	126.3454	267	500.0866	122.9	112.8382
76	500.1	86.72	154.1543	172	500.2067	106.16	126.3454	268	499.98	122.9	112.8382
77	500.0866	86.72	154.1543	173	499.82	106.16	126.3454	269	500.2867	122.9	112.8382
78	499.7267	86.54	155.7434	174	499.9267	106.16	126.3454	270	499.8467	122.72	112.8382
79	500.1	86.72	154.9489	175	500.34	106.16	126.3454	271	499.98	122.72	112.0437
80	499.9	86.72	155.7434	176	499.8467	106.16	127.14	272	499.98	122.72	112.0437
81	499.8467	86.72	156.538	177	499.98	105.98	127.14	273	500.2333	122.72	112.8382
82	500.0866	86.54	157.3325	178	500.0333	106.16	127.14	274	500.06	122.54	112.8382
83	500.1	86.54	157.3325	179	499.98	105.98	127.9345	275	500.1	122.54	112.8382
84	500.0866	86.54	158.127	180	500.06	105.98	127.9345	276	499.98	122.54	113.6328
85	603.8825	86.54	173.2233	181	606.5491	105.98	140.6471	277	606.3491	122.54	125.5509
86	600.3493	86.54	168.4561	182	600.696	105.98	137.469	278	600.696	122.54	121.5782
87	599.9893	86.54	166.0724	183	600.0826	105.98	137.469	279	599.9893	122.54	120.7836
88	599.936	86.54	166.0724	184	600.1627	105.98	137.469	280	600.216	122.36	120.7836
89	599.936	86.54	166.0724	185	600.1893	105.98	137.469	281	599.936	122.36	120.7836
90	599.9627	86.54	166.867	186	600.0426	105.8	137.469	282	599.936	122.36	120.7836
91	600.0426	86.54	167.6615	187	599.9893	105.8	137.469	283	600.016	122.36	120.7836
92	599.936	86.54	167.6615	188	599.9893	105.8	137.469	284	600.0426	122.36	120.7836
93	599.9893	86.54	168.4561	189	600.0426	105.8	137.469	285	600.0826	122.36	120.7836
94	600.016	86.54	168.4561	190	600.0426	105.8	137.469	286	599.8827	122.18	120.7836
95	599.8294	86.54	169.2506	191	599.9893	105.8	137.469	287	600.016	122.18	120.7836
96	599.9094	86.54	170.0451	192	599.9893	105.8	137.469	288	599.9893	122.18	120.7836

Table 12.6. Data obtained from rheometer for the rheological model analysis of drilling fluid with 12.5% FA at 86 °F, 104°F and 122°F

No	Shear rate (1/s)	Tempera ture (°C)	Shear stress (dyne/cm^2)	No	Shear rate (1/s)	Tempera ture. (°C)	Shear stress (dyne/cm^2)	No	Shear rate (1/s)	Tempera ture. (°C)	Shear stress (dyne/cm^2)
1	50.60798	85.1	48.48045	97	50.54881	101.48	32.58964	193	50.18966	118.22	21.46607
2	50.10049	85.1	46.89137	98	50.04966	101.48	31.7951	194	50.04217	118.22	20.67153
3	50.093	85.1	46.89137	99	50.03383	101.48	31.7951	195	50.01133	118.22	19.87699
4	50.11216	85.28	46.09683	100	50.0405	101.48	31.00056	196	50.01133	118.4	19.87699
5	49.93217	85.28	46.09683	101	50.048	101.66	31.00056	197	49.978	118.4	19.87699
6	49.94634	85.28	46.09683	102	50.06383	101.66	31.00056	198	49.99883	118.4	19.87699
7	49.94634	85.28	45.30229	103	50.06133	101.66	31.00056	199	49.99133	118.58	19.87699
8	49.90717	85.46	45.30229	104	50.02134	101.84	31.00056	200	49.99384	118.58	19.87699

9	49.94967	85.46	45.30229	105	49.97717	101.84	31.00056	201	49.99883	118.76	19.87699
10	50.07217	85.46	45.30229	106	50.028	101.84	31.00056	202	50.0355	118.76	19.87699
11	49.93217	85.46	44.50775	107	50.01967	101.84	30.20602	203	49.78634	118.76	19.87699
12	49.9305	85.46	45.30229	108	50.03216	102.02	30.20602	204	50.0355	118.76	19.87699
13	101.7143	85.64	65.96034	109	102.0026	102.02	47.68591	205	102.4576	118.76	34.17872
14	100.1343	85.64	65.1658	110	100.1443	102.2	46.89137	206	100.2927	118.94	34.17872
15	100.016	85.64	64.37126	111	99.99433	102.2	46.89137	207	99.91434	118.94	34.17872
16	99.88934	85.82	64.37126	112	99.991	102.2	46.89137	208	99.93933	119.12	34.17872
17	99.89933	85.82	64.37126	113	99.98433	102.38	46.89137	209	100.1443	119.3	34.17872
18	100.1343	86	63.57672	114	99.98433	102.56	46.09683	210	99.89933	119.48	33.38418
19	99.93767	86	63.57672	115	100.1443	102.56	46.09683	211	99.99433	119.48	33.38418
20	100.131	86	63.57672	116	99.981	102.56	46.09683	212	99.97433	119.66	33.38418
21	99.82934	86.18	62.78218	117	99.93434	102.74	46.09683	213	99.92434	119.66	33.38418
22	99.93933	86.18	62.78218	118	99.93767	102.74	46.09683	214	100.1443	119.84	33.38418
23	99.911	86.18	62.78218	119	100.1693	102.92	45.30229	215	99.92767	120.02	33.38418
24	100.086	86.36	62.78218	120	99.93933	102.92	45.30229	216	100.1593	120.2	33.38418
25	151.8273	86.36	78.67299	121	152.0039	103.1	58.80947	217	152.6606	120.38	45.30229
26	150.154	86.54	78.67299	122	150.144	103.1	58.80947	218	150.1507	120.56	44.50775
27	149.9907	86.54	77.87845	123	150.0107	103.28	58.80947	219	150.0907	120.56	44.50775
28	149.9773	86.54	77.87845	124	149.9973	103.46	58.01493	220	149.944	120.74	44.50775
29	150.0273	86.54	77.87845	125	150.0407	103.64	58.01493	221	149.9773	120.92	44.50775
30	150.0407	86.72	77.87845	126	150.0607	103.82	58.01493	222	149.9273	121.1	44.50775
31	149.9907	86.72	77.08391	127	150.0473	103.82	58.01493	223	149.984	121.28	44.50775
32	150.034	86.72	77.08391	128	150.054	104	58.01493	224	149.9573	121.46	44.50775
33	149.9907	86.9	77.08391	129	150.074	104.18	57.22039	225	150.004	121.64	44.50775
34	150.0607	87.08	77.08391	130	150.054	104.18	57.22039	226	149.9573	121.64	44.50775
35	149.9973	87.08	77.08391	131	150.0607	104.36	57.22039	227	149.9773	121.82	44.50775
36	150.0107	87.08	76.28936	132	150.0407	104.36	57.22039	228	149.9407	122	44.50775
37	201.8186	87.08	90.59109	133	202.6519	104.54	69.1385	229	202.7352	122	54.83677
38	200.0587	87.26	89.79655	134	200.2853	104.72	68.34396	230	200.2053	122.18	54.04223
39	199.9987	87.26	89.79655	135	199.8987	104.72	68.34396	231	200.052	122.36	54.04223
40	199.912	87.44	89.79655	136	199.9253	104.9	68.34396	232	200.0387	122.36	54.04223
41	200.1453	87.44	89.79655	137	199.9187	105.08	68.34396	233	200.0653	122.54	54.04223
42	199.942	87.44	89.79655	138	199.9253	105.08	67.54942	234	200.0187	122.72	54.04223
43	200.1387	87.44	89.00201	139	199.9053	105.08	67.54942	235	200.0187	122.72	54.04223
44	200.0387	87.44	89.00201	140	199.912	105.26	67.54942	236	200.0387	122.9	54.04223
45	199.932	87.62	89.00201	141	199.9053	105.26	67.54942	237	200.032	122.72	54.04223
46	200.172	87.62	89.00201	142	199.9487	105.44	67.54942	238	199.8987	122.9	53.24769
47	199.982	87.62	89.00201	143	199.9553	105.44	67.54942	239	199.8787	122.9	53.24769
48	199.9687	87.62	89.00201	144	199.9353	105.44	67.54942	240	199.8987	122.9	53.24769
49	304.1612	87.62	113.6328	145	305.3944	105.62	87.41293	241	306.7811	122.9	71.52212
50	300.4213	87.62	112.8382	146	300.4947	105.62	86.61839	242	300.5613	123.08	70.72758
51	300.1013	87.62	112.0437	147	300.0013	105.62	86.61839	243	300.208	123.08	70.72758
52	299.948	87.62	112.0437	148	299.9747	105.62	86.61839	244	300.028	123.08	70.72758
53	300.088	87.8	112.0437	149	300.0147	105.62	86.61839	245	300.0013	123.08	70.72758
54	300.1013	87.8	112.0437	150	299.8347	105.62	86.61839	246	300.0013	123.26	70.72758
55	299.948	87.8	112.0437	151	300.0013	105.8	86.61839	247	299.9747	123.26	70.72758
56	299.9147	87.8	112.0437	152	299.8613	105.8	86.61839	248	299.988	123.26	70.72758
57	299.9747	87.98	112.0437	153	300.0813	105.8	86.61839	249	300.0013	123.26	70.72758
58	299.9413	87.98	112.8382	154	299.9013	105.98	86.61839	250	300.0413	123.26	70.72758
59	299.948	87.98	112.8382	155	299.9013	105.98	86.61839	251	300.0013	123.26	70.72758
60	299.928	87.98	112.8382	156	300.1013	105.98	86.61839	252	300.0413	123.26	70.72758
61	404.0772	87.8	135.8799	157	406.1638	105.98	105.6874	253	407.5237	123.26	87.41293
62	400.3773	87.8	134.2908	158	400.5973	105.98	104.8928	254	400.644	123.26	86.61839
63	400.0373	87.98	134.2908	159	400.1107	105.98	104.8928	255	400.0973	123.26	86.61839
64	399.9307	87.98	134.2908	160	399.944	105.98	104.8928	256	399.9307	123.08	86.61839
65	400.084	87.98	134.2908	161	399.9307	105.98	104.8928	257	399.944	123.08	86.61839

66	399.8973	87.98	134.2908	162	399.9707	105.98	104.8928	258	399.9307	123.08	86.61839
67	399.9174	87.98	135.0854	163	399.9707	105.98	104.8928	259	399.9307	123.08	86.61839
68	399.9107	87.98	135.0854	164	400.024	105.98	104.8928	260	400.0707	123.08	86.61839
69	399.9174	87.98	135.0854	165	400.024	105.98	104.8928	261	399.9307	123.08	86.61839
70	399.9174	87.98	135.0854	166	399.9973	105.98	104.8928	262	399.9573	123.08	86.61839
71	399.984	88.16	135.0854	167	399.9973	105.98	104.8928	263	400.0107	123.08	86.61839
72	400.164	88.16	135.0854	168	399.8707	105.98	104.8928	264	399.984	123.08	86.61839
73	504.5265	87.98	154.9489	169	505.5265	105.98	121.5782	265	507.7664	123.08	101.7147
74	500.1	87.98	154.1543	170	500.1266	105.98	120.7836	266	500.46	123.08	100.1256
75	500.1	88.16	154.1543	171	499.9	105.98	120.7836	267	500.2067	122.9	100.1256
76	500.06	87.98	154.9489	172	500.18	105.98	120.7836	268	499.98	122.9	100.9201
77	500.06	87.98	155.7434	173	499.9	105.98	121.5782	269	500.0333	122.72	100.9201
78	499.9267	87.98	155.7434	174	499.8067	105.98	121.5782	270	500.06	122.72	100.9201
79	500.0333	87.98	155.7434	175	500.2067	105.98	121.5782	271	499.9	122.72	100.1256
80	499.9	87.98	155.7434	176	499.8467	105.8	122.3727	272	499.8734	122.72	100.1256
81	499.8467	87.98	156.538	177	500.26	105.8	122.3727	273	499.98	122.72	100.9201
82	499.9533	87.98	156.538	178	499.98	105.8	122.3727	274	500.1	122.72	100.9201
83	500.18	87.98	158.127	179	499.8467	105.8	123.1673	275	499.8067	122.72	100.9201
84	499.9	87.98	158.9216	180	500.1266	105.8	123.1673	276	500.06	122.54	100.9201
85	604.6958	87.98	177.196	181	605.7891	105.8	137.469	277	607.8957	122.54	111.2491
86	600.4693	87.98	178.7851	182	600.5493	105.8	135.0854	278	600.616	122.54	109.6601
87	600.0426	87.98	181.9632	183	599.9893	105.62	132.7017	279	599.9893	122.54	109.6601
88	599.936	87.98	182.7578	184	599.9893	105.8	132.7017	280	600.0693	122.36	110.4546
89	600.1093	87.98	184.3469	185	599.936	105.62	132.7017	281	599.9893	122.36	110.4546
90	599.936	87.98	186.7305	186	600.0826	105.62	131.9072	282	599.9893	122.36	110.4546
91	600.0693	87.98	187.525	187	599.8827	105.62	131.9072	283	600.016	122.36	110.4546
92	600.0693	87.98	189.1141	188	600.0426	105.62	131.9072	284	599.9893	122.36	110.4546
93	600.0426	87.98	189.9087	189	600.0693	105.62	132.7017	285	600.016	122.36	110.4546
94	600.0426	87.98	190.7032	190	600.0426	105.62	132.7017	286	599.9893	122.18	110.4546
95	599.9893	87.98	192.2923	191	599.936	105.44	131.9072	287	600.0426	122.18	110.4546
96	600.0426	87.8	192.2923	192	599.9094	105.62	132.7017	288	600.016	122.18	110.4546

Table 12.7. Data obtained from rheometer for the rheological model analysis of drilling fluid with 15% FA at 86°F, 104°F and 122°F

No	Shear rate (1/s)	Temp. (°C)	Shear stress (dyne/cm^2)	No	Shear rate (1/s)	Temp. (°C)	Shear stress (dyne/cm^2)	No	Shear rate (1/s)	Temp. (°C)	Shear stress (dyne/cm^2)
1	50.23299	84.92	56.42585	97	50.84797	101.66	38.15142	193	49.95634	118.22	19.87699
2	49.94967	85.1	54.83677	98	50.06133	101.66	36.56234	194	49.99883	118.22	19.87699
3	49.9305	85.1	54.83677	99	50.00383	101.66	36.56234	195	49.95467	118.22	19.08245
4	49.96717	85.1	54.04223	100	49.97967	101.84	36.56234	196	49.97217	118.22	19.08245
5	49.94467	85.1	53.24769	101	49.94634	101.84	35.7678	197	49.978	118.22	19.08245
6	49.948	85.1	53.24769	102	50.05633	101.84	35.7678	198	50.018	118.4	19.08245
7	49.96217	85.1	53.24769	103	50.0305	101.84	35.7678	199	49.95134	118.4	19.08245
8	49.95467	85.28	53.24769	104	50.0355	102.02	35.7678	200	50.02633	118.4	19.08245
9	49.9755	85.1	52.45315	105	50.00217	102.02	35.7678	201	50.01133	118.58	19.08245
10	50.03216	85.28	52.45315	106	49.9705	102.02	35.7678	202	49.99133	118.58	18.28791
11	49.958	85.28	52.45315	107	50.01133	102.2	34.97326	203	49.97384	118.58	19.08245
12	50.10049	85.28	52.45315	108	50.06133	102.2	34.97326	204	50.01467	118.76	18.28791
13	101.3959	85.28	75.49482	109	101.7043	102.2	53.24769	205	102.1076	118.76	34.97326
14	100.0643	85.46	74.70028	110	100.1493	102.2	53.24769	206	100.2327	118.76	34.17872

15	99.96267	85.46	73.90574	111	100.0077	102.38	52.45315	207	100.0393	118.76	34.17872
16	99.92767	85.46	73.90574	112	99.98767	102.38	52.45315	208	100.076	118.94	34.17872
17	99.96267	85.46	73.1112	113	100.0793	102.56	52.45315	209	100.0393	119.12	34.17872
18	99.931	85.64	73.1112	114	100.0293	102.56	52.45315	210	100.0543	119.12	34.17872
19	99.946	85.64	73.1112	115	99.946	102.56	52.45315	211	100.001	119.3	34.17872
20	100.1027	85.64	72.31666	116	99.98433	102.74	52.45315	212	100.1143	119.3	34.17872
21	99.98433	85.82	72.31666	117	99.96934	102.74	52.45315	213	99.931	119.48	34.17872
22	99.93933	85.82	72.31666	118	99.956	102.74	52.45315	214	99.96934	119.66	34.17872
23	99.92434	85.82	72.31666	119	100.0127	102.92	52.45315	215	100.0193	119.84	34.17872
24	99.98433	85.82	72.31666	120	100.0193	102.92	51.65861	216	100.0393	120.02	34.17872
25	151.5906	85.82	89.79655	121	151.6739	102.92	65.96034	217	151.9473	120.02	46.09683
26	150.2507	85.82	89.00201	122	150.1507	103.1	66.75488	218	150.2007	120.2	46.09683
27	150.004	86	88.20747	123	150.0107	103.28	65.96034	219	150.1107	120.56	46.09683
28	150.054	86	88.20747	124	149.9973	103.46	65.96034	220	149.944	120.74	46.09683
29	149.9507	86	88.20747	125	150.0107	103.46	65.96034	221	149.874	120.92	46.09683
30	149.9773	86.18	88.20747	126	149.984	103.64	65.96034	222	150.0407	121.1	46.09683
31	149.9973	86.18	87.41293	127	150.0107	103.82	65.96034	223	150.0207	121.28	46.09683
32	150.0407	86.18	87.41293	128	150.0273	103.82	65.96034	224	149.9407	121.46	46.09683
33	150.034	86.36	87.41293	129	149.9773	104	65.1658	225	149.894	121.64	46.09683
34	149.984	86.36	87.41293	130	149.9907	104.18	65.1658	226	149.9707	121.82	46.09683
35	149.9073	86.36	86.61839	131	149.9907	104.18	65.1658	227	149.894	122	46.09683
36	149.9907	86.36	86.61839	132	149.9907	104.36	65.1658	228	150.0107	122.18	46.09683
37	201.4886	86.36	102.5092	133	201.7553	104.36	77.87845	229	202.1186	122.36	57.22039
38	200.122	86.54	101.7147	134	200.0587	104.54	77.08391	230	200.172	122.54	56.42585
39	200.0887	86.54	100.9201	135	200.0953	104.72	77.08391	231	199.9687	122.72	56.42585
40	199.9687	86.72	100.9201	136	200.0453	104.72	77.08391	232	200.1387	122.54	56.42585
41	200.0053	86.72	100.9201	137	199.962	104.9	77.08391	233	199.9953	122.72	57.22039
42	199.9253	86.72	100.9201	138	199.9187	105.08	77.08391	234	199.9987	122.72	57.22039
43	199.962	86.72	100.9201	139	199.912	105.08	77.08391	235	199.942	122.72	57.22039
44	199.9953	86.9	100.1256	140	200.0953	105.26	76.28936	236	200.1453	122.9	57.22039
45	200.0053	86.9	100.1256	141	200.0753	105.26	76.28936	237	200.0053	122.9	57.22039
46	199.9687	86.9	100.1256	142	199.9953	105.26	76.28936	238	199.942	123.08	57.22039
47	200.0053	86.9	100.1256	143	199.982	105.44	76.28936	239	199.9887	123.08	57.22039
48	199.962	86.9	100.1256	144	199.9753	105.44	76.28936	240	199.9487	123.08	57.22039
49	303.3679	86.9	127.9345	145	304.2745	105.44	99.33104	241	305.3544	123.26	77.08391
50	300.228	86.9	127.14	146	300.3346	105.62	98.5365	242	300.628	123.26	76.28936
51	300.128	86.9	126.3454	147	299.9613	105.62	97.74196	243	299.988	123.44	76.28936
52	299.9747	86.9	126.3454	148	300.0147	105.62	97.74196	244	299.9747	123.44	77.08391
53	299.948	86.9	126.3454	149	300.0013	105.8	97.74196	245	300.028	123.62	77.08391
54	300.0813	86.9	126.3454	150	300.0013	105.8	97.74196	246	299.9747	123.44	77.08391

55	299.9413	87.08	127.14	151	300.0413	105.8	97.74196	247	300.0413	123.62	77.08391
56	299.9747	86.9	127.14	152	300.0147	105.98	97.74196	248	300.028	123.62	77.08391
57	300.1147	86.9	127.14	153	300.0547	105.98	97.74196	249	300.028	123.62	77.87845
58	300.0013	87.08	127.14	154	299.8747	105.98	97.74196	250	299.9013	123.62	77.87845
59	299.9747	87.08	127.14	155	300.0413	105.98	97.74196	251	299.9013	123.8	77.87845
60	300.0013	87.08	127.9345	156	300.0547	105.98	97.74196	252	300.068	123.62	77.87845
61	403.2372	87.08	153.3598	157	405.1105	105.98	119.1946	253	406.5438	123.62	97.74196
62	400.264	87.08	152.5653	158	400.3906	105.98	117.6055	254	400.4573	123.62	96.94742
63	400.024	87.08	152.5653	159	400.084	106.16	118.4	255	400.0973	123.62	97.74196
64	400.084	86.9	152.5653	160	399.9107	106.16	118.4	256	399.9107	123.62	97.74196
65	400.0573	86.9	152.5653	161	399.9707	106.16	118.4	257	399.9307	123.62	98.5365
66	399.9573	87.08	153.3598	162	400.0373	106.16	118.4	258	399.9307	123.62	98.5365
67	400.0973	87.08	153.3598	163	399.944	106.16	118.4	259	399.9973	123.62	98.5365
68	399.984	86.9	153.3598	164	399.984	106.16	118.4	260	399.984	123.62	98.5365
69	399.984	86.9	153.3598	165	399.9707	106.16	119.1946	261	400.024	123.62	98.5365
70	399.9973	86.9	154.1543	166	399.984	106.16	119.1946	262	400.0107	123.62	99.33104
71	399.984	86.9	154.9489	167	399.9707	106.16	119.1946	263	399.9107	123.62	99.33104
72	400.0373	86.9	154.9489	168	400.0373	106.16	119.1946	264	399.9973	123.62	99.33104
73	504.9665	86.9	178.7851	169	506.1797	105.98	138.2635	265	506.0064	123.62	115.2218
74	500.2333	86.9	178.7851	170	500.2067	105.98	138.2635	266	500.5933	123.62	114.4273
75	500.2067	86.9	178.7851	171	500.1	105.98	139.0581	267	499.9	123.44	114.4273
76	499.9267	86.9	179.5796	172	499.9	105.98	139.0581	268	500.34	123.44	115.2218
77	499.82	86.9	179.5796	173	499.9	105.98	139.0581	269	499.98	123.44	115.2218
78	500.18	86.9	179.5796	174	499.9267	105.98	139.0581	270	499.9533	123.44	116.0164
79	499.8067	86.9	181.1687	175	500.18	105.98	139.8526	271	499.98	123.26	116.8109
80	500.18	86.9	181.9632	176	499.8734	105.98	139.8526	272	500.0333	123.26	116.8109
81	499.8734	86.9	182.7578	177	500.0866	105.98	139.8526	273	500.06	123.26	117.6055
82	500.2333	86.9	183.5523	178	500.06	105.98	140.6471	274	499.9267	123.08	117.6055
83	499.8734	86.9	183.5523	179	499.9	105.8	140.6471	275	500.2333	123.08	117.6055
84	500.2333	87.08	184.3469	180	499.9267	105.98	140.6471	276	499.8467	123.08	117.6055
85	604.7358	86.9	207.3885	181	605.3491	105.8	157.3325	277	605.9358	123.08	131.9072
86	600.5493	87.08	208.9776	182	600.4693	105.8	155.7434	278	600.576	123.08	130.3181
87	600.136	86.9	209.7722	183	600.016	105.8	158.127	279	600.0426	122.9	130.3181
88	599.9893	86.9	211.3612	184	599.9893	105.8	159.7161	280	600.0426	122.9	131.1127
89	599.9893	86.9	212.1558	185	600.016	105.8	160.5107	281	600.0426	122.9	131.1127
90	600.0426	86.9	212.9503	186	599.9094	105.62	162.0997	282	599.9893	122.9	131.1127
91	600.0426	86.9	213.7449	187	600.016	105.62	162.0997	283	599.9893	122.72	131.1127
92	600.0693	86.9	213.7449	188	599.8827	105.62	162.8943	284	600.016	122.72	131.9072
93	599.9893	86.9	214.5394	189	600.1093	105.62	164.4834	285	599.936	122.72	131.1127
94	600.0426	86.9	214.5394	190	600.1627	105.62	164.4834	286	600.016	122.72	131.9072

95	600.016	86.9	215.334	191	600.0826	105.62	165.2779	287	600.0426	122.72	131.9072
96	600.136	86.9	214.5394	192	599.9893	105.62	165.2779	288	599.9893	122.72	131.9072

Table 12.8. Results of rheological model estimation of the water based drilling fluids with the increasing concentration of FA

KCL ref. mud+0% FA				
Temperature, °F		**86**	**104**	**122**
Bingham Plastic	**μ_p (Pa-s)**	0.01157	0.009396	0.009169
	τ_y (Pa)	4.058	3.059	1.602
	SSE	1.357	0.5828	0.5608
	R^2	0.9874	0.9918	0.9917
	Adjusted R^2	0.9853	0.9904	0.9903
	RMSE	0.4756	0.3117	0.3057
Power-Law	**n**	0.5317	0.5507	0.6915
	K (Pa-s^n)	0.3831	0.268	0.08833
	SSE	0.2151	0.1568	0.05477
	R^2	0.998	0.9978	0.9992
	Adjusted R^2	0.9977	0.9974	0.9991
	RMSE	0.1894	0.1617	0.09554
Herschel-Bulkley	**y_0 (Pa)**	1.48	1.431	0.126
	n	0.6374	0.6923	0.7075
	K (Pa-s^0)	0.1679	0.08992	0.07822
	SSE	0.08022	0.005224	0.05292
	R^2	0.9993	0.9999	0.9992
	Adjusted R^2	0.999	0.9999	0.9989
	RMSE	0.1267	0.03232	0.1029
KCL ref. Mud+7% FA				
Temperature, °F		**86**	**104**	**122**
Bingham Plastic	**μ_p (Pa-s)**	0.01148	0.01034	0.009418
	τ_y (Pa)	4.38	2.597	1.715
	SSE	1.136	0.7596	0.5967
	R^2	0.9893	0.9911	0.9916
	Adjusted R^2	0.9875	0.9897	0.9902
	RMSE	0.4352	0.3558	0.3154
Power-Law	**n**	0.5108	0.612	0.6819
	K (Pa-s^n)	0.4485	0.1829	0.09747
	SSE	0.2421	0.04536	0.005536
	R^2	0.9977	0.9995	0.9999
	Adjusted R^2	0.9973	0.9994	0.9999
	RMSE	0.2009	0.08695	0.03038
Herschel-Bulkley	**m**	0.651	0.6794	0.6876
	K (Pa-s^0)	0.1502	0.1091	0.09334
	τ_y (Pa)	1.974	0.6929	0.04779
	SSE	0.01668	0.004362	0.005297
	R^2	0.9998	0.9999	0.9999
	Adjusted R^2	0.9998	0.9999	0.9999

	RMSE	0.05776	0.02954	0.03255
KCL ref. Mud+9% FA				
Temperature, °F		**86**	**104**	**122**
Bingham Plastic	**μ_p (Pa-s)**	0.01241	0.01092	0.009877
	τ_y (Pa)	4.756	3.267	2.643
	SSE	1.129	1.437	0.8924
	R^2	0.9908	0.9851	0.9886
	Adjusted R^2	0.9893	0.9826	0.9867
	RMSE	0.4339	0.4894	0.3857
Power-Law	**n**	0.5103	0.5694	0.598
	K (Pa-s^n)	0.4871	0.2686	0.1949
	SSE	0.5589	0.08344	0.2782
	R^2	0.9955	0.9991	0.9965
	Adjusted R^2	0.9947	0.999	0.9959
	RMSE	0.3052	0.1179	0.2153
Herschel-Bulkley	**m**	0.6927	0.6045	0.6887
	K (Pa-s^0)	0.1184	0.2042	0.09708
	τ_y (Pa)	2.611	0.4603	0.9017
	SSE	0.1142	0.07008	0.2065
	R^2	0.9991	0.9993	0.9974
	Adjusted R^2	0.9987	0.999	0.9963
	RMSE	0.1511	0.1184	0.2032
KCL ref. Mud+12.5% FA				
Temperature, °F		**86**	**104**	**122**
Bingham Plastic	**μ_p (Pa-s)**	0.01426	0.0108	0.009565
	τ_y (Pa)	3.843	2.835	1.827
	SSE	0.57	1.069	1.103
	R^2	0.9965	0.9886	0.985
	Adjusted R^2	0.9959	0.9867	0.9826
	RMSE	0.3082	0.4222	0.4288
Power-Law	**n**	0.6009	0.601	0.6682
	K (Pa-s^n)	0.2763	0.2078	0.1095
	SSE	1.773	0.09889	0.08094
	R^2	0.9891	0.9989	0.9989
	Adjusted R^2	0.9872	0.9988	0.9987
	RMSE	0.5437	0.1284	0.1161
Herschel-Bulkley	**m**	0.9012	0.6522	0.6895
	K (Pa-s^0)	0.02913	0.14	0.3074)
	τ_y (Pa)	3.244	0.5836	0.2724
	SSE	0.454	0.07227	0.04468
	R^2	0.9972	0.9992	0.9994
	Adjusted R^2	0.9961	0.9989	0.9992
	RMSE	0.3013	0.1202	0.09453
KCL ref. Mud+15% FA				
Temperature, °F		**86**	**104**	**122**

Bingham Plastic	**μ_p (Pa-s)**	0.01637	0.01298	0.0119
	τ_y (Pa)	4.35	3.003	1.418
	SSE	0.3597	0.4392	0.7046
	R^2	0.9983	0.9967	0.9938
	Adjusted R^2	0.998	0.9962	0.9927
	RMSE	0.2449	0.2706	0.3427
Power-Law	**n**	0.6059	0.6353	0.7629
	K (Pa-s^n)	0.3057	0.1927	0.06703
	SSE	2.648	0.5741	0.05329
	R^2	0.9876	0.9957	0.9995
	Adjusted R^2	0.9855	0.995	0.9995
	RMSE	0.6643	0.3093	0.09424
Herschel-Bulkley	**m**	0.9547	0.8243	0.8145
	K (Pa-s^0)	0.02268	0.04649	0.1261
	τ_y (Pa)	4.054	1.937	0.452
	SSE	0.3279	0.1158	0.04639
	R^2	0.9985	0.9991	0.9996
	Adjusted R^2	0.9978	0.9988	0.9994
	RMSE	0.2561	0.1522	0.09632